Risk management in trading activities through the lens of complex systems theory

Anagnostou, I.

Publication date
2020

Document Version
Final published version

License
Other

Risk management in trading activities through the lens of complex systems theory

Ioannis Anagnostou

Risk management in trading activities through the lens of complex systems theory

Risk management in trading activities through the lens of complex systems theory

ACADEMISCH PROEFSCHRIFT

ter verkrijging van de graad van doctor
aan de Universiteit van Amsterdam
op gezag van de Rector Magnificus
prof. dr. ir. K.I.J. Maex
ten overstaan van een door het College voor Promoties
ingestelde commissie,
in het openbaar te verdedigen in de Agnietenkapel
op maandag 30 november 2020, te 17:00 uur

door

Ioannis Anagnostou

geboren te Cholargos

Promotiecommissie:

Promotores:	prof. dr. B.D. Kandhai	Universiteit van Amsterdam
	prof. dr. ir. A.G. Hoekstra	Universiteit van Amsterdam
Overige leden:	prof. dr. C.G.H. Diks	Universiteit van Amsterdam
	prof. dr. M.R.H. Mandjes	Universiteit van Amsterdam
	prof. dr. I. van Lelyveld	Vrije Universiteit Amsterdam
	dr. D. Garlaschelli	Universiteit Leiden/IMT Lucca
	dr. R. Quax	Universiteit van Amsterdam

Faculteit der Natuurwetenschappen, Wiskunde en Informatica

The work described in this thesis was carried out in the Computational Science Lab of the University of Amsterdam in close collaboration with ING Bank and has received funding from the European Union's Horizon 2020 research and innovation programme under the Marie Skłodowska-Curie Grant Agreement no. 675044 (http://bigdatafinance.eu/), Training for Big Data in Financial Research and Risk Management.

ISBN 978-94-6421-100-9

An electronic version of this dissertation is available at
`https://dare.uva.nl/`.

Contents

Summary

The financial crisis of 2008, which led to a near collapse of the banking system and caused enormous losses and damage to billions of people, challenged financial institutions, regulators, and researchers to offer more comprehensive explanations of its causes by revisiting their conventional approach. In the post-crisis era, there has been increasing interest in using ideas from complexity theory to achieve a better understanding of financial markets. Concepts, such as regime shifts, interconnectedness, contagion, feedback, and resilience, have entered the financial vocabulary, but the actual use of models and results from complexity is still at an early stage. Moreover, while recent studies offer potential for better monitoring and supervision of the financial system, little work has been done on incorporating complexity tools in the pricing and risk management of individual portfolios.

The dynamics of complex systems such as financial markets is recorded in time series of activity of their constituting elements. One of the striking effects exhibited by financial time series is sudden changes of behaviour, with the new behaviour often persisting for several periods after the change. These regime shifts - prevalent in stocks, foreign exchange and interest rates, as well as in the behaviour of many macroeconomic variables - may lead to dramatic changes in the market interactions and risk measures. Thus, the identification of regime transitions is of great importance. In an attempt to account for these phenomena, we propose a model for the evolution of exchange rates were drift and volatility are allowed to switch between regimes. We use this model to generate scenarios for counterparty exposure and evaluate the conceptual soundness by carrying out a rigorous backtesting experiment against realised time series for a number of exchange rates. The impact of using a regime-switching model on counterparty exposure is shown to be profound for derivatives with non-linear payoffs.

A central role in understanding and modelling complex systems is played by network science. Complex interactions between different assets and entities, which can be extracted from financial time series or other data, are of great interest with regards to risk management, as shocks may be amplified through strong cascading effects. One of the key contributions of this thesis is the incorporation of contagion effects in portfolio credit risk models using network theory. Systematic risk factors are augmented with a contagious default mechanism which affects the entire universe of credits. Credit stress propagation networks are constructed and contagion parameters are calibrated for infectious defaults. The resulting framework is implemented on synthetic test portfolios wherein the contagion effect is shown to have a significant impact on the tails of the loss distributions. At a later stage we learn Bayesian networks of interactions between issuers, and estimate the contagion effects following a systemic default. Different techniques to learn the structure and parameters of Bayesian networks are studied and evaluated, with the results confirming that the structures are robust. In order to investigate the impact of these effects on credit losses, we carry out simulations and calculate the percentiles of

the loss distribution in the presence of contagion.

One of the most important characteristics of networks is community structure, i.e., the occurrence of nodes that are more densely interconnected locally than with the rest of the network. Communities reveal the intermediate organisation of nodes, and their detection is crucial in the study of complex systems. We discuss a recent community detection method for empirical correlation matrices and apply it to real time series data on credit default swap spreads. We examine the emergent community structure and investigate its evolution over time. A range of dependencies is uncovered which are not immediately obvious from the standard sector and region taxonomy. We argue that this result can be particularly relevant for optimisation and risk management of real portfolios.

Samenvatting

De financiële crisis van 2008, waarbij het bankensysteem bijna ineenstortte en miljarden mensen de consequenties ervaarden, heeft instellingen, toezichthouders en onderzoekers uitgedaagd om diepgaandere verklaringen te vinden voor de oorzaak ervan en om de huidige methodes te herzien. In de periode na de crisis is de belangstelling voor het gebruiken van ideeën afkomstig uit de theorie van complexe systemen om de financiële markten beter te begrijpen erg toegenomen. Begrippen als regimeverschuivingen, onderlinge verbondenheid, besmetting, feedback en veerkrachtigheid zijn al onderdeel geworden van het financiële vocabulaire, maar de daadwerkelijke toepassing van modellen en resultaten uit de complexiteitsleer staat vooralsnog in zijn kinderschoenen. Daar komt bij dat, hoewel recente studies de potentie bieden om het financiële systeem beter te monitoren en te controleren, er nog weinig werk is verricht om onderdelen uit de complexiteitsleer te verwerken in de waardering en het risicobeheer van losse portefeuilles.

De dynamiek van complexe systemen, zoals de financiële markten, is te observeren in tijdsreeksen van de onderliggende elementen. Opvallende effecten die zijn terug te vinden in deze financiële tijdsreeksen, zijn plotselinge gedragsveranderingen, waarbij het nieuwe gedrag meestal een langere periode na de verandering aanhoudt. Deze regimeverschuivingen - veel voorkomend bij aandelen, wisselkoersen en rentes, maar ook bij het gedrag van vele macro-economische variabelen - kunnen leiden tot heftige veranderingen in de interacties tussen markten en de te nemen risicomaatregelen. Zodoende is het identificeren van regimeverschuivingen van groot belang. In een poging om deze fenomenen te verklaren, introduceren we een model voor de ontwikkeling van wisselkoersen waarin de drift en de volatiliteit van toestand kunnen wisselen. We gebruiken dit model om scenarios te generen voor de blootstelling aan tegenpartijrisico en toetsen de conceptuele correctheid door een rigoureuze backtest uit te voeren op de gemodelleerde blootstelling aan tegenpartijrisico van derivaten met een niet-lineaire intrinsieke waarde.

Netwerkwetenschap speelt een centrale rol in het begrijpen en modelleren van complexe systemen. Complexe interacties tussen activa en instellingen, welke kunnen worden onttrokken aan financiële tijdsreeksen of andere gegevens, zijn met het oog op risicomanagement zeer interessant, aangezien economische schokken versterkt kunnen worden door een sterk domino-effect. Een belangrijke bijdrage van dit proefschrift is de verwerking van besmettingseffecten in kredietrisico modellen voor portefeuilles, met behulp van netwerktheorie. Systematische risico-factoren worden uitgebreid met een overdraagbaar default mechanisme dat invloed heeft op het volledige universum van kredieten. Krediet-stress-propagatie netwerken zijn gecreëerd en besmettingsparameters zijn gekalibreerd voor overdraagbare defaults. Het raamwerk dat hieruit voortkomt is geïmplementeerd op kunstmatige test portefeuilles waarbij is aangetoond dat het besmettingseffect een significante impact heeft op de staarten van de verliesverdeling. In

een later stadium trainen we Bayesiaanse netwerken op basis van de interacties tussen uitgevende instellingen en maken we een inschatting van de besmettingseffecten die volgen op een systematische default. Verschillende technieken om de structuur en de parameters van een Bayesiaans netwerk te leren zijn bestudeerd en geëvalueerd, waarbij de resultaten de robuustheid van de structuren bevestigen. Om de impact van deze effecten op kredietverliezen te onderzoeken, doen we simulaties en berekenen we de percentielen van de verliesverdeling waarbij sprake is van besmetting.

Een van de belangrijkste eigenschappen van netwerken is de clustervorming, dat wil zeggen, de aanwezigheid van knopen die lokaal dichter met elkaar verbonden zijn dan met de rest van het netwerk. Clusters onthullen de organisatorische structuur van knopen op mesoscopische schaal en de detectie daarvan is cruciaal in de studie van complexe systemen. We bespreken een recente cluster-detectie methode voor empirische correlatie matrices en passen dit toe op bestaande gegevens van tijdsreeksen voor credit-default swap spreads. We onderzoeken de cluster structuur die hierbij ontstaat en haar ontwikkeling als functie van de tijd. Meerdere afhankelijkheden zijn aangetoond die niet direct voor de hand liggend zijn vanuit een standaard sector- of regiotaxonomie. Wij stellen dat dit resultaat in het bijzonder relevant is voor de optimalisatie en het risicomanagement van echte portefeuilles.

1

Introduction

The global financial crisis laid bare the significant drawbacks of traditional economic and financial models, as these were unable to explain the events that took place in the economy and financial markets in a plausible and realistic manner. In November 2010 Jean-Claude Trichet, then President of the European Central Bank (ECB), pointed out the following during his opening address at the ECB Central Banking Conference:

> When the crisis came, the serious limitations of existing economic and financial models immediately became apparent. As a policy-maker during the crisis, I found the available models of limited help. In fact, I would go further: in the face of the crisis, we felt abandoned by conventional tools.

At the same speech, Trichet challenged the scientific community by highlighting the need to introduce drastically innovative tools in order to complement the existing modelling approaches, tapping into the progress made by scientists developing techniques for the study of complex dynamic systems. Almost a decade later, complexity related concepts such as tipping points, networks, and contagion have entered the financial and regulatory dictionary [1]. However, the effort for incorporating techniques from complexity theory into models used for pricing and risk management of individual portfolios remains challenging.

The purpose of this thesis is to take up this challenge and develop novel risk management models which would view financial markets as complex systems prone to sudden and major changes while consisting of many interacting nodes. A question that remains central to this thesis is the amount of capital that a bank needs to hold to remain solvent. Capital acts as a loss-absorbing cushion that covers losses related to a range of risk types. Figure 1.1 illustrates how adequate capital prevents liabilities from exceeding assets. Insufficient capital buffers translate to a crisis-prone financial system, which would be in need for regular bail-outs. A During the 2007-2009 crisis it became apparent that capital buffers where not adequate for many banks. As a result, after suffering large losses, banks were unable to extend credit, and thus a powerful feedback loop was created between

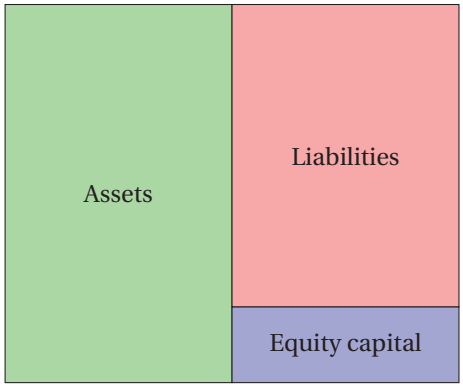

Figure 1.1: A company is considered solvent at a particular time if the value of assets exceeds the value of its liabilities. One of the key roles of risk management is to determine the amount of capital a bank is required to hold as a buffer for future unexpected losses to ensure that it will remain solvent.

banking stress and the real economy. As Lord Turner, former Chairman of the UK Financial Services Authority, highlights in his review on the Global Banking Crisis ([2]): " When the crisis broke, banks did not have sufficient capital buffers to absorb losses, creating the danger of a self-reinforcing feedback loop between weak lending capacity, economic recession, and credit losses." It is therefore critical to ensure that banking risks are sufficiently capitalised for the protection of individual customers, as well as the society as a whole. In response to the crisis, regulators have introduced a thorough and extensive reinforcement of global bank standards, most notably through the Basel III and Basel IV frameworks. Nevertheless, despite the numerous crucial improvements, the revised capital framework still relies heavily on conventional modelling approaches.

In the present thesis, we develop techniques and tools that go beyond the current practice. New tools from time-series and network theory are used along with a range of real-world datasets to implement an integrated complex systems approach for risk modelling and the calculation of capital buffers. This includes new methods of empirical analysis, and the development of new mathematical and computational tools. Our effort is guided by emerging new conceptual paradigms such as network theory and data-driven methods. By merging these ideas into practical simulation and risk measurement tools, our aim is to build the foundations of a new paradigm within risk management.

1.1. The complex systems approach

In 1948 the mathematician Warren Weaver published an influential paper [3] in which he introduced three notions of complexity to characterise natural systems: organised simplicity, disorganised complexity, and organised complexity. Organised simplicity is a property of the systems adequately described by a small number of degrees of freedom, the relationship between which can be described by simple, typically deterministic functions; best example of such systems is the systems dealt with in classical mechanics. These systems are usually analytically tractable, but when the number of degrees of freedom exceeds exceeds a very small number, they become intractable. Disorganised

complexity on the other hand characterises systems involving a very large number of degrees of freedom which do not follow deterministic rules, such as the systems encountered in statistical mechanics. Within this class, simplification can be achieved through the transition from the microscopic to the macroscopic level; description can overlook single particle motion and instead focus on a small number of statistical averages. Individual trajectories do not contribute to the description of the system and, in fact, can be replaced by random variables following a distribution of possible trajectories.

Between these two extremes, Weaver identified a third notion which he called organised complexity. Systems characterised by organised complexity typically involve a moderate to large number of degrees of freedom, by the interactions between which order emerges spontaneously. The macroscopic properties of these systems cannot be seen as averages over the properties of their individual degrees of freedom. As such, individual elements may contribute far beyond their proportion to the behaviour at the aggregate level of the system. This results in situations of diverse order or ordered heterogeneity, where the system is amenable to neither analytical nor statistical treatment and different approaches are necessary.

More than seventy years after the publications of Weaver's paper, significant steps have been taken towards the understanding of complex systems, the study of which has emerged as a scientific field often termed complexity science. However, despite the considerable progress, it remains challenging for scientists to agree upon a single definition that captures all aspects of complexity. The inspired categorisation of Weaver still appears to be the best definition of the purview of complexity science. Some widely known examples of complex systems consisting of dynamic, interacting elements with robust collective properties are ecological systems, brains, and cities.

The first one to conceive the economy as a complex system is thought to be Adam Smith, who described the collective wealth and shared benefits of society as a process emerging from the self-organised behaviour of individuals [4]. Early contributions on complex systems in economics include [5, 6]. The majority of social and economic systems such as traffic flows, crowd behaviour, and financial markets can be viewed as complex systems. Some groundbreaking publications on complex systems in social and economic context can be found in [7, 8].

Complex systems are characterised by tipping points and regime transitions such as epidemic spreading, power blackouts, and the collapse of financial markets. Sudden changes of behaviour are one of the striking effects exhibited by financial time series, with the new behaviour often persisting for several periods after the change. These regime shifts - prevalent in stocks, foreign exchange and interest rates, as well as in the behaviour of many macroeconomic variables - may lead to dramatic changes in portfolio losses and risk measures. In addition, the frequency of extreme events observed in complex systems is much higher than what is suggested by the Gaussian distribution assumed by many standard models. The distribution of earthquakes, material failures, epileptic seizures, and financial returns is distinctly non-normal. This further emphasises the importance of the development of models that can account for these extremes for a complete risk management framework.

The study of complex systems requires methods that span beyond the conventional risk manager's toolbox, such as data mining, non-linear dynamics, theory of critical tran-

sitions, network theory, and agent-based modelling. In this thesis, much of the emphasis in extending quantitative risk management is on network theory, considering that financial markets consist of interacting nodes such as companies and governments, each of which is acting in the context of networks in which the behaviour of the node is not fixed, but evolves in response to the behaviour of others. Network theory can provide us with tools and insights that enable us to make sense of the complex interconnected nature of financial systems. Following the global financial crisis crisis, network-based models have been frequently used to study contagion phenomena [9–14] and measure systemic risk [15–18]. However, despite the growing literature on network models in finance, their actual use for risk management remains at a very early stage.

One of the most relevant features encountered in many complex systems is hierarchical structure. In his influential paper "The architecture of complexity" [5], Herbert A. Simon argues that hierarchy is one of the main structural schemes used by the architect of complexity. Simon defines as hierarchical system a system consisting of sub-systems that are complex systems which in turn consist of complex systems themselves. Resolving the organisation of a complex system's constituting units at the mesoscale, i.e. at an intermediate level between the microscopic dynamics of individual units and the macroscopic dynamics of the system as a whole is an active topic in complex systems research. In network representations this amounts to identifying groups of nodes which are tightly connected to each other inside the group and loosely connected to the rest of the nodes in the network. A large interdisciplinary community of scientists has been working on solving this very hard problem over the past few years; a review of the most methods developed can be found in [19]. In risk management, where we often have to deal with high-dimensional vectors of risk factors, resolving the structure of financial markets can provide valuable insights.

1.2. Quantitative risk management

In the Concise Oxford English Dictionary risk is defined as "hazard, a chance of bad consequences, loss or exposure to mischance". With financial risk in mind, McNeil, Frey, and Embrechts [20] find the definitions "any event or action that may adversely affect an organisation's ability to achieve its objectives and execute its strategies" and "the quantifiable likelihood of loss or less-than-expected returns" relevant. Although all these definitions cover certain of the key elements of risk, it is impossible to capture all of its aspects in a single one-sentence definition. However, it is clear that risk is strongly related to uncertainty about future events.

This thesis is concerned about methods and techniques to measure and model financial risk, which is part of the risk management process. In an attempt to explain what risk management is really about, H. Felix Kloman [21] writes:

> What is risk management? To many analysts, politicians, and academics it is the management of environmental and nuclear risks, those technology generated macro-risks that appear to threaten our existence. To bankers and financial officers it is the sophisticated use of such techniques as currency hedging and interest-rate swaps. To insurance buyers or sellers it is coordination of insurable risks and the reduction of insurance costs. To hospital

> administrators it may mean "quality assurance". To safety professionals it is reducing accidents and injuries.

According to Kloman, risk management as the range of techniques that we are beginning to use to manage our lives and organisations more efficiently in the face of "unprecedented uncertainty". In short, risk management is a discipline for ensuring resilience to future events that may cause adverse effects. It is important to note that financial institutions are not passive towards risk. In fact they are actively pursuing risk in order to generate returns, since risk is what drives returns. As such, risk management is a fundamental competence of financial institutions.

The focus of this thesis is on credit risk, one of the most important types of financial risk. Credit risk is the risk of losses arising from the failure of a borrower or a counterparty to fulfil its contractual obligations. This includes both default risk and the risk of losses due to the downgrade of a counterparty in a rating system. Default is the actual failure of a borrower or counterparty to fulfil their obligation, for example to repay their loan or pay interest on a loan or bond.

Credit risk is ubiquitous in bank portfolios. It is clear that instruments such as loans and bonds are subject to credit risk. It may be less clear, but over-the-counter (OTC) derivatives such as forwards and interest rate swaps[1] are also subject to credit risk, since default of one of the contracted parties may significantly affect the payoff of the transaction. In addition, there is a dedicated market for credit derivatives such as credit default swaps, which will be introduced later in the thesis.

The management of credit risk involves a range of activities. First and foremost, banks need to determine the amount of capital they require in order to absorb credit-risk related losses. Apart from capital calculations, it is important for banks to diversify and optimise their portfolios of credit-risky instruments with risk-return considerations. As far as credit derivatives are concerned, banks need credit risk management to price and hedge their trades as well as to manage collateral. Finally, the global financial crisis highlighted the significance of counterparty credit risk management in the OTC derivatives portfolios. Some of the banks heavily involved in OTC derivative transactions realised huge losses or —in the case of Lehman Brothers— even collapse. Counterparty credit risk management is now a key focus for all banks and at the centre of many recent regulatory developments.

1.2.1. Credit risk variables

A challenge inherent in credit risk modelling is that default events are rare and they occur unexpectedly. When they do occur, however, defaults lead to major losses, the size of which is not known beforehand. The main focus of risk management within banks lies in the possibility of these extreme losses, rather than on traditional financial risk measurement.

When measuring the risk of losses over a fixed time horizon, typically one year, we are mainly concerned with the probability that an issuer[2] or a counterparty will default by the time horizon, a quantity known as *probability of default* or PD. The probability of

[1] A forward is a non-standardised contract between two parties to buy or sell an asset at a certain future time for a certain price. An interest rate swap is a contract involving exchange of interest payments between two parties. For more details see [22]

[2] An issuer is a legal entity that develops, registers and sells securities to finance its operations.

Figure 1.2: In order to determine the exposure for an OTC derivative transaction typically one has to simulate the future state of all underlying risk factors, and evaluate the value of the transaction on that state. By doing this for a large number of paths and time points, a future exposure distribution is obtained. The figure shows simulated Monte Carlo paths from time $t = t_0$ that are transformed into an exposures by calculating the transaction value at all the simulated states.

default is strongly related to the credit quality and its measurement is often the first step in credit risk management. In cases where the loss depends on the exact time that default takes place, such as OTC derivatives, it is necessary to consider the entire distribution of default times rather than just the probability of default occurring within a fixed period

When a bank is offering a loan or buying a bond, it is quite straightforward to determine its exposure, since this consists mainly of the principal with some additional uncertainty stemming from the possibility of missed interest payments. For OTC derivatives however, determining the exposure is far more involved, since it is a stochastic variable depending on the evolution of a range of factors and the exact time at which default takes place. For the exposure to be determined typically one has to simulate the future state of all underlying risk factors, and evaluate the value of the transaction on that state, as illustrated in Figure 1.2. In practice the concept used is *exposure-at-default* or EAD, which represents the extent to which the bank is exposed in the event of and at the time of default.

Default does not necessarily imply that the entire exposure is lost. In case a residential mortgage holder defaults, for example, the lender can sell the property that was used as collateral and recover part of the exposure. Similarly, if a bond issuer defaults, the bond holders are partly compensated for their losses by the sale of the issuer's assets. The percentage of loss incurred over the total exposure is known as *loss-given-default* or LGD.

EAD, PD and LGD are not independent quantities. For example, in a period of economic distress when many residential mortgage holders default, house prices are also likely to be low and, as a result, LGDs are likely to be correspondingly high. This is an example of positive correlation between PDs and LGDs. Nevertheless, this dependence

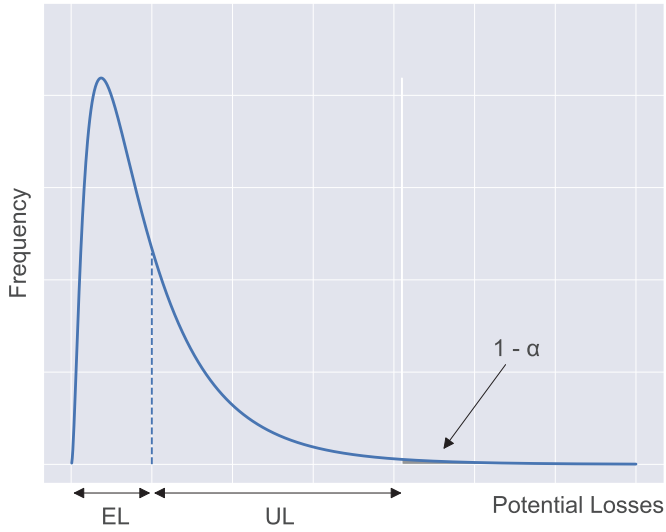

Figure 1.3: Potential losses are typically distinguished in Expected Losses (EL) which are relatively predictable and covered by provisions, and Unexpected Losses (UL) which are less predictable and are covered by capital. To determine how much capital is required to cover UL, risk managers usually apply a tail risk measure such as Value-at-Risk (VaR) at a given confidence level α to the loss distribution obtained using a credit risk model.

not in the scope of this thesis.

1.2.2. Credit risk models

Credit risk models have two main uses: the analysis of instruments subject to credit risk and the management of credit portfolios. For credit-risky instruments such as OTC derivatives, the payoff of the transaction depends on the exact time of default. It is therefore necessary to use dynamic models that study the evolution of risk as a stochastic process over time. On the other hand, when credit risk models are used for portfolio management the focus is mainly on determining the portfolio loss distribution for a fixed period of time and computing the corresponding risk measures and capital on the basis of this distribution. As a result, static distributional models are often sufficient.

Regardless of being static or dynamic, credit risk models can be classified in structural or firm-value on the one hand and reduced-form on the other hand. Structural models originate from the model of Merton [23] and are concerned with the mechanism by which default takes place. In Merton's model default of a firm takes place if at the end of a given period the value of its assets falls below the value of its liabilities. More broadly, in structural models default takes place when a stochastic variable falls below a critical threshold. Because of that structural models are often termed threshold models. Reduced-form models leave the mechanism unspecified and model directly the time to default.

With credit risk in mind, it is important to distinguish potential losses in Expected Losses (EL) and Unexpected Losses (UL). Expected losses are relatively predictable and

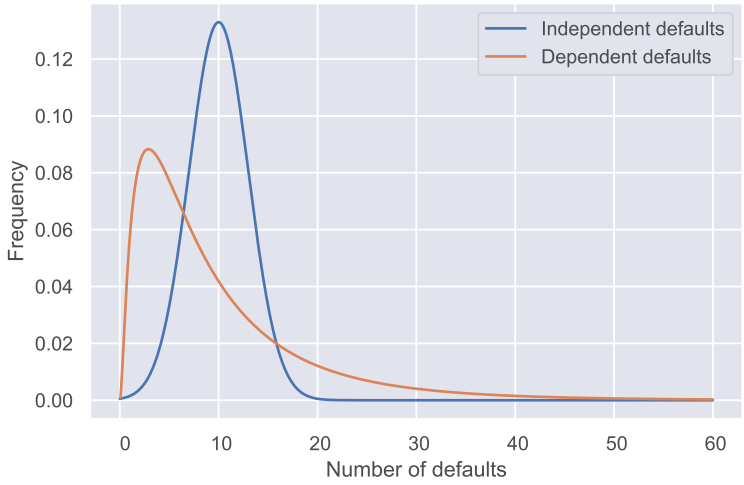

Figure 1.4: The figure shows the loss distributions for two homogeneous portfolios consisting of one thousand issuers with probability of default equal to 0.01. The blue line represents the distribution of defaults when independence is assumed, while the distribution represented by the orange line is generated using the Asymptotic Single Risk Factor Model ([24]) and assuming a correlation of 0.1. It can be seen that even when relatively low correlation is introduced, the impact on losses can be dramatic.

their management is therefore straightforward. Banks typically cover expected losses with provisions in their balance sheet. The focus of risk managers is mainly on losses that exceed EL, as these pose a serious threat to capital. To determine how much capital is required to cover UL, usually a risk measure is applied to the loss distribution obtained using a credit risk model. The focus is on risk measure relating to the tail of the loss distribution such as Value-at-Risk (VaR). VaR at a confidence level α is defined in such a way such that the probability of a loss greater than VaR is at most α while the probability of a loss less than VaR is at least $1-\alpha$. In other words, VaR at a confidence level α can be seen as the $(1-\alpha)$-quantile of the loss distribution. Figure 1.3 provides a visual representation of EL and UL for a stylised loss distribution.

A major concern in credit risk management is the occurrence of disproportionately many defaults of different issuers in a particular period of time. As a result, the dependence structure of the default events is a major issue in credit risk management. The impact of default dependence in a loss distribution for a credit portfolio is critical. In particular, increasing dependence is reflected in the loss distribution by a shift of the distribution to the left and a longer right tail. This is illustrated by Figure 1.4, where the loss distribution of a homogeneous portfolio consisting of one thousand independent issuers is compared to the loss distribution of an otherwise similar portfolio where there is dependence between defaults. As a result, modelling default dependence is a key issue.

It is important to note are two distinct sources of dependence between defaults. On the one hand, performance of different issuers depends on certain common underlying factors, such as interest rates or economic growth. These factors drive the evolution of a company's financial success, which is measured in terms of its rating class or the

probability of default. On the other hand, default of an issuer may, too, have a direct impact on the probability of default of a second dependent issuer, a phenomenon known as contagion. Through contagion, economic distress initially affecting only one issuer can spread to a significant part of the portfolio or even the entire system. An example of such a transmission of pressure is the Russian crisis of 1998-1999 which saw the defaults of corporate and sub-sovereign issuers heavily clustered following the sovereign default [25].

1.3. Challenges that we attempt to tackle

The techniques and tools developed in this thesis go beyond current practice and address some of the key challenges in risk management that have been raised repeatedly by critics. In the following we elaborate on these issues, as they where outlined by McNeil, Frey, and Embrechts [20].

Extremes matter. A paramount challenge in risk management is the need to handle unexpected, abnormal or extreme outcomes, rather than the expected, normal or average outcomes in contrast with many traditional applications. In financial markets, as in other complex systems, extreme values occur much more frequently than what normal models would suggest. This is in line with the view expressed by the former Chair of the Federal Reserve of the United States, Alan Greenspan, during the Joint Central Bank Research Conference in 1995:

> From the point of view of the risk manager, inappropriate use of the normal distribution can lead to an understatement of risk, which must be balanced against the significant advantage of simplification. From the central bank's corner, the consequences are even more serious because we often need to concentrate on the left tail of the distribution in formulating lender-of-last-resort policies. Improving the characterisation of the distribution of extreme values is of paramount importance.

More than a decade after Greenspan, Lord Turner expressed a similar view in his review of the global banking crisis [2]:

> Price movements during the crisis have often been of a size whose probability was calculated by models (even using longer term inputs) to be almost infinitesimally small. This suggests that the models systematically underestimated the chances of small probability high impact events. Models frequently assume that the full distribution of possible events, from which the observed price movements are assumed to be a random sample, is normal in shape. But there is no clearly robust justification for this assumption and it is possible that financial market movements are inherently characterised by fat-tail distributions.

The largest part of this thesis is dedicated to the development of models that depart from the Gaussian framework and account for phenomena such as heavy tails, volatility, and extreme values. This effort is taking place whether the concern is the distribution of

individual risk factors for counterparty credit risk or the distribution of losses in a credit portfolio.

The interdependence of risks. Another major challenge is introduced by the multivariate nature of risk. In general, we are concerned about some expression of total risk that is dependent on high-dimensional vectors of underlying risk factors such as individual credit spreads or counterparty default indicators. In this multivariate modelling set-up, what presents a particular challenge is the ability to accommodate for situations where extreme outcomes are dependent. In other words, it is essential to account for scenarios where many of these factors move against us concurrently, for instance multiple issuers default at a given period of time. In connection to this the below quote is found in Business Week, September 1998.

> Extreme, synchronised rises and falls in financial markets occur infrequently but they do occur. The problem with the models is that they did not assign a high enough chance of occurrence to the scenario in which many things go wrong at the same time – the "perfect storm" scenario.

State-of-the-art models used in industry assume a Gaussian dependence structure which underestimates the probability of joint large movements of risk factors. This underestimation may have tremendous implications for the performance of risk-management. Practitioners have considered alternative copulas with more extreme tail-dependence in order to obtain more heavy-tailed loss distributions. In this case however, the joint distribution is defined a priori by the choice of the copula function. In this thesis we argue that instead of considering an alternative copula, it is necessary to consider an entirely different channel of dependence known as contagion and view portfolios as networks.

More than a decade ago, in his speech "Why banks failed the stress-test", Bank of England banker Andrew G. Haldane expressed the view that regulatory requirements need to adjust for network considerations:

> Any asset portfolio is, in essence, a financial network. So the balance sheet of a large financial institution is a network, with nodes defined by the assets and links defined by the correlations among those assets. The financial system is similarly a network, with nodes defined by the financial institutions and links defined by the financial interconnections between these institutions. Evaluating risk within these networks is a complex science; indeed, it is the science of complexity. When assessing nodal risk, it is not enough to know your counterparty; you need to know your counterparty's counterparty too. In other words, there are network externalities.
>
> In financial networks, these externalities are often referred to as contagion or spillovers. There have been many examples of such spillover during this crisis, with Lehman Brothers' failure a particularly painful one. That is why there have been recent calls to calibrate regulatory requirements to these risk externalities.

The network externalities mentioned by Haldane were also identified as one of the reasons that contributed to the global financial crisis by Lord Turner:

> The models used implicitly assume that the actions of the individual firm, reacting to market price movements, are both sufficiently small in scale as not themselves to affect the market equilibriums, and independent of the actions of other firms. But this is a deeply misleading assumption if it is possible that developments in markets will induce similar and simultaneous behaviour by numerous players.

Today, more than a decade after the crisis, little progress has been made in incorporating network effects in models for capital calculations.

The problem of scale. A further important challenge is the scale of the considered portfolios. In many cases, it is likely that the considered portfolios contain the entire position of a bank in credit-risky instruments. This renders the calibration of comprehensive models for all the considered risk factors nearly impossible with dimension reduction the only plausible approach. In order to achieve this dimension reduction, one must be able to identify the key risk drivers in an efficient manner and focus on modelling these.

In other words, an across-the-board approach needs to be adopted. In the context of portfolio credit risk models, the interest lies in capturing the dependence between defaults rather than identifying the mechanism by which each individual default takes place. It is common practice to start from financial return time-series and attempt to calibrate a parsimonious factor model which captures the same dependence structure. These factors, however, in most industry models are not statistical but rather assigned by economic arguments such as geography and industry sector. This raises the question of how much confidence can be placed in the model parameters derived in such a way and how confident can one be on the weight of the systematic risk component, i.e. the risk influencing all issuers. In other model specifications, statistical factors are derived using principal component analysis (PCA), a dimensionality reduction technique. However, PCA does not directly address the objective of identifying certain unobservable factors accounting for the correlation structure between the observed variables; at best, it provides an approximation to the required factors ([26, Section 7.3]). In this thesis, we use the community structure of the credit market to obtain representative factors that capture dependencies beyond the standard industry sector and geographic region factor specifications.

1.4. Outline of the thesis

In Chapter 2 the main focus in on the challenge presented by the presence of extreme outcomes in the evolution of foreign exchange rates which are among the most important risk factors for counterparty exposure. The widely used Geometric Brownian Motion (GBM) is not able to capture stylised facts of financial time series such as volatility clustering and heavy-tailedness in the returns distribution. Instead of using a process with jumps or stochastic volatility for the modelling of exchange rates, we propose a data-driven approach where the volatility and drift are able to switch between regimes, more specifically they are governed by an unobservable Markov chain. Hence, exchange rates are modelled as a hidden Markov models (HMMs) and scenarios for counterparty exposure are generated using this approach. Backtesting results are presented for a number

of exchange rates. The use of a regime-switching model is found to have a significant impact on capital for derivatives with non-linear payoff.

Chapters 3 and 4 are concerned with the challenge presented by the interdependence of risks. Chapter 3 presents a portfolio credit risk model that can account for default contagion. State-of-the-art portfolio credit risk models assume that dependence between defaults is fully captured by dependence on common underlying factors. This assumption however has been questioned repeatedly in light of empirical evidence. As a result, practitioners have traditionally relied on models with alternative copulas with more extreme tail dependence or stressed correlations. A different approach is adopted here; systematic risk factors are augmented with a contagious default mechanism which affects the entire universe of credits. Stress propagation networks are constructed using real credit spread data in order to estimate contagion effects. The resulting framework is implemented on synthetic tests portfolios and the contagion effect is shown to increase markedly the capital required to cover unexpected losses.

Chapter 4 extends the work presented in Chapter 3 by using Bayesian network methods to uncover the direct and indirect relationships between issuers and estimate contagion effects. A range of techniques to learn the structure and parameters of financial networks from real credit default swaps data are studied and evaluated. The methods are demonstrated in detail in a stylised portfolio and the impact on standard risk metrics is estimated. The impact on capital is found to be in line with the results of Chapter 3.

The mesoscale structure of the credit market is studied in Chapter 5, where the main challenge addressed is the problem of scale. With credit default swap time-series data as a starting point, a principled community detection technique for correlation matrices is used to resolve the market community structure. The communities identified have similarities that cannot be traced back to the standard “industry sector” or “geographic region” taxonomies. The obtained groups are used as factors for capturing the dependence structure in a model for capitalising risk from trading activities.

The results of the work presented in this thesis are summarised and discussed in Chapter 6

2

Risk factor evolution for counterparty credit risk under a hidden Markov model

One of the key components of counterparty credit risk (CCR) measurement is generating scenarios for the evolution of the underlying risk factors such as interest and exchange rates, equity and commodity prices, and credit spreads. The geometric Brownian motion (GBM) is a widely used method for modelling the evolution of exchange rates. An important limitation of the GBM is that, due to the assumption of constant drift and volatility, stylised facts of financial time series such as volatility clustering and heavy-tailedness in the returns distribution cannot be captured. We propose a model where the volatility and drift are able to switch between regimes, more specifically they are governed by an unobservable Markov chain. Hence, we model exchange rates as a hidden Markov models (HMMs) and generate scenarios for counterparty exposure using this approach. A numerical study is carried out and backtesting results for a number of exchange rates are presented. The impact of using a regime-switching model on counterparty exposure is found to be profound for derivatives with non-linear payoff.

2.1. Introduction

One of the main factors that amplified the financial crisis of 2007–2008 was the failure to capture major risks associated with over-the-counter (OTC) derivative-related exposures [27]. Counterparty exposure, at any future time, is the amount that would be lost in the event that a counterparty to a derivative transaction would default, assuming zero recovery at that time. Banks are required to hold regulatory capital against their current and future exposures to all counterparties in OTC derivative transactions.

A key component of the counterparty exposure framework is modelling the evolution

Parts of this chapter have been published in Risks **7**, 66 (2019) [P1]

of underlying risk factors, such as interest and exchange rates, equity and commodity prices, and credit spreads. Risk Factor Evolution (RFE) models are, arguably, the most important part of counterparty exposure modelling, since small changes in the underlying risk factors may have a profound impact on the exposure and, as a result, on the regulatory and economic capital buffers. It is, therefore, crucial for financial institutions to put significant effort in the design and calibration of RFE models and, in addition, have a sound framework in place in order to assess the forecasting capability of the model.

Although the Basel Committee on Banking Supervision has stressed the importance of the ongoing validation of internal models method (IMM) for counterparty exposure [28], there are no strict guidelines on the specifics of this validation process. As a result, there is some degree of ambiguity regarding the regulatory requirements that financial institutions are expected to meet. In an attempt to reduce this ambiguity, [29] introduced a complete framework for counterparty credit risk (CCR) model backtesting which is compliant with Basel III and the new Capital Requirements Directives (CRD IV). A detailed backtesting framework for CCR models was also introduced by [30], who expanded the corresponding framework for Value-at-Risk (VaR) models by the Basel Committee [31].

The most ubiquitous model for the evolution of exchange rates is the geometric Brownian motion (GBM). Under GBM, the exchange rate dynamics are assumed to follow a continuous-time stochastic process, in which the returns are log-normally distributed. Although simplicity and tractability render GBM a particularly popular modelling choice, it is generally accepted that it cannot adequately describe the empirical facts exhibited by real exchange rate returns [32]. More specifically, exchange rate returns can be leptokurtic, exhibiting tails that exceed those of the normal distribution. As a result, a scenario-generation framework based on GBM may assign unrealistically low probabilities to extreme scenarios, leading to the under-estimation of counterparty exposure and, consequently, regulatory and economic capital buffers.

The main reason for the inability of GBM to produce return distributions with realistically heavy tails is the assumption of constant drift and volatility parameters. In this chapter, we present a way to address this limitation without entirely departing from the convenient GBM framework. We propose a model where the GBM parameters are allowed to switch between different states, governed by an unobservable Markov process. Thus, we model exchange rates with a hidden Markov model (HMM) and generate scenarios for counterparty exposure using this approach.

A HMM is a mathematical model in which the system being modelled is assumed to follow a Markov chain whose states are hidden from the observer. HMMs have a broad range of applications, in speech recognition [33], computational biology [34], gesture recognition [35], and in other areas of artificial intelligence and pattern recognition [36]. HMMs have gained significant popularity in the mathematical and computational finance fields. The application of HMMs in financial and economic time-series was pioneered by Hamilton in Hamilton (1988, 1989). Since then, a significant amount of literature has been published, focusing on the ability of HMMs to reproduce stylised facts of asset returns [39–41], asset allocation [42–44], and option pricing [45–47].

Our work expands the counterparty exposure literature by introducing a hidden Markov model for the evolution of exchange rates. We provide a detailed description

of HMMs and their estimation process. In our numerical experiments, we use GBM and HMM to generate scenarios for the Euro against two major and two emerging currencies. We perform a thorough backtesting exercise, based on the framework proposed by [30], and find similar performances for GBM and a two-state HMM. Finally, we use the generated scenarios to calculate credit exposure for foreign exchange (FX) options, and find significant differences between the two models, which are even more pronounced for deep out-of-the-money instruments.

The remainder of the chapter is organised as follows. Section 2.2 provides the fundamentals of HMMs, along with the algorithms for determining their parameters from data. Section 2.3 gives background information on modelling the evolution of exchange rates. Section 2.4 outlines the framework for performance evaluation of RFE models. A numerical study is presented in Section 2.5. Finally, in Section 2.6, we draw conclusions and discuss future research directions.

2.2. An introduction to hidden Markov models

The hidden Markov model (HMM) is a statistical model in which a sequence of observations is generated by a sequence of unobserved states. The hidden state transitions are assumed to follow a first-order Markov chain. The theory of hidden Markov models (HMMs) originates from the work of Baum et al. in the late 1960s ([48], [49]). In the rest of this section, we introduce the theory of hidden Markov models (HMMs), following [50].

2.2.1. Formal definition of an HMM

In order to formally define a hidden Markov model (HMM), the following elements are required:

1. N, the number of hidden states. Even though the states are not directly observed, in many practical applications they have some physical interpretation. For instance, in financial time-series, hidden states may correspond to different phases of the business cycle, such as prosperity and depression. We denote the states by $X = \{X_1, X_2, ..., X_N\}$, and the state at time t by q_t.

2. M, the number of distinct observation symbols per state. These symbols represent the physical output of the system being modelled. The individual symbols are denoted by $V = \{v_l, v_2, ..., v_M\}$.

3. The transition probability distribution between hidden states, $A = \{a_{ij}\}$, where

$$a_{ij} = P\left[q_{t+i} = X_j | q_t = X_i\right], \qquad 1 \leq i, j \leq N. \tag{2.1}$$

4. The observation symbol probability distribution in state j, $B = \{b_j(k)\}$, where

$$b_j(k) = P\left[v_k \text{ at } t | q_t = X_j\right], \qquad 1 \leq j \leq N, 1 \leq k \leq M. \tag{2.2}$$

5. The initial distribution of the hidden states, $\pi = \{\pi_i\}$, where

$$\pi_i = P\left[q_1 = X_i\right], \qquad 1 \leq i \leq N. \tag{2.3}$$

The parameter set of the model is denoted by $\lambda = (A, B, \pi)$. A graphical representation of a hidden Markov model with two states and three discrete observations is given by Figure 2.1.

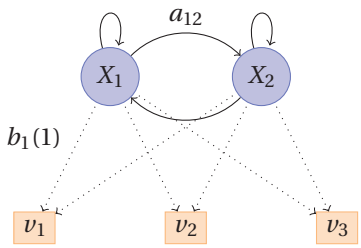

Figure 2.1: A hidden Markov model (HMM) with two states and three discrete observations, where a_{ij} is the probability of transition from state X_i to state X_j and $b_j(k)$ is the emission probability for symbol v_k in state X_j.

In the case where there are an infinite amount of symbols for each hidden state, v_k is omitted and the observation probability $b_j(k)$, conditional on the hidden state X_j, can be replaced by

$$b_j(O_t) = P(O_t|q_t = X_j).$$

If the observation symbol probability distributions are Gaussian, then

$$b_j(O_t) = \phi(O_t|u_j, \sigma_j), \tag{2.4}$$

where $\phi(\cdot)$ is the Gaussian probability density function, and u_j and σ_j are the mean and standard deviation of the corresponding state X_j, respectively. In that case, the parameter set of the model is $\lambda = (A, u, \sigma, \pi)$, where u and σ are vectors of means and standard deviations, respectively.

2.2.2. The three basic problems for HMMs

The idea that HMMs should be characterised by three fundamental problems originates from the seminal paper of Rabiner [50]. These three problems are the following:

Problem 1 (Likelihood). Given the observation sequence $O = O_1 O_2 ... O_T$ and a model $\lambda = (A, B, \pi)$, how do we compute the conditional probability $P(O|\lambda)$ in an efficient manner?

Problem 2 (Decoding). Given the observation sequence $O = O_1 O_2 ... O_T$ and a model λ, how do we determine the state sequence $Q = q_1 q_2 ... q_T$ which optimally explains the observations?

Problem 3 (Learning). How do we select model parameters $\lambda = (A, B, \pi)$ that maximise $P(O|\lambda)$?

2.2.3. Solutions to the three basic problems

Likelihood

Our objective is to calculate the likelihood of a particular observation sequence, $O = O_1 O_2 \cdots O_T$, given the model λ. The most intuitive way of doing this is by summing the joint probability of O and Q for all possible state sequences Q of length T:

$$P(O|\lambda) = \sum_{\text{all } Q} P(O|Q,\lambda) \cdot P(Q|\lambda). \tag{2.5}$$

The probability of a particular observation sequence O, given a state sequence $Q = q_1 q_2 \cdots q_T$, is

$$\begin{aligned} P(O|Q,\lambda) &= \prod_{t=1}^{T} P(O_t|q_t,\lambda) \\ &= b_{q_1}(O_1) \cdot b_{q_2}(O_2) \cdots b_{q_T}(O_T), \end{aligned} \tag{2.6}$$

as we have assumed that the observations are independent. The probability of a state sequence Q can be written as

$$P(Q|\lambda) = \pi_{q_1} a_{q_1 q_2} a_{q_2 q_3} \cdots a_{q_{T-1} q_T}. \tag{2.7}$$

The joint probability of O and Q is the product of the above two terms; that is,

$$P(O,Q|\lambda) = P(O|Q,\lambda) \cdot P(Q|\lambda). \tag{2.8}$$

Although the calculation of $P(O|\lambda)$ using the above definition is rather straightforward, the associated computational cost is huge.

Thankfully, a dynamic programming approach, called the Forward Algorithm, can be used instead.

Consider the forward variable $\alpha_i(t)$, defined as

$$\alpha_t(i) = P(O_1 O_2 \cdots O_t, q_t = X_i|\lambda). \tag{2.9}$$

We can solve for $\alpha_t(i)$ inductively using Algorithm 1.

Algorithm 1 The Forward Algorithm

1. Initialisation:

$$\alpha_1(i) = \pi_i b_i(O_1), \qquad 1 \le i \le N. \tag{2.10}$$

2. Induction:

$$\alpha_{t+1}(j) = \left[\sum_{i=1}^{N} \alpha_t(i) a_{ij}\right] b_j(O_{t+1}), \qquad \begin{aligned} 1 &\le t \le T-1 \\ 1 &\le j \le N. \end{aligned} \tag{2.11}$$

3. Termination:

$$P(O|\lambda) = \sum_{i=1}^{N} \alpha_T(i). \tag{2.12}$$

Correspondingly, we can define a backward variable $\beta_t(i)$ as

$$\beta_t(i) = P(O_{t+1} O_{t+2} \cdots O_T | q_t = X_i, \lambda). \tag{2.13}$$

Again, we can solve for $\beta_t(i)$ inductively using Algorithm 2.

Algorithm 2 The Backward Algorithm

1. Initialisation:

$$\beta_T(i) = 1, \qquad 1 \le i \le N. \tag{2.14}$$

2. Induction:

$$\beta_t(i) = \sum_{j=1}^{N} a_{ij}\, b_j(O_{t+1}) \beta_{t+1}(j), \qquad \begin{aligned} t &= T-1, T-2, ..., 1 \\ 1 &\le i \le N. \end{aligned} \tag{2.15}$$

Decoding
In order to identify the best sequence $Q = \{q_1 q_2 \cdots q_T\}$ for the given observation sequence $O = \{O_1 O_2 \cdots O_T\}$, we need to define the quantity

$$\delta_t(i) = \max_{q_1, q_2, ..., q_{t-1}} P(q_1 q_2 \cdots q_t = i, O_1 O_2 \cdots O_t | \lambda). \tag{2.16}$$

By induction, we have

$$\delta_{t+1}(j) = \left[\max_i \delta_t(i) a_{ij}\right] \cdot b_j(O_{t+1}). \tag{2.17}$$

To actually retrieve the state sequence, it is necessary to keep track of the argument which maximises Equation 2.17, for each t and j. We do so via the array $\psi_t(j)$. The complete procedure for finding the best state sequence is presented in Algorithm 3.

Algorithm 3 Viterbi algorithm

1. Initialisation:

$$\begin{aligned} \delta_1(i) &= \pi_i b_i(O_1), \qquad 1 \le i \le N \quad (2.18) \\ \psi_1(i) &= 0. \quad (2.19) \end{aligned}$$

2. Recursion:

$$\begin{aligned} \delta_t(j) &= \max_{1\le i\le N} \left[\delta_{t-1}(i)a_{ij}\right] b_j(O_t), \qquad 2 \le t \le T \\ & \qquad\qquad 1 \le j \le N \quad (2.20) \\ \psi_t(j) &= \arg\max_{1\le i\le N} \left[\delta_{t-1}(i)a_{ij}\right] \qquad 2 \le t \le T \\ & \qquad\qquad 1 \le j \le N. \quad (2.21) \end{aligned}$$

3. Termination:

$$\begin{aligned} P^* &= \max_{1\le i\le N} [\delta_T(i)] \\ q_T^* &= \arg\min_{1\le i\le N} [\delta_T(i)]. \quad (2.22) \end{aligned}$$

4. Sequence back-tracking:

$$q_t^* = \psi_{t+1}(q_{t+1}^*), \qquad t = T-1, T-2, \cdots, 1. \quad (2.23)$$

Learning

The model which maximises the probability of an observation sequence O, given a model $\lambda = (A, B, \pi)$, cannot be determined analytically. However, a local maximum can be found using an iterative algorithm, such as the Baum-Welch method or the expectation-maximization (EM) method [51]. In order to describe the iterative procedure of obtaining the HMM parameters, we need to define $\xi_t(i, j)$, the probability of being at the state X_i at time t, and the state X_j at time $t+1$, given the model and observation sequence; that is,

$$\xi_t(i, j) = P(q_t = X_i, q_{t+1} = X_j | O, \lambda). \quad (2.24)$$

Using the earlier defined forward and backward variables, $\xi_t(i, j)$ can be rewritten as

$$\xi_t(i, j) = \frac{\alpha_t(i)a_{ij}b_j(O_{t+1})\beta_{t+1}(j)}{P(O|\lambda)}. \quad (2.25)$$

We define

$$\gamma_t(i) = \sum_{j=i}^{N} \xi_t(i,j) \tag{2.26}$$

as the probability of being in state X_i at time t. It is clear that

$$\sum_{t=i}^{T-1} \gamma_t(i) = \text{expected number of transitions from } X_i, \text{ and} \tag{2.27}$$

$$\sum_{t=i}^{T-1} \xi_t(i,j) = \text{expected number of transitions from } X_i \text{ to } X_j. \tag{2.28}$$

Using these formulas, the parameters of a HMM can be estimated, in an iterative manner, as follows:

$$\hat{\pi}_i = \gamma_1(i) = \text{expected number of times in state } X_i \text{ at time } t = 1; \tag{2.29}$$

$$\begin{aligned} \hat{a}_{ij} &= \frac{\sum_{t=i}^{T-1} \xi_t(i,j)}{\sum_{t=i}^{T-1} \gamma_t(i)} \\ &= \frac{\text{expected number of transitions from } X_i \text{ to } X_j}{\text{expected number of transitions from } X_i}; \end{aligned} \tag{2.30}$$

$$\begin{aligned} \hat{b}_j(k) &= \frac{\sum_{t=1}^{T} \mathbf{1}_{\{O_t = v_k\}} \gamma_t(j)}{\sum_{t=1}^{T} \gamma_t(j)} \\ &= \frac{\text{expected number of times in state } j \text{ and observing symbol } v_k}{\text{expected number of times in state } j}. \end{aligned} \tag{2.31}$$

If $\lambda = (A, B, \pi)$ is the current model and $\hat{\lambda} = (\hat{A}, \hat{B}, \hat{\pi})$ is the re-estimated one, then it has been shown, by [48, 49], that $P(O|\hat{\lambda}) \geq P(O|\lambda)$.

In case the observation probabilities are Gaussian, the following formulas are used to update the model parameters u and σ:

$$\hat{u}_j = \frac{\sum_{t=1}^{T} \gamma_t(j) O_t}{\sum_{t=1}^{T} \gamma_t(j)}, \tag{2.32}$$

$$\hat{\sigma}_j = \sqrt{\frac{\sum_{t=1}^{T} \gamma_t(j)(O_t - u_j)^2}{\sum_{t=1}^{T} \gamma_t(j)}}. \tag{2.33}$$

2.3. Modelling the evolution of exchange rates

As discussed in the introduction, the first step in calculating the future distribution of counterparty exposure is the generation of scenarios using the models that represent the evolution of the underlying market factors. These factors typically include interest and exchange rates, equity and commodity prices, and credit spreads. This chapter is concerned with the modelling of exchange rates.

2.3.1. Geometric Brownian motion

In mathematical finance, the geometric Brownian motion (GBM) model is the stochastic process which is usually assumed for the evolution of stock prices [22]. Due to its simplicity and tractability, GBM is also a widely used model for the evolution of exchange rates.

A stochastic process, S_t, is said to follow a GBM if it satisfies the following stochastic differential equation:

$$dS_t = \mu S_t dt + \sigma S_t dW_t, \tag{2.34}$$

where W_t is a Wiener process, and μ and σ are constants representing the drift and volatility, respectively.

The analytical solution of Equation (2.34) is given by:

$$S_t = S_0 \exp\left(\left(\mu - \frac{\sigma^2}{2}\right)t + \sigma W_t\right). \tag{2.35}$$

With this expression in hand, and knowing that $W_t \sim N(0,t)$, one can generate scenarios simply by generating standard normal random numbers.

2.3.2. A hidden Markov model for drift and volatility

One of the main shortcomings of the GBM model is that, due to the assumption of constant drift and volatility, some important characteristics of financial time-series, such as volatility clustering and heavy-tailedness in the return distribution, cannot be captured. To address these limitations, we consider a model with an additional stochastic process. The observations of the exchange rates are assumed to be generated by a discretised GBM, in which both the drift and volatility parameters are able to switch, according to the state of an unobservable process which satisfies the Markov property. In other words, the conditional probability distribution of future states depends solely upon the current state, not on the sequence of states that preceded it. The observations also satisfy a Markov property with respect to the states (i.e., given the current state, they are independent of the history).

Thus, we consider a hidden Markov model with Gaussian emissions $\lambda = (A, u, \sigma, \pi)$, as was presented in Section 2.2.1. We denote the hidden states by $X = \{X_1, X_2, ..., X_N\}$, and the state at time t as q_t. The unobservable Markov process governs the distribution of the log-return process $Y = \{Y_2, ..., Y_T\}$, where $Y_t = \log \frac{S_t}{S_{t-1}}$, $t = 2, ..., T$. The dynamics of Y are then as follows:

$$Y_t = u(q_t) + \sigma(q_t) Z_t, \tag{2.36}$$

where $u(q_t) = \left(\mu(q_t) - \frac{\sigma^2(q_t)}{2}\right)$ and $Z_t \sim N(0,1)$ are independent standard normal random numbers.

The transition probabilities of the hidden process, as well as the drift and volatility of the GBM, can be estimated from a series of observations, using the algorithms presented in Section 2.2. The number of hidden states has to be specified in advance. In many practical applications, the number of hidden states can be determined based on intuition. For example, stock markets are often characterised as "bull" or "bear", based on whether they are appreciating or depreciating in value. A bull market occurs when returns are positive and volatility is low. On the other hand, a bear market occurs when returns are negative and volatility is high. It would, therefore, be in line with intuition to assume that stock market observations are driven by a two-state process. The number of states can also be determined empirically; for example, using the Akaike information criterion (AIC) or the Bayesian information criterion (BIC). Once the model parameters have been estimated, scenarios can be generated by generating the hidden Markov chain and sampling the log-returns from the corresponding distributions.

2.4. RFE model performance evaluation

2.4.1. Backtesting

In this sub-section, we give a brief overview of a framework for the backtesting of RFE models. For a more detailed description, the reader is referred to [30]. Backtesting is the process of comparing the distributions given by the RFE models with the realised history of the corresponding risk factors. In accordance with regulatory requirements, RFE models have to be backtested at multiple forecasting horizons, making use of various distributional tests [28].

To test whether a set of realisations can reasonably be modelled as arising from a specific distribution, we use the Probability Integral Transform (PIT) (see [52]), defined as

$$F(x_n) = \int_{-\infty}^{x_n} f(u)\,du, \tag{2.37}$$

where x_n is the realisation of a random variable and $f(\cdot)$ is its predicted density. Note that, if one applies PIT using the true density of x_n to construct a set of values, it follows that the distribution of the constructed set will simply be $\mathcal{U}(0,1)$. As a result, one is able to evaluate the quality of the model $f(\cdot)$ for x_n, simply by measuring the distance between the distribution of the constructed set and $\mathcal{U}(0,1)$.

For a given set of realisations x_{t_i} of the risk factor to be tested, we set a starting point t_{start} and an ending point t_{end}. The size of the backtesting window is then $T_b = t_{end} - t_{start}$. If the time horizon over which we want to test our model is Δ, we proceed as follows:

1. We set $t_1 = t_{start}$. We, then, calculate the PIT $F(x_{t_1+\Delta})$ of the realised value at $t_1 + \Delta$ using the model risk factor distribution for that point. If an analytical expression is not available, the distribution can be approximated numerically. This yields a value F_1.

2. We, then, move forward to $t_2 = t_1 + \Delta$. We calculate $F(x_{t_2+\Delta})$ using the model risk factor distribution at $t_2 + \Delta$ and obtain a value F_2.

3. We repeat the above, until $t_i + \Delta = t_{end}$.

This exercise yields a set $\{F_i\}_{i=1}^{K}$, where K is the number of steps taken. As mentioned previously, if the empirical distribution of the realisations is the same as the predicted distribution, then the constructed set $\{F_i\}_{i=1}^{K}$ will be uniformly distributed.

In order to measure the distance d between the distribution of the constructed set and $\mathscr{U}(0,1)$ we can use a number of metrics, such as:

The Anderson–Darling metric:

$$\begin{aligned} d_{AD} &= \int_{-\infty}^{\infty} (F_e(x) - F(x))^2 \, \omega(F(x)) \, dF(x) \\ \omega(x) &= \frac{1}{x(1-x)}, \end{aligned} \tag{2.38}$$

the Cramer–von Mises metric:

$$\begin{aligned} d_{CVM} &= \int_{-\infty}^{\infty} (F_e(x) - F(x))^2 \, \omega(F(x)) \, dF(x) \\ \omega(x) &= 1, \text{ or} \end{aligned} \tag{2.39}$$

the Kolmogorov–Smirnov metric:

$$d_{KS} = \sup_x |F_e(x) - F(x)|, \tag{2.40}$$

where F_e is the empirical and F is the theoretical cumulative distribution function. Note that each of these metrics provides a single distance value $\tilde{d}$ between the distribution of the realised set and $\mathscr{U}(0,1)$. To obtain an understanding of whether this distance is acceptable, we simulate time-series using the model being tested. Although the simulated time-series will follow the model by definition, there will still be some distance, d, due to numerical noise. By repeating this experiment a sufficiently large number of times (say, M), we can obtain a set $\{d_i\}_{i=1}^{M}$ and approximate, numerically, its cumulative distribution function $\psi(d)$. With $\psi(d)$ in hand, we can assess the distance $\tilde{d}$, as follows: If $\tilde{d}$ falls in a range with high probability with respect to $\psi(d)$, then the probability of the model being accurate is high. By defining d_y and d_r as the 95th and the 99.99th percentiles, respectively, we can obtain three colour bands for model performance:

- Green band: $\tilde{d} \in [0, d_y)$;
- Yellow band: $\tilde{d} \in [d_y, d_r)$; and
- Red band: $\tilde{d} \in [d_r, \infty)$.

An example of the three-colour scoring scheme is shown in Figure 2.2. The backtesting process can be carried out for a set of time horizons, and for every horizon a single result can be produced, in terms of a probability $\psi(\tilde{d})$ and a colour band.

2.4.2. Long-term percentiles of distribution cones

Backtesting provides a statistical judgement of the performance of the model for relatively short-term forecast horizons. Assessing the distribution cones of the risk factor evolution provides insight into the behaviour of the model for long forecast horizons. The high and low percentiles of the distribution cones need to be compared to the long-term percentiles of the observed risk factor data. Please note that assessing the long-term percentiles needs expert judgement to some extent, as it is difficult to statistically unambiguously state what the long-term percentile of a distribution cone should be.

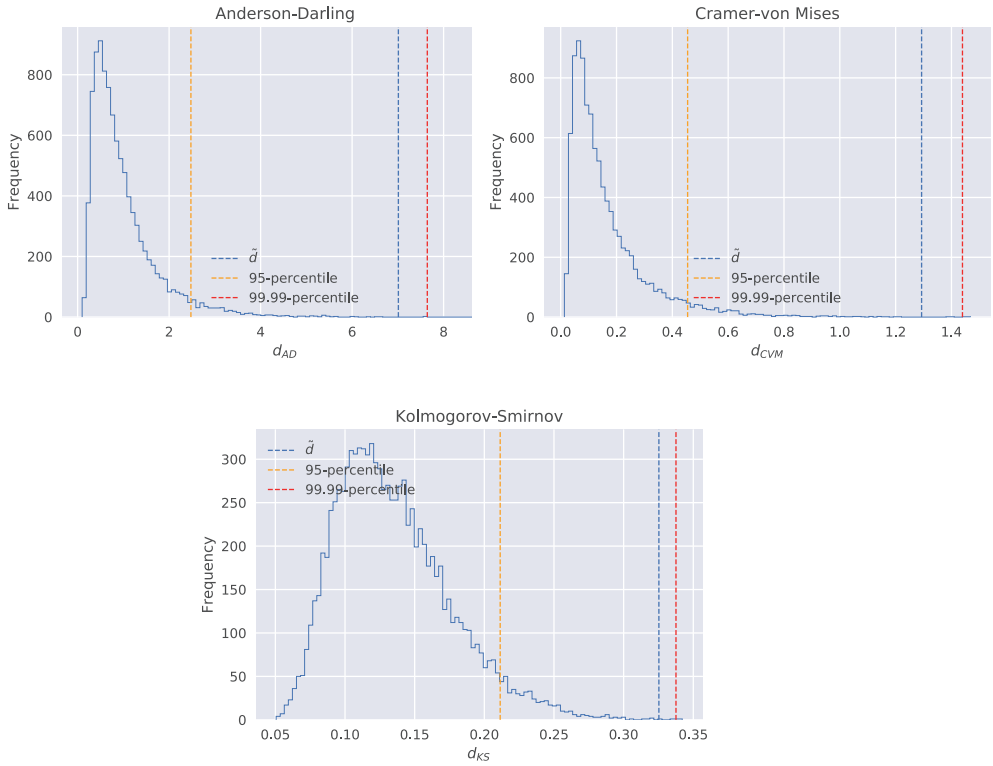

Figure 2.2: Examples of the three-colour scoring scheme. The model in the example receives yellow scores for all three metrics, as $d_y < \tilde{d} < d_r$.

2.5. Numerical experiments

2.5.1. Overview of data selections

In order to evaluate the performance of the HMM approach, we used the foreign exchange rates of the Euro against two G10 and two emerging-market currencies. We used daily observations, between 1 January 2004 and 31 December 2016, for the following FX rates:

- USD/EUR,

- GBP/EUR,
- RUB/EUR, and
- MXN/EUR.

2.5.2. Selection of the number of hidden states

Choosing the appropriate number of hidden states for a HMM is not a trivial task. Two commonly used criteria for model comparison are the Akaike information criterion (AIC):

$$\text{AIC} = -2\log L + 2p, \tag{2.41}$$

and the Bayesian information criterion (BIC):

$$\text{BIC} = -2\log L + p\log T, \tag{2.42}$$

where L is the likelihood of the fitted model, p is the number of free parameters in the model, and T denotes the number of observations [53]. The number of free parameters in a HMM with a Gaussian distribution for each hidden state is:

$$p = N^2 + 2N - 1, \tag{2.43}$$

where N is the number of hidden states. Thus, in both criteria, the second term is a penalty term which increases with increasing N. Compared to the AIC, the penalty term of the BIC has more weight when $T > e^2$ and, therefore, the BIC often favours models with fewer parameters than the AIC does.

A bank that uses internal models to measure exposure for capital purposes must use at least three years of historical data for calibration, where the parameters have to be updated quarterly or more frequently, if market conditions warrant. During the course of backtesting, re-calibration of the RFE model parameters needs to be done at the same frequency as for production to make the re-calibration effects visible [28]. Consequently, in the backtesting exercise that follows (in Section 2.5.3), we use calibration blocks of three years and move the block forward by one quarter every time.

To choose the appropriate number of hidden states, we calibrate HMMs with 2–5 states for each of the three-year blocks and calculate the AIC and BIC. The results are shown in Figures 2.3–2.6. Based on the AIC results, the performance of HMMs with 2, 3, 4, or 5 states is almost the same for the emerging-market currencies. For USD/EUR, models with higher number of hidden states seem to perform better while, for GBP/EUR, the two-state model is preferable. However, based on the BIC, the HMM with two states is the best candidate for all four currency pairs. Therefore, we focus on the HMM with two states for the rest of our numerical experiments.

2.5.3. Model backtesting

We applied the backtesting algorithm (presented in Section 2.4) using observations between 1 January 2004 and 31 December 2016 for the selected FX rates. We used a calibration window T_c of three years with quarterly re-calibration ($\delta_c = 3$ months). The length of the backtesting window was $T_b = 10$ years and we tested model performance for time horizons Δ of length 1 week, 2 weeks, 1 month, and 3 months.

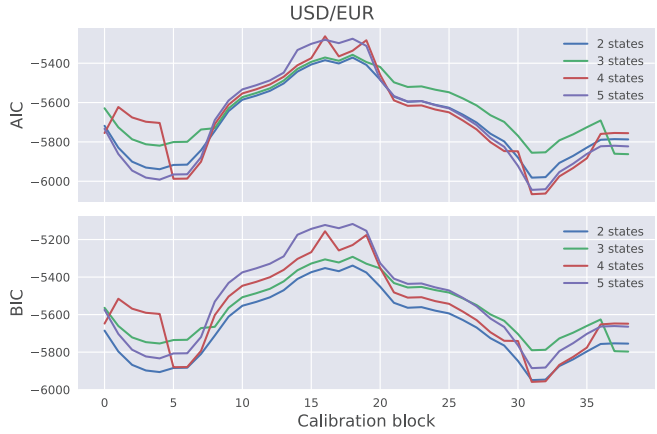

Figure 2.3: AIC and BIC for HMMs calibrated using USD/EUR time series.

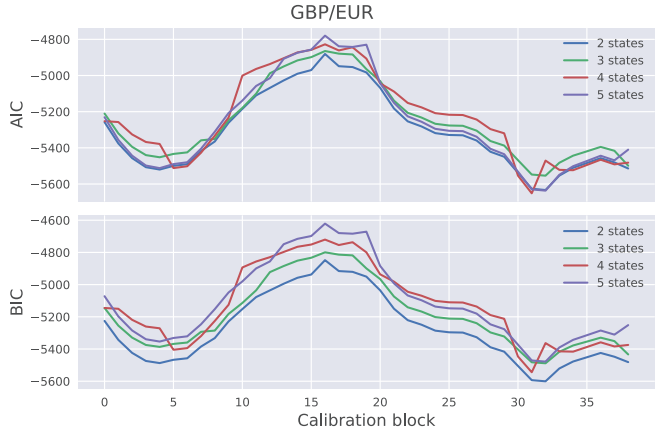

Figure 2.4: AIC and BIC for HMMs calibrated using GBP/EUR time series.

In order to generate scenarios of length Δ, the following steps were taken. At every time point t with $1 \leq t \leq \Delta$ and, given the current hidden state $q_t = X_i$, the next hidden state $q_{t+1} = X_j$ was chosen using the transition probability matrix A. The observation O_t was then generated, according to the corresponding emission probability distribution b_j. The initial hidden state q_0 was assumed to be the most probable state at the end of the learning procedure.

It is important to note that the backtesting procedure provides a statistical assessment of the model performance for relatively short-term forecast horizons. For instance, a backtesting window T_b of 10 years and a time horizon $\Delta = 1$ year would translate to only 10 independent points. As a result, the statistical relevance of the backtesting exercise

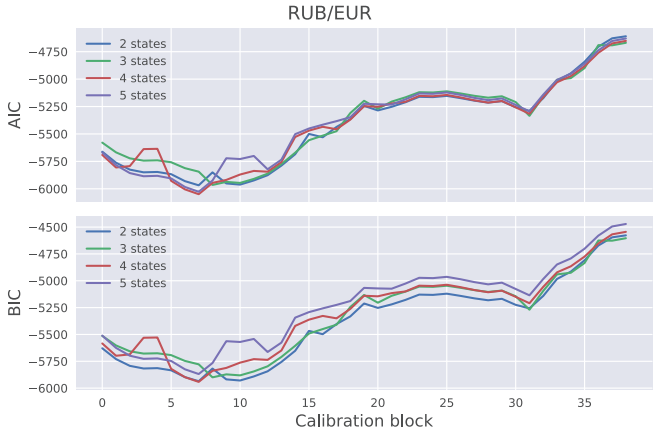

Figure 2.5: AIC and BIC for HMMs calibrated using RUB/EUR time series.

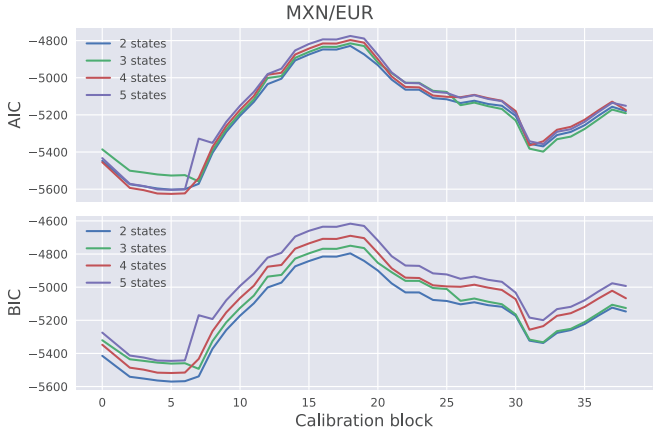

Figure 2.6: AIC and BIC for HMMs calibrated using MXN/EUR time series.

would be limited. In order to gain an insight into model behaviour for longer forecast horizons, we consider the distribution cones of the risk factor evolution. The high and the low percentiles of the distribution cones are compared to observed risk factor data.

In the following, we discuss the results obtained for each of the FX rates.

USD/EUR

Table 2.1 summarises the results of the backtesting exercise for USD/EUR, in terms of probabilities as well as colour bands. When the forecasting horizon was 1 week, both the GBM and the two-state HMM scored yellow under the Anderson–Darling and the Cramer–von Mises metrics, and green under the Kolmogorov–Smirnov metric. For the two-week forecasting horizon, both models obtained a yellow score under all three metrics. Finally,

for the longer horizons (1 and 3 months), both models performed significantly better, with green scores under all metrics. The backtesting results do not indicate any notable difference in performance between the HMM and the GBM.

Table 2.1: Backtesting results for USD/EUR with calibration window $T_c = 3$ years, frequency of re-calibration $\delta_c = 3$ months, and backtesting window $T_b = 10$ years. GBM, geometric Brownian motion.

Time Horizon	GBM			HMM2		
	AD	CVM	KS	AD	CVM	KS
1W	0.9783	0.9709	0.9192	0.9884	0.9846	0.9189
2W	0.9553	0.9507	0.9831	0.9744	0.9662	0.9890
1M	0.4849	0.5829	0.5620	0.6486	0.6957	0.6023
3M	0.3476	0.2130	0.1156	0.6145	0.4968	0.3397

In order to gain an insight into the performance of the models for longer time horizons, we present, in Figure 2.7, the 5th and 95th percentiles of the forecast distributions for a horizon of 7 years, between 2011 and end of 2016. It can be seen that the HMM gave slightly more conservative forecasts, compared to the GBM, but the realised time-series fell within the 90% probability region under both models, at the end of the 7 year period.

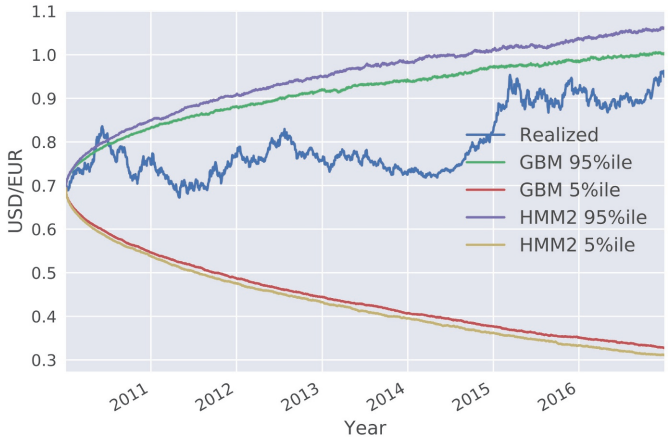

Figure 2.7: Percentiles of long-term distribution cones for USD/EUR under GBM and HMM with two states.

GBP/EUR

The backtesting results for GBP/EUR are summarised in Table 2.2. The two models achieved similar performance when the time horizon was 2 weeks or longer. When the forecasting horizon was 2 weeks, both models scored yellow. In the 1-month horizon, both models had green scores under the Anderson–Darling and Cramer–von Mises metrics, and a yellow score under the Kolmogorov–Smirnov metric. The scores were green for both models under all metrics when the time horizon was 3 months. The greatest difference between the two models was observed for the 1-week forecasting horizon,

where the two-state model performed significantly better, scoring green under all three metrics, while the corresponding scores for GBM were yellow.

Table 2.2: Backtesting results for GBP/EUR with calibration window $T_c = 3$ years, frequency of re-calibration $\delta_c = 3$ months, and backtesting window $T_b = 10$ years.

Time Horizon	GBM			HMM2		
	AD	CVM	KS	AD	CVM	KS
1W	0.9861	0.9816	0.9820	0.8698	0.9280	0.6391
2W	0.9936	0.9919	0.9964	0.9934	0.9920	0.9952
1M	0.9085	0.8965	0.9594	0.9299	0.9140	0.9726
3M	0.8702	0.8273	0.8716	0.8573	0.8014	0.8535

Figure 2.8 shows the 5th and 95th percentiles of the forecast distributions between 2011 and end of 2016. Similarly to the results for USD/EUR, HMM gave slightly more conservative forecasts and the realised time-series fell within the 90% probability region under both models, at the end of the 7 year period. However, in 2016, the realised time-series fell outside the 95th percentile of the GBM distribution, while it was still within this bound for the HMM.

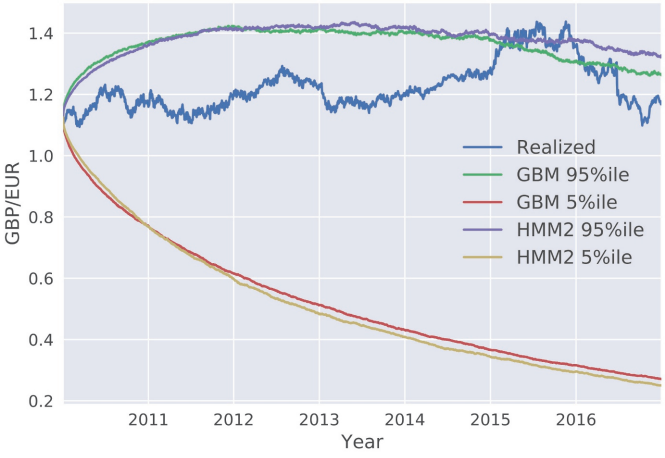

Figure 2.8: Percentiles of long-term distribution cones for GBP/EUR under GBM and HMM with two states.

RUB/EUR

Table 2.3 presents the results of the backtesting exercise for RUB/EUR. It can be seen that both GBM and HMM did not perform very well when the forecasting horizon was 1 week, with HMM having yellow scores under every metric. The results were similar for the 2 week forecasting horizon. In the longer time horizons, however, both models performed better. HMM outperformed the one-state model GBM, achieving green scores in the 1-month horizon. The scores were green for both models when the forecasting horizon was 3 months.

Table 2.3: Backtesting results for RUB/EUR with calibration window $T_c = 3$ years, frequency of re-calibration $\delta_c = 3$ months, and backtesting window $T_b = 10$ years.

Time Horizon	GBM			HMM2		
	AD	CVM	KS	AD	CVM	KS
1W	0.9991	0.9988	0.9988	0.9997	0.9996	0.9996
2W	0.9992	0.9989	0.9992	0.9996	0.9996	0.9988
1M	0.9830	0.9809	0.9446	0.9485	0.9457	0.8898
3M	0.5526	0.1406	0.0651	0.4399	0.3394	0.1624

Figure 2.9 shows the percentiles of the long-term distribution cones for RUB/EUR. It is clear that the difference between GBM and HMM was more pronounced, with the HMM yielding significantly more conservative forecasts. The realised time-series was close to the 95th percentile of the GBM distribution until mid-2014, exceeding it on a number of occasions in 2011 and in 2013. Despite a sharp decline in 2015, the realised time-series remained above the 5th percentile for both models throughout the 7 year period.

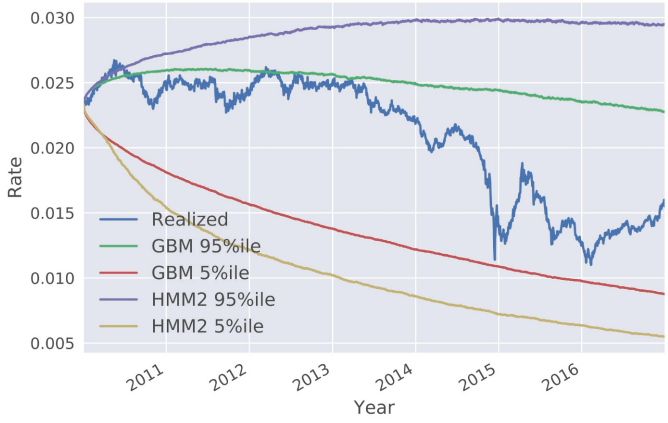

Figure 2.9: Percentiles of long-term distribution cones for RUB/EUR under GBM and HMM with two states.

MXN/EUR

Table 2.4 summarises the results of the backtesting exercise for MXN/EUR, in terms of scores as well as colour bands. Both HMM and GBM had yellow scores for the shorter time horizons (1 and 2 weeks), under all metrics. The models performed better for the longer time horizons (1 and 3 months), achieving green scores. Figure 2.10 shows the long-term distribution cones. Similar to the GBP/EUR case, we do not observe a clear difference in performance between GBM and HMM with two states.

Table 2.4: Backtesting results for MXN/EUR, with a 3-year calibration window, quarterly re-calibration, and a 10-year backtesting window.

Time Horizon	GBM			HMM2		
	AD	CVM	KS	AD	CVM	KS
1W	0.9967	0.9955	0.995	0.9967	0.9956	0.9938
2W	0.9895	0.9864	0.9677	0.9841	0.9768	0.9742
1M	0.5185	0.5963	0.7136	0.5501	0.6071	0.6225
3M	0.7124	0.6643	0.4422	0.7045	0.7373	0.6563

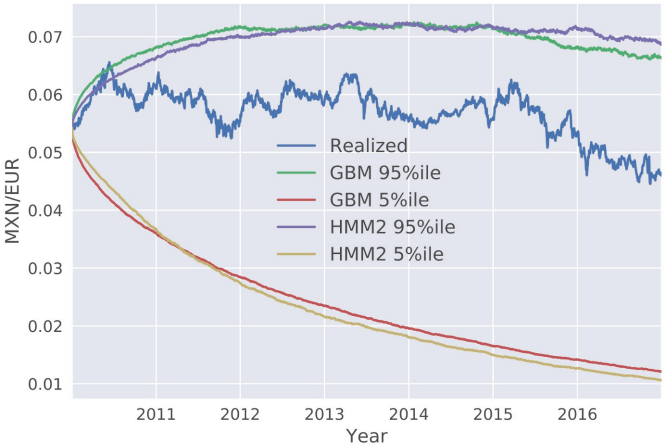

Figure 2.10: Percentiles of long-term distribution cones for MXN/EUR under GBM and HMM with two states.

2.5.4. Impact on credit exposure: a case study for FX options

Exposure at default (EAD)

Prior to presenting the case study on FX options, we provide a brief introduction to credit exposure calculation. For a more detailed description, the reader is referred to [54] and [55].

When a financial institution is permitted to use the IMM to calculate credit exposure, the following steps need to be taken:

1. *Scenario Generation.* Market scenarios are simulated for a fixed set of exposure dates $\{t_k\}_{k=1}^{N}$ in the future, using the RFE models.

2. *Instrument Valuation.* Instrument valuation is performed for each exposure date and for each simulated scenario.

The outcome of this process is a set of realisations of credit exposure at each exposure date in the future. One can then estimate the expected exposure EE_k as the average exposure at future date t_k, where the average is taken across all simulated scenarios of the relevant risk factors.

The Expected Positive Exposure (EPE) is defined as the weighted average of the EE over the first year

$$\text{EPE} = \sum_{k=1}^{\min(1 \text{ year, maturity})} \text{EE}_k \times \Delta t_k, \tag{2.44}$$

where the weights $\Delta_{t_k} = t_k - t_{k-1}$ are the proportion that an individual expected exposure represents over the entire one-year time horizon.

In order to account for potential non-conservative ageing effects, a modification is necessary. First, an Effective EE profile is obtained from the EE profile by adding the non-decreasing constraint for maturities below one year. Effective EE can be calculated, recursively, as follows:

$$\text{Effective EE}_k = \max\{\text{Effective EE}_{k-1}, \text{EE}_k\}, \tag{2.45}$$

where the current date is denoted as t_0 and EE_0 equals the current exposure.

Effective EPE can, then, be calculated from the Effective EE profile, in the same way that EPE is calculated from the EE profile:

$$\text{Effective EPE} = \sum_{k=1}^{\min(1 \text{ year, maturity})} \text{Effective EE}_k \times \Delta t_k. \tag{2.46}$$

Finally, the Exposure at Default (EAD) is the product of a multiplier α and the Effective EPE

$$\text{EAD} = \alpha \times \text{Effective EPE}. \tag{2.47}$$

The multiplier α, introduced by [56], is a correction coefficient that accounts for wrong-way risk. Under the IMM, α is fixed at a rather conservative level of 1.4. However, banks using the IMM have an option to use their own estimate of α, with the prior approval of the supervisor and a floor of 1.2.

Results

In order to study the impact of using a two-state HMM, instead of a GBM, on regulatory and economic capital, we consider the case of FX call options on the RUB/EUR rate. The rationale behind this choice was that the Russian currency suffered a crisis in 2014, which will be included in our calibration data set.

Our starting date was 2 January 2016. We estimated the parameters of a GBM and a two-state HMM, using three years of data (between January 2013 and December 2015). Following the methodology presented in Section 2.5.4, we generated market scenarios for the following set of future exposure dates:

$$\{t_k\}_{k=1}^{9} = \{1 \text{ week}, 2 \text{ weeks}, 3 \text{ weeks}, 4 \text{ weeks}, 2 \text{ months}, 3 \text{ months}, 6 \text{ months}, 9 \text{ months}, 1 \text{ year}\}. \tag{2.48}$$

For each generated scenario and each exposure date, option valuation was performed using the Garman–Kohlhagen model ([57]).

The value of a call option at time t is given by the analytical formula

$$C_t = S_t e^{-r_f(T-t)} N(x + \sigma\sqrt{T-t}) - K e^{-r_d(T-t)} N(x), \tag{2.49}$$

where

$$x \equiv \frac{\ln(S_t/K) + \left(r_d - r_f - \left(\sigma^2/2\right)\right)(T-t)}{\sigma\sqrt{T-t}},$$

S_t it the spot price of the deliverable currency at time t (domestic units per foreign unit),

K is the strike price of the option (domestic units per foreign unit),

$T-t$ is the time to maturity,

r_d is the domestic risk-free interest rate,

r_f is the foreign risk-free interest rate,

σ is the volatility of the spot currency price, and

$N(\cdot)$ = cumulative normal distribution function.

Note that, in the formula, both spot and strike price are quoted in units of domestic currency per unit of foreign currency. As a result, the option price will be in the same units, as well. In order to obtain the market value of a position in such an option, it is necessary to multiply by a notional amount Λ in the foreign currency.

In our example, the foreign and domestic currencies are RUB and EUR, respectively. In order to achieve a candid comparison of the two RFE models for the exchange rate, we do not consider interest rate and volatility as risk factors for FX options. Instead, we make the simplistic assumptions of $r_d = r_f = 0$ and constant volatility $\sigma = 0.15$ (equal to the supervisory volatility for foreign exchange options in the standardised approach, see [58]). The notional amount Λ is set to RUB 100,000,000. The spot RUB/EUR exchange rate on 2 January 2016 was $S_0 = 0.01263$.

The credit exposure values for out-of-the-money (OTM) call options on the RUB/EUR exchange rate, for a range of strike prices, are illustrated in Figure 2.11a. The impact of using a two-state HMM, instead of a GBM, is shown in Figure 2.11b. These results are summarised in Table 2.5. It is clear that exposure values under HMM exceeded the exposure values under GBM markedly for deep-out-the-money options. This difference would have a direct impact on how these positions would be capitalised against counterparty default, with a difference that could exceed 400% for the strike price $K = 0.023$. It is also important to note that, given the exchange rate movements over recent years, it is not unrealistic for the moneyness of such options to change dramatically, leading to large unexpected losses. For in-the-money call options, the two models produced identical exposure values. Thus, these results are omitted from this chapter.

Table 2.5: Credit exposure values for out-of-the-money (OTM) options on the RUB/EUR exchange rate.

Strike K	Credit Exposure		Impact (%)
	GBM	HMM2	
0.014	29,507.54	29,013.22	−1.68
0.015	13,684.44	12,838.95	−6.18
0.016	5981.10	5939.89	−0.69
0.017	2598.64	3199.17	23.11
0.018	1207.04	1740.47	44.19
0.019	580.34	973.64	67.77
0.020	285.70	595.99	108.61
0.021	143.08	401.04	180.29
0.022	70.20	269.96	284.60
0.023	31.87	165.56	419.47

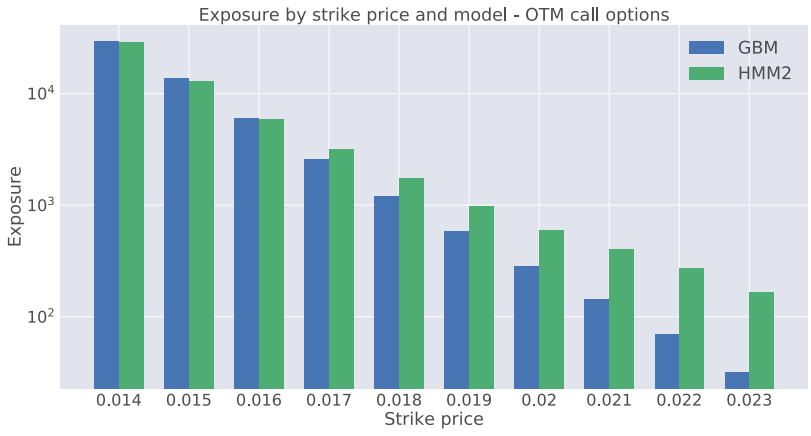

(a)

Figure 2.11: *Cont.*

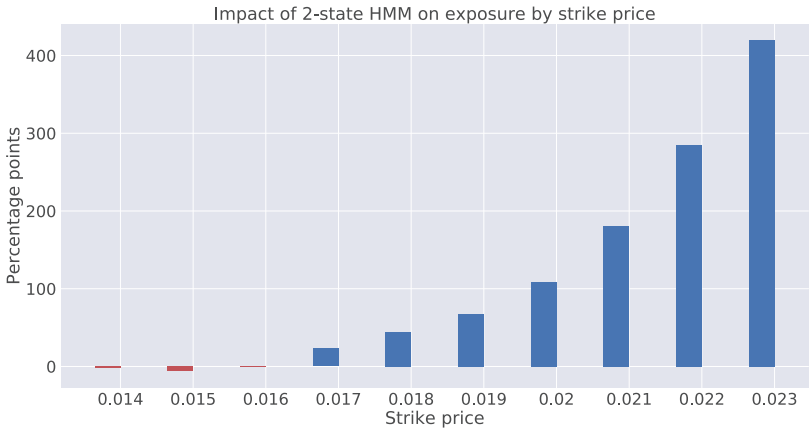

(b)

Figure 2.11: Credit exposure values for out-of-the-money (OTM) call options on the RUB/EUR exchange rate (a) and the impact of using a two-state HMM, instead of a GBM (b).

2.6. Concluding remarks

In this chapter, we presented a hidden Markov model for the evolution of exchange rates with regards to counterparty exposure. In the proposed model, the observations of the exchange rates were assumed to be generated by a discretised GBM, in which both the drift and volatility parameters are able to switch, according to the state of a hidden Markov process. The main motivation of using such a model is the fact that GBM can assign unrealistically low probabilities to extreme scenarios, leading to the under-estimation of counterparty exposure and the corresponding capital buffers. The proposed model is able to produce distributions with heavier tails and capture extreme movements in exchange rates without entirely departing from the convenient GBM framework.

We generated exchange rate scenarios for four currency pairs: USD/EUR, GBP/EUR, RUB/EUR, and MXN/EUR. A risk factor evolution model backtesting exercise was performed, in line with Basel III requirements, and the percentiles of the long-term distribution cones were obtained. The performances of the one-state and two-state models (GBM and the two-state HMM, respectively) were found to be very similar, with the two-state model HMM being slightly more conservative. However, when the generated scenarios were used to calculate exposure profiles for options on the RUB/EUR exchange rate, we found significant differences between the results of the two models. These differences were even more pronounced for deep out-of-the-money options.

Our study highlights some of the limitations of backtesting as a tool for comparing the performance of RFE models. Backtesting can be a useful way to objectively assess model performance. However, it can only be performed over short time horizons; with our available data, we could perform a statistically sound test of modelling assumptions for a time horizon of maximum length three months. It is, therefore, important to put effort into the interpretation of backtesting results, before they are translated into conclusions

about model performance. Our results show how two models with similar performances in a backtesting exercise can result in very different exposure values and, consequently, in very different regulatory and economic capital buffers. This can lead to regulatory arbitrage and potentially weaken financial stability and, further, turn into a systemic risk.

The research presented in this chapter can be extended in a number of ways, such as considering the evolution of risk factors other than exchange rates. Another topic worthy of investigation is the enhancement of the backtesting framework presented by [30], by considering statistical tests similar to the ones presented by [59] and [60]. Finally, an interesting research direction is the development of an agent-based simulation model with heterogeneous modelling approaches, with regards to the RFE models. This model could potentially give valuable insights into the impact of heterogeneous models in financial stability.

3

Incorporating contagion in portfolio credit risk models using network theory

Portfolio credit risk models estimate the range of potential losses due to defaults or deteriorations in credit quality. Most of these models perceive default correlation as fully captured by the dependence on a set of common underlying risk factors. In light of empirical evidence, the ability of such a conditional independence framework to accommodate for the occasional default clustering has been questioned repeatedly. Thus, financial institutions have relied on stressed correlations or alternative copulas with more extreme tail dependence. In this chapter, we propose a different remedy - augmenting systematic risk factors with a contagious default mechanism which affects the entire universe of credits. We construct credit stress propagation networks and calibrate contagion parameters for infectious defaults. The resulting framework is implemented on synthetic test portfolios wherein the contagion effect is shown to have a significant impact on the tails of the loss distributions.

3.1. Introduction

One of the main challenges in measuring the risk of a bank's portfolio is modelling the dependence between default events. Joint defaults of many issuers over a fixed period of time may lead to extreme losses; therefore, understanding the structure and the impact of default dependence is essential. To address this problem, one has to take into consideration the existence of two distinct sources of default dependence. On the one hand, performance of different issuers depends on certain common underlying factors, such as interest rates or economic growth. These factors drive the evolution of a company's financial success, which is measured in terms of its rating class or the probability of default. On the other hand, default of an issuer may, too, have a direct impact on the probability

Parts of this chapter have been published in Complexity **2018** (2018) [P2]

of default of a second dependent issuer, a phenomenon known as contagion. Through contagion, economic distress initially affecting only one issuer can spread to a significant part of the portfolio or even the entire system. A good example of such a transmission of pressure is the Russian crisis of 1998-1999 which saw the defaults of corporate and sub-sovereign issuers heavily clustered following the sovereign default [25].

Most portfolio credit risk models used by financial institutions neglect contagion and rely on the conditional independence assumption according to which, conditional on a set of common underlying factors, defaults occur independently. Examples of this approach include the Asymptotic Single Risk Factor (ASRF) model [24], industry extensions of the model presented by Merton [23] such as the KMV [61, 62] and CreditMetrics [63] models, and the two-factor model proposed recently by Basel Committee on Banking Supervision for the calculation of Default Risk Charge (DRC) to capture the default risk of trading book exposures [64]. A considerable amount of literature has been published on the conditional independence framework in standard portfolio models, see, e.g. [65] and [20].

Although conditional independence is a statistically and computationally convenient property, its empirical validity has been questioned on a number of occasions, where researchers investigated whether dependence on common factors can sufficiently explain the default clustering which occurs from time to time. Schönbucher and Schubert [66] suggest the default correlations that can be achieved with this approach are typically too low in comparison with empirical default correlations, although this problem becomes less severe when dealing with large diversified portfolios. Das et. al. [67] use data on U.S. corporations from 1979-2004 and reject the hypothesis that factor correlations can sufficiently explain the empirically observed default correlations in the presence of contagion. Since a realistic credit risk model is required to put the appropriate weight on scenarios where many joint defaults occur, one may choose to use alternative copulas with tail dependence which have the tendency to generate large losses simultaneously [68]. In that case, however, the probability distribution of large losses is specified a priori by the chosen copula, which seems rather unintuitive [69].

One of the first models to consider contagion in credit portfolios was developed by Davis and Lo [70]. They suggest a way of modelling default dependence through infection in a static framework. The main idea is that any defaulting issuer may infect any other issuer in the portfolio. Giesecke and Weber [71] propose a reduced-form model for contagion phenomena, assuming that they are due to the local interaction of companies in a business partner network. The authors provide an explicit Gaussian approximation of the distribution of portfolio losses and find that, typically, contagion processes have a second-order effect on portfolio losses. Lando and Nielsen [72] use a dynamic model in continuous time based on the notion of mutually exciting point processes. Apart from reduced form models for contagion, which aim to capture the influence of infectious defaults to the default intensities of other issuers, structural models were developed as well. Jarrow and Yu [73] generalise existing models to include issuer-specific counterparty risks and illustrate their effect on the pricing of defaultable bonds and credit derivatives. Eggloff et. al. [74] use network-like connections between issuers that allow for a variety of infections between firms. However, their structural approach requires a detailed microeconomic knowledge of debt structure, making the application of this model in

practice more difficult than that of Davis and Lo's simple model. In general, since the interdependencies between borrowers and lenders are complicated, structural analysis has mostly been applied to a small number of individual risks only.

Network theory can provide us with tools and insights that enable us to make sense of the complex interconnected nature of financial systems. Hence, following the 2008 crisis, network-based models have been frequently used to measure systemic risk in finance. Among the first papers to study contagion using network models was [9], where Allen and Gale show that a fully connected and homogeneous financial network results in an increased system stability. Contagion effects using network models have also been investigated in a number of related articles, see, e.g. [10–14]. The issue of too-central-to-fail was shown to be possibly more important than too-big-to-fail by Battiston et. al. in [15], where DebtRank, a metric for the systemic impact of financial institutions was introduced. DebtRank was further extended in a series of articles, see e.g. [16–18]. The need for development of complexity-based tools in order to complement existing financial modelling approaches was emphasised by Battiston et. al. [1], who called for a more integrated approach among academics from multiple disciplines, regulators, and practitioners.

Despite substantial literature on portfolio credit risk models and contagion in finance, specifying models which take into account both common factors and contagion while distinguishing between the two effects clearly, still proves challenging. Moreover, most of the studies on contagion using network models focus on systemic risk and the resilience of the financial system to shocks. The qualitative nature of this line of research can hardly provide quantitative risk metrics that can be applied to models for measuring the risk of individual portfolios. The aforementioned drawback is perceived as an opportunity for expanding the current body of research by contributing a model that would account for common factors and contagion in networks alike. Given the wide use of factor models for calculating regulatory and economic capital, as well as for rating and analysing structured credit products, an extended model that can also accommodate for infectious default events seems crucial.

In this chapter we take up this challenge by introducing a portfolio credit risk model that can account for two channels of default dependence: common underlying factors and financial distress propagated from sovereigns to corporates and sub-sovereigns. We augment systematic factors with a contagion mechanism affecting the entire universe of credits, where the default probabilities of issuers in the portfolio are immediately affected by the default of the country where they are registered and operating. Our model allows for extreme scenarios with realistic numbers of joint defaults, while ensuring that the portfolio risk characteristics and the average loss remain unchanged. To estimate the contagion effect, we construct a network using credit default swaps (CDS) time series. We then use CountryRank, a network-based metric, introduced in [75] to quantify the impact of a sovereign default event on the credit quality of corporate issuers in the portfolio. In order to investigate the impact of our model on credit losses, we use synthetic test portfolios for which we generate loss distributions and study the effect of contagion on the associated risk measures. Finally, we analyse the sensitivity of the contagion impact to rating levels and CountryRank. Our analysis shows that credit losses increase significantly in the presence of contagion. Our contribution in this chapter is thus threefold: First,

we introduce a portfolio credit risk model which incorporates both common factors and contagion. Second, we use a credit stress propagation network constructed from real data to quantify the impact of deterioration of credit quality of the sovereigns on corporates. Third, we present the impact of accounting for contagion which can be useful for banks and regulators to quantify credit, model, or concentration risk in their portfolios.

The rest of the chapter is organised as follows. Section 3.2 provides an overview of the general modelling framework. Section 3.3 presents the portfolio model with default contagion and illustrates the network model for the estimation of contagion effects. In Section 3.4 we present empirical analysis of two synthetic portfolios. Finally, in Section 3.5 we summarise our findings and draw conclusions.

3.2. Merton-type models for portfolio credit risk

Most financial institutions use models that are based on some form of the conditional independence assumption, according to which issuers depend on a set of common underlying factors. Factor models based on the Merton model are particularly popular for portfolio credit risk. Our model extends the multi-factor Merton model to allow for credit contagion. In this section we present the basic portfolio modelling setup, outline the model of Merton, and explain how it can be specified as a factor model. A more detailed presentation of the multivariate Merton model is provided by [20].

3.2.1. Basic setup and notations

This subsection introduces the basic notation and terminology that will be used throughout this chapter. In addition, we define the main risk characteristics for portfolio credit risk.

The uncertainty of whether an issuer will fail to meet its financial obligations or not is measured by its *probability of default*. For comparison reasons, this is usually specified with respect to a fixed time interval, most commonly one year. The probability of default then describes the probability of a default occurring in the particular time interval. The *exposure at default* is a measure of the extent to which one is exposed to an issuer in the event of, and at the time of, that issuer's default. The default of an issuer does not necessarily imply that the creditor receives nothing from the issuer. The percentage of loss incurred over the overall exposure in the event of default is given by the *loss given default*. Typical values lie between 45% and 80%.

Consider a portfolio of m issuers, indexed by $i = 1, ..., m$, and a fixed time horizon of $T = 1$ year. Denote by e_i the exposure at default of issuer i and by p_i its probability of default. Let q_i be the loss given default of issuer i. Denote by Y_i the default indicator, in the time period $[0, T]$. All issuers are assumed to be in a non-default state at time $t = 0$. The default indicator Y_i is then a random variable defined by

$$Y_i = \begin{cases} 1 & \text{if issuer } i \text{if issuer } defaults \\ 0 & \text{otherwise} \end{cases} \tag{3.1}$$

which clearly satisfies $P(Y_i = 1) = p_i$. The overall portfolio loss is defined as the random

variable

$$L := \sum_{i=1}^{m} q_i e_i Y_i \tag{3.2}$$

With credit risk in mind, it is useful to distinguish potential losses in *expected losses*, which are relatively predictable and thus can easily be managed, and *unexpected losses*, which are more complicated to measure. Risk managers are more concerned with unexpected losses and focus on risk measures relating to the tail of the distribution of L.

3.2.2. The model of Merton

Credit risk models are typically distinguished in structural and reduced-form models, according to their methodology. Structural models try to explain the mechanism by which default takes place, using variables such as asset and debt values. The model presented by Merton in [23] serves as the foundation for all these models. Consider an issuer whose asset value follows a stochastic process $(V_t)_{t\geq 0}$. The issuer finances itself with equity and debt. No dividends are paid and no new debt can be issued. In Merton's model the issuer's debt consists of a single zero-coupon bond with face value B and maturity T. The value at time t of equity and debt are denoted by S_t and B_t and the issuer's asset value is simply the sum of these, i.e.

$$V_t = S_t + B_t, \qquad t \in [0,T] \tag{3.3}$$

Default occurs if the issuer misses a payment to its debtholders, which can happen only at the bond's maturity T. At time T there are only two possible scenarios:

(i) $V_T > B$: the value of the issuer's assets is higher than its debt. In this scenario the debtholders receive $B_T = B$, the shareholders receive the remainder $S_T = V_T - B$, and there is no default.

(ii) $V_T \leq B$: the value of the issuer's assets is less than its debt. Hence, the issuer cannot meet its financial obligations and defaults. In that case, shareholders hand over control to the bondholders, who liquidate the assets and receive the liquidation value in lieu of the debt. Shareholders pay nothing and receive nothing, therefore we obtain $B_T = V_T$, $S_T = 0$.

For these simple observations we obtain the below relations

$$S_T = max(V_T - B, 0) = (V_T - B)^+ \tag{3.4}$$

$$B_T = min(V_T, B) = B - (B - V_T)^+ \tag{3.5}$$

Equation 3.5 implies that the issuer's equity at maturity T can be determined as the price of a European call option on the asset value V_t with strike price B and maturity T, while 3.5 implies that the value of debt at T is the sum of a default-free bond that guarantees payment of B plus a short European put option on the issuer's assets with strike price B.

It is assumed that under the physical probability measure P the process $(V_t)_{t\geq 0}$ follows a geometric Brownian motion of the form

$$dV_t = \mu_V V_t dt + \sigma_V V_t dW_t, \qquad t \in [0,T] \tag{3.6}$$

where $\mu_V \in \mathbb{R}$ is the mean rate of return on the assets, $\sigma_V > 0$ is the asset volatility and $(W_t)_{t\geq 0}$ is a Wiener process. The unique solution at time T of the stochastic differential equation 3.6 with initial value V_0 is given by

$$V_T = V_0 \exp\left(\left(\mu_V - \sigma_V^2/2\right)T + \sigma_V W_T\right) \tag{3.7}$$

which implies that

$$\ln V_T \sim \mathcal{N}\left(\ln V_0 + \left(\mu_V - \sigma_V^2/2\right)T, \sigma_V^2 T\right) \tag{3.8}$$

Hence, the real-world probability of default at time T, measured at time $t = 0$, is given by

$$\begin{aligned} P(V_T \leq B) &= P(\ln V_T \leq \ln B) \\ &= \Phi\left(\frac{\ln(B/V_0) - \left(\mu_V - \sigma_V^2/2\right)T}{\sigma_V\sqrt{T}}\right) \end{aligned} \tag{3.9}$$

A core assumption of Merton's model is that asset returns are lognormally distributed, as can be seen in Equation 3.8. It is widely acknowledged, however, that empirical distributions of asset returns tend to have heavier tails; thus, Equation 3.9 may not be an accurate description of empirically observed default rates.

3.2.3. The multivariate Merton model

The model presented in 3.2.2 is concerned with the default of a single issuer. In order to estimate credit risk at a portfolio level, a multivariate version of the model is necessary. A multivariate geometric Brownian motion with drift vector $\boldsymbol{\mu}_V = (\mu_1, ..., \mu_m)'$, vector of volatilities $\boldsymbol{\sigma}_V = (\sigma_1, ..., \sigma_m)$ and correlation matrix Σ, is assumed for the dynamics of the multivariate asset-value process $(\mathbf{V}_t)_{t\geq 0}$ with $\mathbf{V}_t = (V_{t,1}, ..., V_{t,m})'$, so that for all i

$$V_{T,i} = V_{0,i} \exp((\mu_i - \frac{1}{2}\sigma_i^2)T + \sigma_i W_{T,i}) \tag{3.10}$$

where the multivariate random vector $\mathbf{W}_T$ with $\mathbf{W}_T = (W_{T,1}, ..., W_{T,m})'$ is satisfying $\mathbf{W}_T \sim N_m(\mathbf{0}, T\Sigma)$. Default takes place if $V_{T,i} \leq B_i$ where B_i is the debt of company i. It is clear that the default probability in the model remains unchanged under simultaneous strictly increasing transformations of $V_{T,i}$ and B_i. Thus, one may define

$$X_i := \frac{\ln V_{T,i} - \ln V_{0,i} - (\mu_i - \frac{1}{2}\sigma_i^2)T}{\sigma_i\sqrt{T}} \tag{3.11}$$

$$d_i := \frac{\ln B_i - \ln V_{0,i} - (\mu_i - \frac{1}{2}\sigma_i^2)T}{\sigma_i\sqrt{T}} \tag{3.12}$$

and then default equivalently occurs if and only if $X_i \leq d_i$. Notice that X_i is the standardised asset-value log-return $\ln V_{T,i} - \ln V_{0,i}$. It can be easily shown that the transformed variables satisfy $(X_1, ..., X_m)' \sim N_m(\mathbf{0}, \Sigma)$ and their copula is the Gaussian copula. Thus, the probability of default for issuer i is satisfying $p_i = \Phi(d_i)$, where $\Phi(\cdot)$ denotes the cumulative distribution function of the standard normal distribution. A graphical representation of Merton's model is shown in Figure 3.1. In most practical implementations

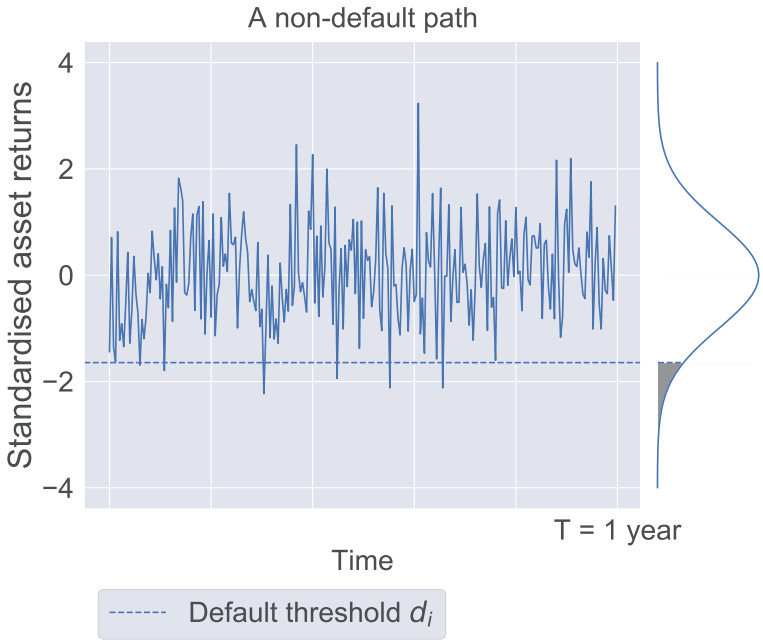

Figure 3.1: In Merton's model, default of issuer i occurs if at time T asset value $V_{T,i}$ falls bellow debt value B_i, or equivalently if $X_i := (\ln V_{T,i} - \ln V_{0,i} - (\mu_i - \frac{1}{2}\sigma_i^2)T)/\sigma_i\sqrt{T}$ falls below the critical threshold $d_i := (\ln B_{T,i} - \ln V_{0,i} - (\mu_i - \frac{1}{2}\sigma_i^2)T)/\sigma_i\sqrt{T}$. Since $X_i \sim \mathcal{N}(0,1)$, i's default probability, represented by the shaded area in the distribution plot, is satisfying $p_i = \Phi(d_i)$. Note that default can only take place at time T does not depend on the path of the asset value process.

of the model, portfolio losses are modelled by directly considering an m-dimensional random vector $\mathbf{X} = (X_1, ..., X_m)'$ with $\mathbf{X} \sim N_m(\mathbf{0}, \Sigma)$ containing the standardised asset returns, and a deterministic vector $\mathbf{d} = (d_1, ..., d_m)$ containing the critical thresholds with $d_i = \Phi^{-1}(p_i)$ for given default probabilities p_i, $i = 1, ..., m$. The default probabilities are usually estimated by historical default experience using external ratings by agencies or model-based approaches.

3.2.4. Merton model as a factor model

The number of parameters contained in the correlation matrix Σ grows polynomially in m, and thus, for large portfolios it is essential to have a more parsimonious parametrisation which is accomplished using a factor model. Additionally, factor models are particularly attractive due to the fact that they offer an intuitive interpretation of credit risk in relation to the performance of industry, region, global economy, or any other relevant indexes that may affect issuers in a systematic way. In the following we show how Merton's model can be understood as a factor model. In the factor model approach, asset returns are linearly dependent on a vector $\mathbf{F}$ of $p < m$ common underlying factors satisfying $\mathbf{F} \sim N_p(0, \Omega)$. Issuer i's standardised asset return is assumed to be driven by a

issuer-specific combination $\tilde{F}_i = \boldsymbol{\alpha}_i' \mathbf{F}$ of the systematic factors

$$X_i = \sqrt{\beta_i}\tilde{F}_i + \sqrt{1-\beta_i}\epsilon_i \tag{3.13}$$

where $\tilde{F}_i$ and $\epsilon_1, ..., \epsilon_m$ are independent standard normal variables, and ϵ_i represents the idiosyncratic risk. Consequently, β_i can be seen as a measure of sensitivity of X_i to systematic risk, as it represents the proportion of the X_i variation that is explained by the systematic factors. The correlations between asset returns are given by

$$\begin{aligned} \rho(X_i, X_j) &= \text{Cov}[X_i, X_j] \\ &= \left(1-\beta_i\right)\mathbf{1}_{\{i=j\}} + \sqrt{\beta_i\beta_j}\,\text{Cov}[\tilde{F}_i, \tilde{F}_j] \\ &= \left(1-\beta_i\right)\mathbf{1}_{\{i=j\}} + \sqrt{\beta_i\beta_j}\,\boldsymbol{\alpha}_i'\Omega\boldsymbol{\alpha}_j \end{aligned} \tag{3.14}$$

since $\tilde{F}_i$ and $\epsilon_1, ..., \epsilon_m$ are independent and standard normal and $\text{var}(X_i) = 1$.

3.3. A model for credit contagion

In the multi-factor Merton model specified in 3.2.4, the standardised asset returns X_i, $i = 1, ..., m$, are assumed to be driven by a set of common underlying systematic factors, and the critical thresholds d_i, $i = 1, ..., m$, are satisfying $d_i = \Phi^{-1}(p_i)$ for all i. The only source of default dependence in such a framework is the dependence on the systematic factors. In the model we propose, we assume that in the event of a sovereign default, contagion will spread to the corporate issuers in the portfolio that are registered and operating in that country, causing default probability to be equal to their CountryRank. In Subsection 3.3.1 we demonstrate how to calibrate the critical thresholds so that each corporate's probability of default conditional on the default of the corresponding sovereign equals its CountryRank, while its unconditional default probability remains unchanged. In Subsection 3.3.2 we show how to construct a credit stress propagation network and estimate the CountryRank parameter.

3.3.1. Incorporating contagion in factor models

Consider a corporate issuer C_i, and its country of operation S. Denote by p_{C_i} the probability of default of C_i. Under the standard Merton model, default occurs if C_i's standardised asset return X_{C_i} falls below its default threshold d_{C_i}. The critical threshold d_{C_i} is assumed to be equal to $\Phi^{-1}(p_{C_i})$ and is independent of the state of the country of operation S. In the proposed model, a corporate is subject to shocks from its country of operation; its corresponding state is described by a binary state variable. The state is considered to be stressed in the event of sovereign default. In this case, the issuer's default threshold increases, causing it more likely to default, as the contagion effect suggests. In case the corresponding sovereign does not default, the corporates liquidity state is considered stable. We replace the default threshold d_{C_i} with $d^*_{C_i}$, where

$$d^*_{C_i} = \begin{cases} d^{sd}_{C_i} & \text{if the corresponding sovereign defaults} \\ d^{nsd}_{C_i} & \text{otherwise} \end{cases} \tag{3.15}$$

or equivalently

$$d^*_{C_i} = \mathbf{1}_{\{Y_S=1\}} d^{sd}_{C_i} + \mathbf{1}_{\{Y_S=0\}} d^{nsd}_{C_i} \tag{3.16}$$

We denote by p_S the probability of default of the country of operation, and by γ_{C_i} the CountryRank parameter which indicates the increased probability of default of C_i given the default of S. An example of the new default thresholds is shown in Figure 3.2. Our objective is to calibrate $d^{sd}_{C_i}$ and $d^{nsd}_{C_i}$ in such way that the overall default rate remains unchanged and $P(Y_{C_i} = 1|Y_S = 1) = \gamma_{C_i}$. Denote by

$$\phi_2(x,y;\rho) := \frac{1}{2\pi\sqrt{1-\rho^2}} \exp\left(-\frac{x^2+y^2-2\rho xy}{2(1-\rho^2)}\right) \tag{3.17}$$

$$\Phi_2(h,k;\rho) := \int_{-\infty}^{h}\int_{-\infty}^{k} \phi_2(x,y;\rho)\,dy\,dx \tag{3.18}$$

the density and distribution function of the bivariate standard normal distribution with correlation parameter $\rho \in (-1,1)$. Note that $d^*_{C_i}(\omega) = d^{sd}_{C_i}$ for $\omega \in \{Y_{C_i} = 1, Y_S = 1\} \subset \{Y_S = 1\}$, and $d^*_{C_i}(\omega) = d^{nsd}_{C_i}$ for $\omega \in \{Y_{C_i} = 1, Y_s = 0\} \subset \{Y_S = 0\}$. We rewrite $P(Y_{C_i} = 1|Y_S = 1)$ in the following way

$$\begin{aligned} P(Y_{C_i} = 1|Y_S = 1) &= \frac{1}{P(Y_S=1)} P(Y_{C_i} = 1, Y_S = 1) && (3.19)\\ &= \frac{1}{p_S} P\left[X_{C_i} < d^{sd}_{C_i}, X_S < d_S\right] && (3.20)\\ &= \frac{1}{p_S} \Phi_2(d^{sd}_{C_i}, d_S; \rho_{SC_i}) && (3.21) \end{aligned}$$

Using the above representation and given $d_S = \Phi^{-1}(p_S)$ and ρ_{SC_i} one can solve the equation

$$P(Y_{C_i} = 1|Y_S = 1) = \gamma_{C_i} \tag{3.22}$$

over $d^{sd}_{C_i}$. We proceed to the derivation of $d^{nsd}_{C_i}$ in such way that the overall default probability remains equal to p_{C_i}. This constraint is important, since contagion is assumed to have no impact on the average loss. Clearly,

$$\begin{aligned} p_{C_i} &= P(Y_{C_i} = 1) && (3.23)\\ &= P(Y_{C_i} = 1, Y_S = 1) + P(Y_{C_i} = 1, Y_S = 0) && (3.24)\\ &= P(Y_{C_i} = 1|Y_s = 1)P(Y_S = 1) + P(Y_{C_i} = 1, Y_S = 0) && (3.25) \end{aligned}$$

and thus

$$P(Y_{C_i} = 1, Y_S = 0) = p_{C_i} - \gamma_{C_i} p_S \tag{3.26}$$

The left-hand side of the above equation can be represented as follows

$$\begin{aligned} P(corp.def \cap nosov.def) &= P\left[X_{C_i} < d^{nsd}_{C_i}, X_S > d_S\right] && (3.27)\\ &= P\left[X_{C_i} < d^{nsd}_{C_i}\right] - P\left[X_{C_i} < d^{nsd}_{C_i}, X_S < d_S\right] && (3.28)\\ &= \Phi(d^{nsd}_{C_i}) - \Phi_2(d^{nsd}_{C_i}, d_S; \rho_{SC_i}) && (3.29) \end{aligned}$$

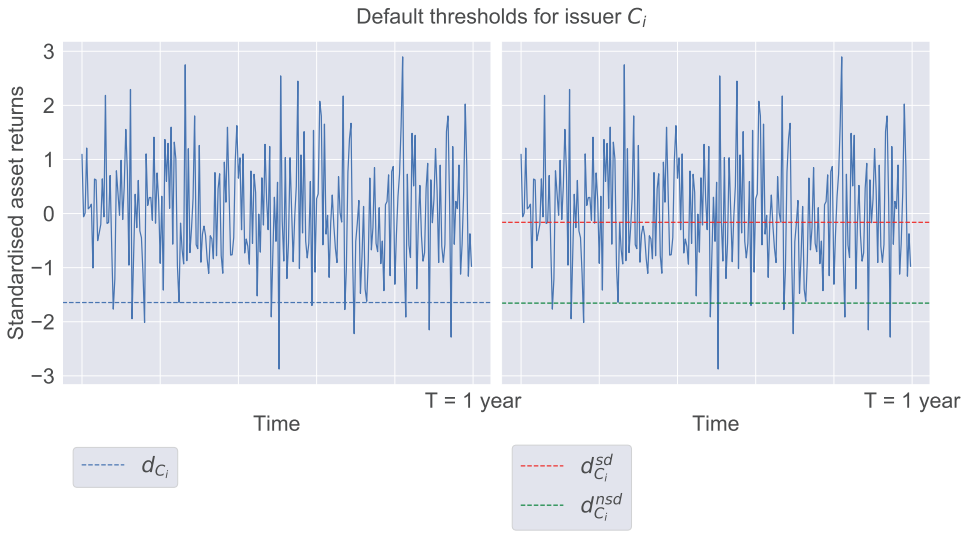

Figure 3.2: Under the standard Merton model, the default threshold d_{C_i} for corporate issuer C_i is set to be equal to $\Phi^{-1}(p_{C_i})$. Under the proposed model, the threshold increases in the event of sovereign default, making C_i's default more likely as the contagion effect suggests.

By use of the above and given $d_S = \Phi^{-1}(p_S)$ and ρ_{SC_i} one can solve the previous equation over $d_{C_i}^{nsd}$.

3.3.2. Estimation of CountryRank

In this section, we elaborate on the estimation of the CountryRank parameter [75], which serves as the probability of default of the corporate conditional on the default of the sovereign. In addition, we provide details on the construction of the credit stress propagation network.

CountryRank

In order to estimate contagion effects in a network of issuers, an algorithm such as DebtRank [76], is necessary. In the DebtRank calculation process, stress propagates even in the absence of defaults and each node can propagate stress only once before becoming inactive. The level of distress for a previously undistressed node is given by the sum of incoming stress from its neighbours with a maximum value of 1. Summing up the incoming stress from neighbouring nodes seems reasonable when trying to estimate the impact of one node or a set of nodes to a network of interconnected balance sheets where links represent lending relationships. However, when trying to quantify the probability of default of a corporate node given the infectious default of a sovereign node, one has to consider that there is significant overlap in terms of common stress, and thus, by summing we may be accounting for the same effect more than once. This effect is amplified in dense networks constructed from CDS data. Therefore, we introduce CountryRank as an alternative measure which is suited for our contagion model.

We assume that we have a hypothetical credit stress propagation network, where the nodes correspond to the issuers, including the sovereign, and the edges correspond to the impact of credit quality of one issuer on the other. The details of the network construction will be presented in Section 3.3.2. Given such a network, the CountryRank of the nodes can be defined recursively as follows:

- First, we stress the sovereign node and as result its CountryRank is 1.

- Let γ_S be the CountryRank of the sovereign and $e_{(j,k)}$ denote the edge weight between nodes j and k. Given a node C_i, let $p = S\,C_1\,C_2 \ldots C_{i-1}\,C_i$ be a path without cycles from the sovereign node S, to the node C_i. The *weight* of the path p is defined as:

$$w(p) = \gamma_S e_{(1,2)} \ldots e_{(i-1,i)} \tag{3.30}$$

  where $e_{(j,k)}$ are the respective edge weights between nodes j and k for $j \in \{1,\ldots,i-1\}$ and $k \in \{2,\ldots,i\}$. Let $p_1,\ldots,p_m$ be the set of all acyclic paths from the sovereign node to the corporate node C_i and $w(p_1)$, …, $w(p_m)$ be the corresponding weights. Then the CountryRank of node C_i is defined as

(3.31)

In order to compute the conditional probability of default of a corporate given the sovereign default analytically, we would need the joint distribution of probabilities of default of the nodes, which has an exponential computational complexity, and it is therefore intractable. Thus, we approximate the conditional probability by choosing the path with the maximum weight in the above definition for CountryRank.

The example below in Figure 3.3 illustrates calculation of CountryRank for a hypothetical network. The network consists of a sovereign node S and corporate nodes C_1, C_2, C_3, C_4. The edge labels indicate weights in network between two nodes. We initially stress the sovereign node which results in a CountryRank of 1 for node S. In the next step, the stress propagates to nodes C_1 and as a result its CountryRank is 0.9. Then, node C_2 gets stressed giving it a CountryRank value 0.8. For node C_3, there are two paths from node S, so we pick the path through node C_2 having a higher weight of 0.48. Finally, there are three paths from node S to node C_4, and the path with maximum weight is 0.27.

Network construction

Credit default swap spreads are market-implied indicators of probability of default of an entity. A credit default swap is a financial contract in which a protection seller A insures a protection buyer B against the default of a third party C. More precisely, regular coupon payments with respect to a contractual notional N and a fixed rate s, the CDS spread, are swapped with a payment of $N(1-RR)$ in the case of the default of C, where RR, the so-called recovery rate, is a contract parameter which represents the fraction of investment which is assumed be recovered in the case of default of C.

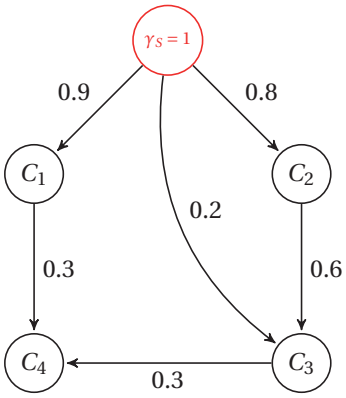

(a) Sovereign node in stress

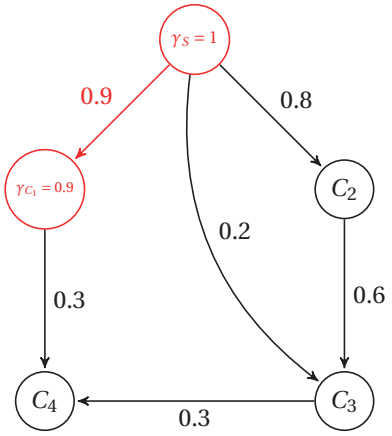

(b) Stress propagates to node C_1

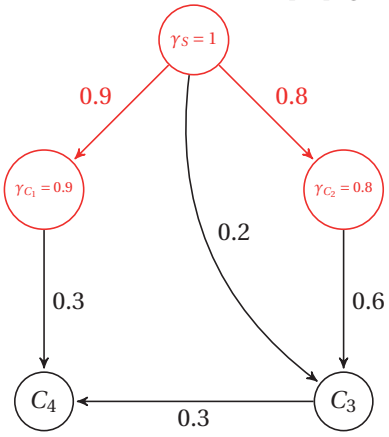

(c) Stress propagates to node C_2

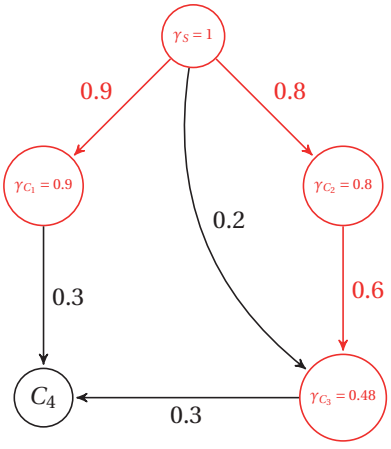

(d) Stress propagates to node C_3

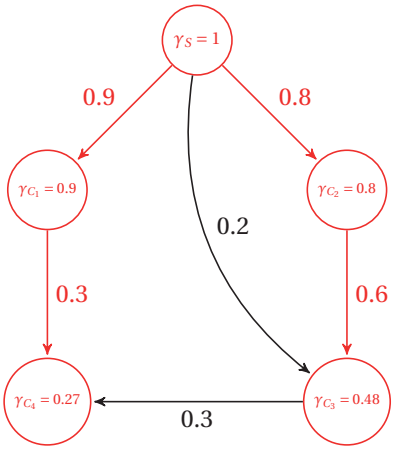

(e) Stress propagates to node C_4

Figure 3.3: Illustration of the CountryRank parameter using a hypothetical network. The subfigures (a) - (e) show the propagation of stress in the network starting from the sovereign node to corporate nodes. At each step, the stress spreads to a node using the path with the maximum weight from the sovereign node.

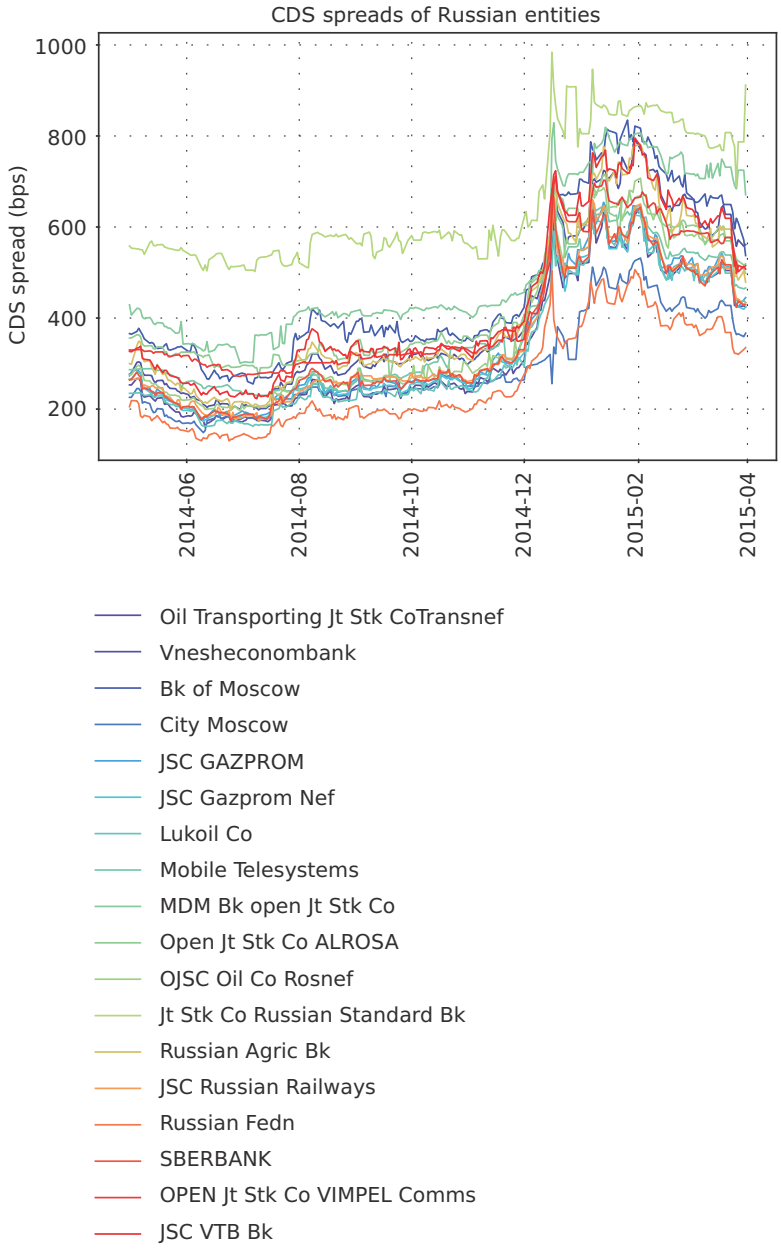

Figure 3.4: Time series of CDS spreads of Russian issuers.

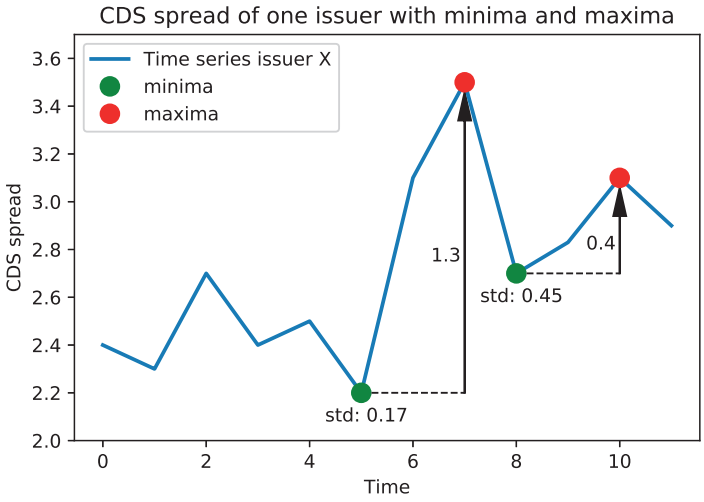

Figure 3.5: A *modified ϵ-drawup* is defined as an upward movement in the time series at a local minimum, in which the amplitude of the movement is greater than a threshold ϵ. The ϵ parameter at time t is set to be the standard deviation in the time series between days $t-n$ and t, where n is chosen to be 10 days. In the above example, the first green minimum is recorded as a *modified ϵ-drawup*, while the second is not.

Modified ϵ-drawup. We would like to measure to what extent changes in CDS spreads of different issuers occur simultaneously. For this, we use the notion of a *modified ϵ-drawup* to quantify the impact of deterioration of credit quality of one issuer on the other. Modified ϵ- drawup is an alteration of the ϵ-drawups notion which is introduced in [77]. In that article, the authors use the notion of ϵ-drawups to construct a network which models the conditional probabilities of spike-like co-movements among pairs of CDS spreads. A modified ϵ-drawup is defined as an upward movement in the time series in which the amplitude of the movement, that is the difference between the subsequent local maximum and current local minimum, is greater than a threshold ϵ. We record such local minima as the modified ϵ-drawups. The ϵ parameter for a local minimum at time t is set to be the standard deviation in the time series between days $t-n$ and t, where n is chosen to be 10 days. An illustration of the modified ϵ-drawup definition is shown in Figure 3.5. Figure 3.6 shows the time series of Russian Federation CDS with the calibrated modified ϵ-drawups using a history of 10 days for calibration.

Filtering market impact. Since we would like to measure the co-movement of the time series i and j, we exclude the effect of the external market on these nodes as follows. We calibrate the ϵ-drawups for the CDS time series of an index that does not represent the region in question, for instance for Russian issuers we choose the iTraxx index which is the composite CDS index of 125 CDS referencing European investment grade credit. Then, we filter out those ϵ-drawups of node i which are the same as the ϵ-drawups of the iTraxx index including a time lag τ. That is, if iTraxx has a modified ϵ-drawup on day t, then we remove the modified ϵ-drawups of node i on days $t, t+1, \ldots, t+\tau$. We choose a

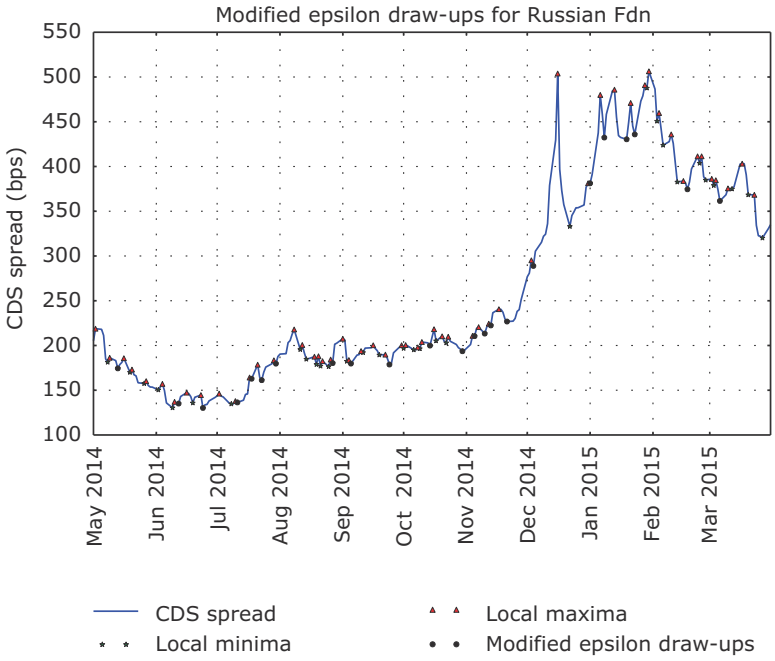

Figure 3.6: Time series for Russian Federation with local minima, local maxima and modified ϵ-drawups.

time lag of 3 days for our calibration based on the input data which is consistent with the choice in [77].

Edges. After identifying the ϵ-drawups for all the issuers and filtering out the market impact, the edges in our network are constructed as follows. The weight of an edge in the credit stress propagation network from node i to node j is the conditional probability that if node i has an epsilon draw-up on day t then node j also has an epsilon draw-up on days $t, t+1, \ldots, t+\tau$, where τ is the time lag. More precisely, let N_i be the number of ϵ-drawups of node i after filtering using iTraxx index and N_{ij} epsilon draw-ups of node i which are also epsilon draw-ups for node j with the time lag τ. Then, the edge weight w_{ij} between nodes i and j is defined as $w_{ij} = N_i/N_{ij}$. Figure 3.7 shows the minimum spanning tree of the credit stress propagation network constructed using the CDS spread time series data of Russian issuers.

Uncertainty in CountryRank. We test the robustness of our CountryRank calibration by varying the number of days used for ϵ-parameter. Figure A.3 in Appendix A.2 shows that the ϵ-parameter for Russian Federation CDS time series remains stable when we vary the number of days. We initially obtain time series of ϵ-parameters by calculating standard deviation in the last $n = 10, 15$ and 20 days on all local minima indices of Russian Federation CDS. Subsequently, we calculate the mean of the absolute differences between the epsilon time series calculated and express this in units of the mean of Rus-

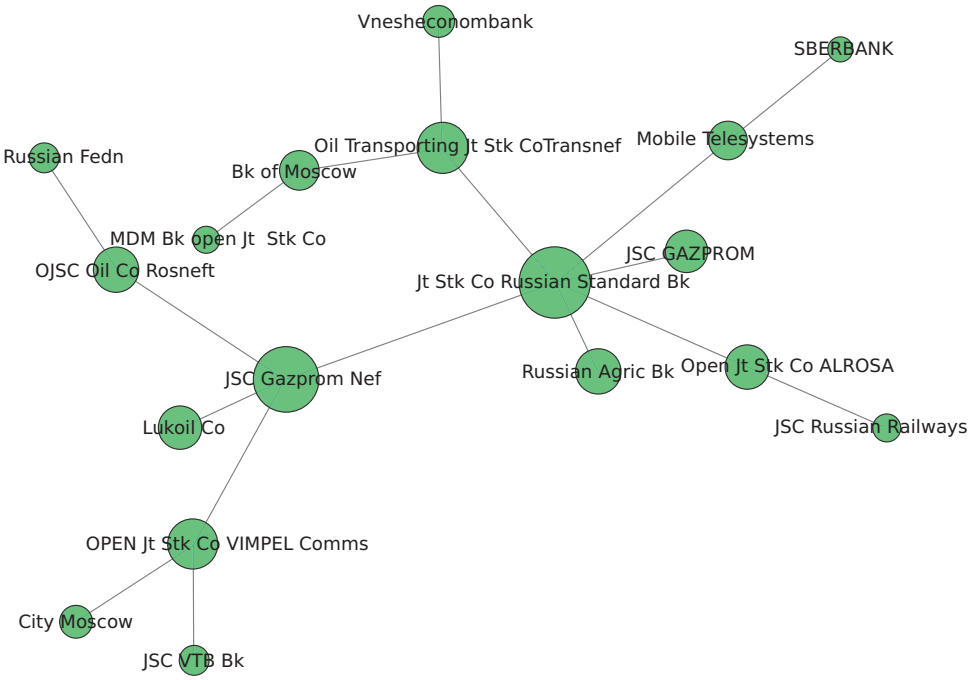

Figure 3.7: Minimum spanning tree for Russian issuers.

sian Federation CDS time series. The percentage difference is 1.38% between the 10 day ϵ parameter is 1.38% and 15 day ϵ parameter, and 2.22% between the 10 day and 20 day ϵ parameters.

Further, we quantify the uncertainty in CountryRank parameter as follows. For an corporate node, we calculate the absolute difference in CountryRank calculated using $n = 15, 20$ days with CountryRank using $n = 10$ days for the ϵ parameter. We then calculate this difference as a percentage of the CountryRank calculated using 10 days for ϵ parameter for all corporates and then compute their mean. The mean difference between CountryRank calibrated using $n = 15$ days and $n = 10$ days is 6.84%, and $n = 20$ days and $n = 10$ days is 9.73% for the Russian CDS data set.

3.4. Numerical experiments

We implement the framework presented in Section 3.3 to synthetic test portfolios and discuss the corresponding risk metrics. Further, we perform a set of sensitivity studies and explore the results.

3.4.1. Factor model

We first set up a multi-factor Merton model, as it was described in Section 3.2. We define a set of systematic factors that will represent region and sector effects. We choose 6 region and 6 sector factors, for which we select appropriate indexes, as shown in Table

3.1. We then use 10 years of index time series to derive the region and sector returns $F_{R(j)}$, $j = 1,...,6$ and $F_{S(k)}$, $k = 1,...,6$ respectively, and obtain an estimate of the correlation matrix Ω, shown in Figure 3.8. Subsequently, we map all issuers to one region and one sector factor, $F_{R(i)}$ and $F_{S(i)}$ respectively. For instance, a Dutch bank will be associated with Europe and Financial factors. As a proxy of individual asset returns we use 10 years of equity or CDS time series, depending on the data availability for each issuer. Finally, we standardise the individual returns time series $\left(X_{i,t}\right)$ and perform the following Ordinary Least Squares regression against the systematic factor returns

$$X_{i,t} = \alpha_{R(i)} F_{R(i),t} + \alpha_{S(i)} F_{S(i),t} + \epsilon_{i,t} \tag{3.32}$$

to obtain $\hat{\alpha}_{R(i)}$, $\hat{\alpha}_{S(i)}$, and $\hat{\beta}_i = R^2$, where R^2 is the coefficient of determination, and it is higher for issuers whose returns are largely affected by the performance of the systematic factors.

Factor	Index
Europe	MSCI EUROPE
Asia	MSCI AC ASIA
North America	MSCI NORTH AMERICA
Latin America	MSCI EM LATIN AMERICA
Middle East and Africa	MSCI FM AFRICA
Pacific	MSCI PACIFIC
Materials	MSCI WRLD/MATERIALS
Consumer products	MSCI WRLD/CONSUMER DISCR
Services	MSCI WRLD/CONSUMER SVC
Financial	MSCI WRLD/FINANCIALS
Industrial	MSCI WRLD/INDUSTRIALS
Government	ITRAXX SOVX GLOBAL LIQUID INVESTMENT GRADE

Table 3.1: Systematic factor - Index mapping.

3.4.2. Synthetic test portfolios

To investigate the properties of the contagion model, we set up 2 test portfolios. For these portfolios, the resulting risk measures are compared to those of the standard latent variable model with no contagion. Portfolio A consists of 1 Russian government bond and 17 bonds issued by corporations registered and operating in the Russian Federation. As it is illustrated in Table 3.2, the issuers are of medium and low credit quality. Portfolio B represents a similar but more diversified setup with 4 sovereign bonds issued by Germany, Italy, the Netherlands, and Spain, and 76 corporate bonds by issuers from the aforementioned countries. The sectors represented in portfolios A and B are shown in Table 3.3. Both portfolios are assumed to be equally weighted with a total notional of €10 million.

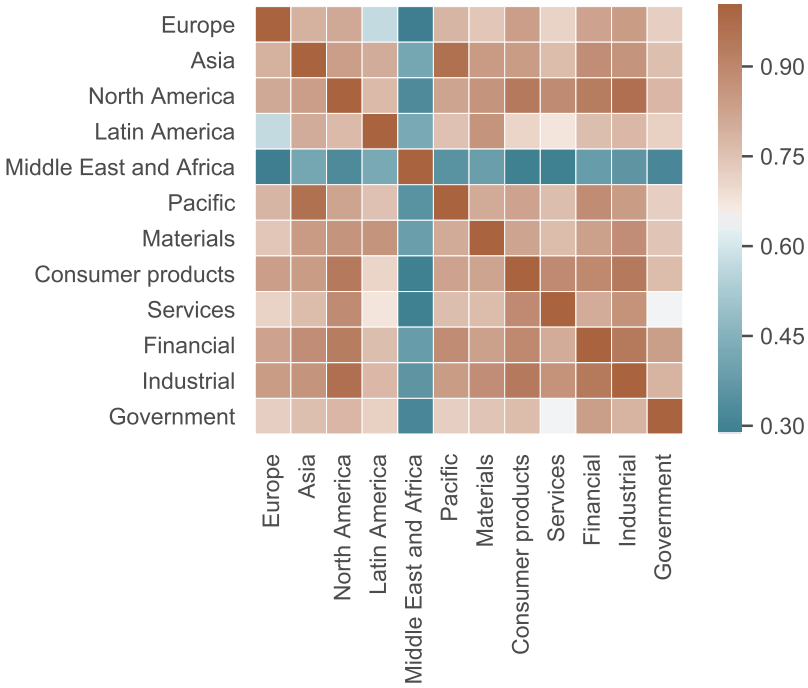

Figure 3.8: Estimated systematic factor correlation matrix $\hat{\Omega}$.

Rating	Portfolio A		Portfolio B	
	Issuers	%	Issuers	%
AAA	-	0.00%	3	3.75%
AA	-	0.00%	3	3.75%
A	-	0.00%	22	27.50%
BBB	1	5.56%	39	48.75%
BB	15	83.33%	9	11.25%
B	2	11.11%	3	3.75%
CCC/C	-	0.00%	1	1.25%

Table 3.2: Rating classification for the test portfolios.

3.4.3. Credit stress propagation network

We use credit default swap data to construct the stress propagation network network. The CDS raw data set consists of daily CDS liquid spreads for different maturities from 1 May 2014 to 31 March 2015 for Portfolio A and 1 July 2014 to 31 December 2015 for Portfolio B. These are averaged quotes from contributors rather than exercisable quotes. In addition, the data set also provides information on the names of the underlying reference entities,

Sector	Portfolio A		Portfolio B	
	Issuers	%	Issuers	%
Materials	5	27.78%	12	15.00%
Consumer products	-	0.00%	12	15.00%
Services	3	16.67%	19	23.75%
Financial	7	38.89%	25	31.25%
Industrial	-	0.00%	6	7.50%
Government	3	16.67%	6	7.50%

Table 3.3: Sector classification for the test portfolios.

recovery rates, number of quote contributors, region, sector, average of the ratings from Standard & Poor's, Moody's, and Fitch Group of each entity and currency of the quote. We use the normalised CDS spreads of entities for the 5 year tenor for our analysis. The CDS spreads time series of Russian issuers are illustrated in Figure 3.4.

3.4.4. Simulation study

In order to generate portfolio loss distributions and derive the associated risk measures we perform Monte Carlo simulations. This process entails generating joint realisations of the systematic and idiosyncratic risk factors, and comparing the resulting critical variables with the corresponding default thresholds. By this comparison we obtain the default indicator Y_i for each issuer and this enables us to calculate the overall portfolio loss for this trial. The only difference between the standard and the contagion model is that in the contagion model we first obtain the default indicators for the sovereigns, and their values determine which default thresholds are going to be used for the corporate issuers. The quantiles of the generated loss distributions as well as the percentage increase due to contagion are illustrated in Table 3.4. A liquidity horizon of 1 year is assumed throughout and the figures are based on a simulation with 10^6 samples.

For Portfolio A, the 99.90% quantile of the loss distribution under the standard factor model is €2,258,857, which corresponds to approximately 23% of the total notional. This figure jumps to €4,968,393 (almost 50% of the notional) under the model with contagion. As shown in Panel 1, contagion has a minimal effect on the 99% quantile, while at 99.5%, 99.90% and 99.99% it results to an increase of 108%, 120%, and 61% respectively. This is to be expected as the probability of default for Russian Federation is less than 1% and thus, in more than 99.9% of our trials default will not take place and contagion will not be triggered. For Portfolio B, the 99.90% quantile is considerably lower under both the standard and the contagion model, at €775,773 or 8% of the total notional and €1,009,426 or 10% of the total notional respectively, reflecting lower default risk. One can observe that the model with contagion yields low additional losses at 99% and 99.5% quantiles, with a more significant impact at 99.90% and 99.99% (30% and 37% respectively). An illustration of the additional losses due to contagion is given by Figure 3.9.

Panel 1: Portfolio A.

Quantile	Loss - standard model	Loss - contagion model	Contagion impact	
99%	1,115,153	1,162,329	47,176	4%
99.50%	1,443,579	3,003,949	1,560,370	108%
99.90%	2,258,857	4,968,393	2,709,536	120%
99.99%	3,543,441	5,713,486	2,170,045	61%
average loss	71,807	71,691		

Panel 2: Portfolio B.

Quantile	Loss - standard model	Loss - contagion model	Contagion impact	
99%	373,013	379,929	6,915	2%
99.50%	471,497	520,467	48,971	10%
99.90%	775,773	1,009,426	233,653	30%
99.99%	1,350,279	1,847,795	497,516	37%
average loss	44,850	44,872		

Table 3.4: Portfolio losses for the test portfolios and additional risk due to contagion.

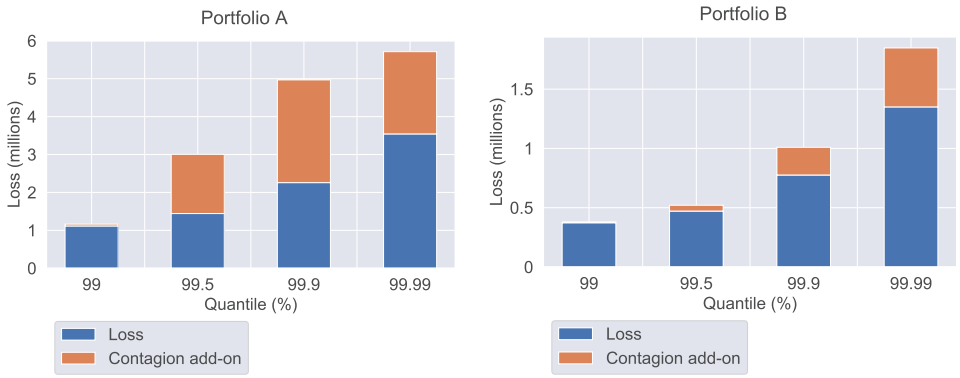

Figure 3.9: Additional losses due to contagion for Portfolios A and B.

3.4.5. Sensitivity analysis

In the following we present a series of sensitivity studies and discuss the results. To achieve a candid comparison, we choose to perform this analysis on the single-sovereign portfolio A. We vary the ratings of sovereign and corporates, as well as the CountryRank parameter, to draw conclusions about their impact on the loss distribution and verify the model properties.

Sovereign rating

We start by exploring the impact of the credit quality of the sovereign. Table 3.5 shows the quantiles of the generated loss distributions under the standard latent variable model and the contagion model when the rating of the Russian Federation is 1 and 2 notches higher than the original rating (BB). It can be seen that the contagion effect appears less strong when the sovereign rating is higher. At the 99.9% quantile, the contagion impact drops from 120% to 62% for an upgraded sovereign rating of BBB. The drop is even higher, when upgrading the sovereign rating to A, with only 11% additional losses due to contagion. Apart from having a less significant impact at the 99.9% quantile, it is clear that, with a sovereign rating of A, the contagion impact is zero at the 99% and 99.5% levels, where the results of the contagion model match those of the standard model. This is to be expected since a rating of A corresponds to a probability of default less than 0.01%, and as explained in 3.4.4, when sovereign default occurs seldom, the contagion effect can hardly be observed.

Sovereign rating	Quantile	Loss standard model	Loss contagion model	Contagion impact	
BB	99%	1,115,153	1,162,329	47,176	4%
	99.50%	1,443,579	3,003,949	1,560,370	108%
	99.90%	2,258,857	4,968,393	2,709,536	120%
	99.99%	3,543,441	5,713,486	2,170,045	61%
BBB	99%	1,115,153	1,115,153	-	0%
	99.50%	1,443,009	1,490,755	47,746	3%
	99.90%	2,229,742	3,613,625	1,383,883	62%
	99.99%	3,496,264	5,432,236	1,935,972	55%
A	99%	1,114,583	1,114,583	-	0%
	99.50%	1,443,009	1,443,009	-	0%
	99.90%	2,229,737	2,469,922	240,185	11%
	99.99%	3,455,199	5,056,639	1,601,439	46%

Table 3.5: Varying the sovereign rating.

Corporate default probabilities

In the next test, the impact of corporate credit quality is investigated. As Table 3.6 illustrates, contagion has smaller impact when the corporate default probabilities are increased by 5%, which is in line with intuition since the autonomous (not sovereign induced) default probabilities are quite high, meaning that they are likely to default whether the corresponding sovereign default or not. For the same reason, the impact is even less significant when the corporate default probabilities are stressed by 10%.

CountryRank

In the last test, the sensitivity of the contagion impact to changes in the CountryRank is investigated. In Table 3.7 we test the contagion impact when CountryRank is stressed

Corporate default probabilities	Quantile	Loss standard model	Loss contagion model	Contagion impact	
Unstressed	99%	1,115,153	1,162,329	47,176	4%
	99.50%	1,443,579	3,003,949	1,560,370	108%
	99.90%	2,258,857	4,968,393	2,709,536	120%
	99.99%	3,543,441	5,713,486	2,170,045	61%
Stressed by 5%	99%	1,115,153	1,250,570	135,417	12%
	99.50%	1,443,579	3,003,949	1,560,370	108%
	99.90%	2,333,935	4,968,393	2,634,458	113%
	99.99%	3,584,506	5,713,486	2,128,979	59%
Stressed by 10%	99%	1,162,329	1,260,422	98,093	8%
	99.50%	1,503,348	3,003,949	1,500,602	100%
	99.90%	2,375,570	4,968,393	2,592,823	109%
	99.99%	3,642,099	5,713,486	2,071,387	57%

Table 3.6: Varying corporate default probabilities.

by 15% and 10% respectively. The results are in line with intuition, with a milder contagion effect for lower CountryRank values and a stronger effect in case the parameter is increased.

CountryRank	Quantile	Loss standard model	Loss contagion model	Contagion impact	
Unstressed	99%	1,115,153	1,162,329	47,176	4%
	99.50%	1,443,579	3,003,949	1,560,370	108%
	99.90%	2,258,857	4,968,393	2,709,536	120%
	99.99%	3,543,441	5,713,486	2,170,045	61%
Stressed by 5%	99%	1,115,153	1,162,329	47,176	4%
	99.50%	1,443,579	3,196,958	1,753,379	121%
	99.90%	2,258,857	5,056,634	2,797,777	124%
	99.99%	3,543,441	5,713,495	2,170,054	61%
Stressed by 10%	99%	1,115,153	1,162,329	47,176	4%
	99.50%	1,443,579	3,389,398	1,945,818	135%
	99.90%	2,258,857	5,296,249	3,037,392	134%
	99.99%	3,543,441	5,801,727	2,258,286	64%

Table 3.7: Varying CountryRank.

3.5. Concluding remarks

In this chapter, we present an extended factor model for portfolio credit risk which offers a breadth of possible applications to regulatory and economic capital calculations, as well as to the analysis of structured credit products. In the proposed framework, systematic risk factors are augmented with an infectious default mechanism which affects the entire portfolio. Unlike models based on copulas with more extreme tail behaviour, where the dependence structure of defaults is specified in advance, our model provides an intuitive approach, by first specifying the way sovereign defaults may affect the default probabilities of corporate issuers, and then deriving the joint default distribution. The impact of sovereign defaults is quantified using a credit stress propagation network constructed from real data. Under this framework, we generate loss distributions for synthetic test portfolios and show that the contagion effect may have a profound impact on the upper tails.

Our model provides a first step towards incorporating network effects in portfolio credit risk models. The model can be extended in a number of ways such as, for instance, accounting for stress propagation from a sovereign to corporates even without sovereign default, or taking into consideration contagion between sovereigns. Another interesting topic for future research is characterising the joint default distribution of issuers in credit stress propagation networks using Bayesian network methodologies, which may facilitate an improved approximation of the conditional default probabilities in comparison to the maximum weight path in the current definition of CountryRank. This research direction is explored in Chapter 4. Finally, a conjecture worthy of further investigation is that a more connected structure for the credit stress propagation network leads to increased values for the CountryRank parameter, and, as a result, to higher additional losses due to contagion.

4

Contagious defaults in a credit portfolio: a Bayesian network approach

The robustness of credit portfolio models is of great interest for financial institutions and regulators, since misspecified models translate to insufficient capital buffers and a crisis-prone financial system. In this chapter, we propose a method to enhance credit portfolio models based on the model of Merton by incorporating contagion effects. While in most models the risks related to financial interconnectedness are neglected, we use Bayesian network methods to uncover the direct and indirect relationships between credits, while maintaining the convenient representation of factor models. A range of techniques to learn the structure and parameters of financial networks from real credit default swaps data are studied and evaluated. Our approach is demonstrated in detail in a stylised portfolio and the impact on standard risk metrics is estimated.

4.1. Introduction

In recent years, there has been an increasing interest in modelling credit risk by practitioners as well as academics (see e.g., [78–83]). Portfolio credit risk models are concerned with the occurrence of large losses due to defaults or deteriorations in credit quality. In practice, these models have a wide range of applications, such as regulatory and economic capital measurements, portfolio management, and risk-adjusted pricing. The robustness of such models is of great interest both for financial institutions and regulators, since misspecified models could lead to insufficient capital buffers, which in turn would result in a crisis-prone financial system and the need for regular bail-outs.

The key challenge in portfolio credit risk modelling is the incorporation of default dependence. Joint defaults of many issuers to which a portfolio is exposed to may lead

Parts of this chapter have been published in Journal of Credit Risk **16**, pp. 1-26 (2020) [P3]

to extreme losses. Therefore, understanding the relationship between default events is crucial. In most portfolio credit risk models existing in the literature, defaults of individual issuers depend on a set of common underlying risk factors; these describe the state of a sector, region, or the economy as a whole. Notable examples of this approach are the Asymptotic Single Risk Factor (ASRF) model ([24]) in the Basel regulations and industrial adaptations of Merton model ([23]) such as the CreditMetrics ([63]) and KMV models ([61, 62]).

Many researchers have challenged the claim that default dependence can be fully explained by dependence on common underlying factors, on the grounds that such models often fail to capture default clustering that does occur from time to time. [66] suggest that in most cases the default correlations that can be achieved with common factors are not as high as the ones in empirical data. [67] perform statistical tests and reject the hypothesis that factor correlations can sufficiently explain the empirically observed default correlations. Thus, it becomes evident that an additional channel of default dependence needs to be considered.

Besides dependence on common factors, joint defaults might occur as a result of direct links between issuers, a phenomenon known as contagion. [70] were among the first to introduce contagion in credit risk models by considering that any default might infect another issuer in the portfolio. [73] tried to generalise already existing models, included particular specifications of the issuers and focused on their effect on bonds and credit derivatives. [74] introduced network theory to allow for a variety of infections, however the model required detailed information making its application more difficult than expected.

Following the financial crisis, there has been a significant interest in using network-based methods for financial stability and systemic risk (see e.g., [1, 14, 76, 84–86]). Next to network models, there is a growing literature on particle systems with mean-field interaction, considered, e.g., in [87–91]. Nevertheless, the use of these methods for valuation and measurement of risk charges such as capital is limited. In Chapter 3 we introduced a portfolio credit risk model that can account for both channels of default dependence: common underlying factors and contagion from sovereigns to corporates and sub-sovereigns. We augmented systematic risk factors with a contagious default mechanism where the default probabilities of issuers in the portfolio are immediately affected by a sovereign default. To estimate the contagion effect we used a network constructed from CDS time series and introduced CountryRank, a network based metric that approximates the probability of default of a node conditional on the infectious default of a sovereign. The chapter presents a thorough approach of how contagion effects can be introduced to portfolio credit risk modes using complex networks. However, the underlying network in Chapter 3 is based on one-to-one relationships between issuers. While this can capture the direct relationships effectively, it is well-known that the associations between entities might be indirect and often mediated through others. In this chapter we use Probabilistic Graphical Models (PGM) to learn the network using the data in a holistic manner. This extends the one-to-one approach and provides a more natural and accurate representation of the network. Moreover, we can efficiently approximate the joint default probability distribution of the issuers in a PGM.

PGMs are a powerful framework for representing complex relationships using prob-

ability distributions. Their ability to model associations in complex datasets has proven them particularly useful for a wide range of machine learning problems, including natural language processing ([92]), medical diagnosis ([93]), and genetic linkage analysis ([94]). One of the most important classes of PGMs is Bayesian networks (BNs). More recently, there have been attempts to utilise BNs for solving financial problems. In particular, [95] presented a method to calculate portfolio losses in the presence of stress events using BNs. Nevertheless, his approach, relies on the ability of the risk manager to identify causal links and subjectively assign probabilities. [96] developed a structural default model for interconnected financial institutions, but the need for balance sheet data makes its applicability limited. [97] used credit default swaps (CDS) data to learn the structure of interbank networks, which would enable policy makers to make decisions on the too-big-to-fail problem. In order to learn the BN, the author uses the log of CDS spreads under the assumption of normality. However, this strong assumption is barely supported by empirical evidence.

In this chapter, we overcome the need for making assumptions about the distribution of CDS spreads by introducing a discretisation method based on the notion of *modified ϵ-drawups* (see Section 3.3.2). This transformation enables us to utilise algorithms for structure and parameter learning that assume discrete random variables, without having to sacrifice the interpretability of the resulting models. We use the discretised CDS time series to learn a BN of interactions between issuers, and to estimate the contagion effects following a sovereign default. Different techniques to learn the structure and parameters of financial networks are studied and evaluated, with the results confirming that the structures are robust. In order to investigate the impact of these effects on credit losses, we carry out simulations and calculate the quantiles of the loss distribution in the presence of contagion. Finally, we perform a comparative analysis with the results obtained in Chapter 3.

The rest of the chapter is organised as follows. Section 4.2 presents BNs and outlines the methods for learning their structure and parameters. Section 4.3 demonstrates a method to learn BNs for CDS data. In Section 4.4, we present empirical analysis on a synthetic test portfolio. Finally, in Section 4.5 we summarise and draw conclusions. Additional information is included in the Appendices.

4.2. Bayesian networks

A Bayesian network (BN) is a graphical model that allows us to represent and reason about an uncertain domain. The nodes in a BN represent random variables, and the edges represent the direct dependencies between variables [98].

The graphical structure $\mathcal{G} = (\mathcal{V}, \mathcal{E})$ of a BN is a *directed acyclic graph* (DAG), where $\mathcal{V} = \{X_1, ..., X_n\}$ is a finite vertex set and $\mathcal{E} \subseteq \{(i, j) : X_i, X_j \in \mathcal{V}, i \neq j\}$ is a set of edges without any self-loops. The DAG defines a factorisation of the joint probability distribution of $\mathcal{V}$, into a set of local probability distributions, one for each variable. The form of the factorisation states that every random variable X_i directly depends only on its parents Pa_{X_i}:

$$P(X_1, \ldots, X_n) = \prod_{i=1}^{n} P(X_i | \text{Pa}_{X_i}) \tag{4.1}$$

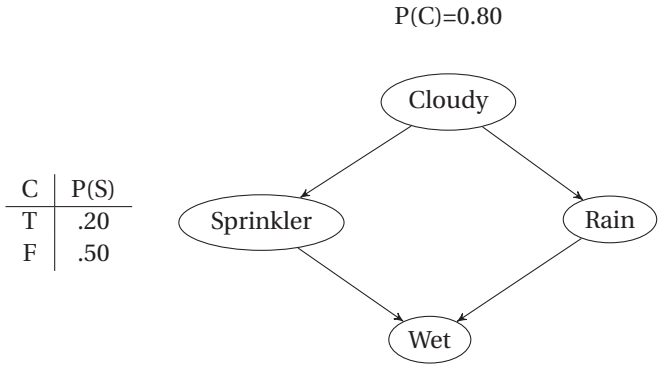

C	P(S)
T	.20
F	.50

C	P(R)
T	0.60
F	0.10

S	R	P(W)
T	T	0.99
T	F	0.90
F	T	0.90
F	F	0.00

Figure 4.1: A Bayesian network with Conditional Probability Tables (CPTs).

BNs have a useful property of *conditional independence* that allows us to represent a joint distribution in a tractable manner. For example, even if the random variables $X_1, \ldots, X_n$ follow a binomial distribution, we would need $2^n - 1$ probabilities to represent their joint distribution. With a BN, the order of representation of joint distribution is linear in the number of variables.

In order to demonstrate this representation, we provide a commonly used example from [99], illustrated in Figure 4.1. We consider that the grass can appear wet in the morning either because the sprinkler was on during the night or because it rained. Note that these events are not mutually exclusive: it is possible that the sprinkler was on and it rained at the same time. Thus, we have two binary-valued random variables, *Sprinkler* (S) and *Rain* (R). In addition, we have two binary-valued variables, *Cloudy* (C) and *Wet* (W), which are correlated to both *Sprinkler* and *Rain*. The strength of these relationships is shown in the Conditional Probability Tables (CPTs). For example, we see that $P(W|S,R) = 0.99$, and thus, $P(\neg W|S,R) = 1 - 0.99 = 0.01$. Since the C node has no parents, its CPT specifies the prior probability that it is cloudy, which in this case is equal to 0.5. Overall, our probability space has $2^4 = 16$ values which correspond to all the possible assignments of these four variables. By the chain rule of probability, the joint probability of all the nodes in the graph is:

$$P(C,S,R,W) = P(C)P(S|C)P(R|C,S)P(W|C,S,R). \tag{4.2}$$

By using conditional independence relationships, this can be rewritten as:

$$P(C,S,R,W) = P(C)P(S|C)P(R|C)P(W|S,R), \tag{4.3}$$

where it was possible to simplify the third term because *Rain* is independent of *Sprinkler*

given its parent *Cloudy*, and the last term because *Wet* is independent of *Cloudy* given its parents *Season* and *Rain*. Thus, it is clear that the conditional independence relationships allow for a more compact representation of the joint probability distribution.

Although, in theory, there are many possible options for the distributions of the random variables in a BN, the literature has mainly focused on two cases [100]:

- *Multinomial variables*: this representation is used for discrete/categorical data and is often referred to as the discrete case. This assumption is the most common in the literature, and its corresponding Bayesian networks are called discrete Bayesian networks.

- *Multivariate normal variables*: this representation is used for continuous data and therefore referred to as the continuous case. These Bayesian networks are referred to as Gaussian Bayesian networks.

In this work, the nodes in BNs represent random variables characterising issuers of debt and the edges how these issuers influence each other. More specifically, the random variables of interest are the probabilities of default. It should be noted that, since BNs are DAGs, the existence of cycles or loops is neglected in our analysis. It can be argued, however, that the magnitude of such second order effects may be negligible as far as the contagion process is concerned[1]. To learn the structure and parameters of the BNs we use time series of CDS spreads. The rest of this section describes the process of learning the structure and parameters of a BN from data.

4.2.1. Learning

In order to estimate the joint probability distribution from a BN, we first need to learn both the structure and the parameters of the network from data. We will explain the parameter learning followed by structure learning. The reason for this order is the use of some parameter estimation techniques in the latter.

Parameter learning. Suppose we have a collection of n random variables $X_1,\dots,X_n$ such that the number of states of the random variable X_i are $1,2,\dots,r_i$ and the number of configurations of parents of X_i are $1,2,\dots,q_i$. The parameters which have to be estimated in this case are:

$$\theta_{ijk} = P(X_i = j \,|\, \mathrm{Pa}_{X_i} = k), \qquad i \in \{1,\dots,n\},\ j \in \{1,\dots,r_i\} \text{ and } k \in \{1,\dots,q_i\}.$$

We use $\theta_{\mathcal{G}} = \{\theta_{ijk} \,|\, i \in \{1,\dots,n\},\ j \in \{1,\dots,r_i\},\ k \in \{1,\dots,q_i\}\}$ to denote the parameter vector.

[1] Several contributions in the contagion literature, for instance [101–104], take advantage of conditional independence relationships in order to approximate the probability of contagion with a closed-form expression. The authors of the above papers test their approximations to the contagion probability when applied to finite networks that entail cycles by performing numerical simulations, and show that the analytic approximations work surprisingly well. These results can be seen as a test on the actual relevance of second order, cycle effects in contagion processes. Taking this into consideration, we believe that we can neglect the existence of cycles in our financial networks without compromising our contagion analysis.

Let us assume that we know the structure of a BN. There are two different methods for learning the parameters: Maximum Likelihood Estimation (MLE) and Bayesian estimation. MLE is based on choosing the parameters which maximise the likelihood of the data. Given a data set $\mathscr{D}$, the MLE method chooses parameters $\hat{\theta}_{\mathscr{G}}$ such that:

$$\hat{\theta}_{\mathscr{G}} = \arg\max_{\theta_{\mathscr{G}} \in \Theta_{\mathscr{G}}} L(\theta_{\mathscr{G}} : \mathscr{D}) = \arg\max_{\theta_{\mathscr{G}} \in \Theta_{\mathscr{G}}} P(\mathscr{D} : \theta_{\mathscr{G}}) = \arg\max_{\theta_{\mathscr{G}} \in \Theta_{\mathscr{G}}} \prod_m P(\xi[m] : \theta_{\mathscr{G}}),$$

where $\Theta_{\mathscr{G}}$ is the space of possible values of $\theta_{\mathscr{G}}$, $\xi[m]$ is the m-th instance of $\mathscr{D}$.

The alternative Bayesian estimation method is based on assuming a prior distribution over the parameters $P(\theta_{\mathscr{G}})$, and updating it with each instance of the data to obtain the posterior distribution, $P(\theta_{\mathscr{G}} \,|\, \mathscr{D})$ using the Bayes rule as follows:

$$P(\theta_{\mathscr{G}} \,|\, \xi[1], \ldots, \xi[M]) = \frac{P(\xi[1], \ldots, \xi[M] \,|\, \theta_{\mathscr{G}})\, P(\theta_{\mathscr{G}})}{P(\xi[1], \ldots, \xi[M])}, \tag{4.4}$$

where the denominator is a normalising factor and $P(\xi[1], \ldots, \xi[M] \,|\, \theta_{\mathscr{G}})$ is the likelihood.

The choice of the prior distribution is key for the Bayesian estimation procedure. From Equation 4.4, we can see that the posterior distribution is proportional to the product of the likelihood and the prior. Therefore, we need to choose the prior in such a way that it can be updated easily after each new sample, while maintaining the form of the posterior distribution. It is well-known that the Dirichlet distribution is the conjugate prior for the multinomial distribution ([105, Section 17.3.2]), which means that if the prior distribution of the multinomial parameters is Dirichlet then the posterior distribution is also a Dirichlet distribution. Since we deal with multinomial variables in our case, we choose a Dirichlet distribution as the prior for our experiments.

Structure learning. The structure learning for a BN is essentially an optimisation problem where we minimise a score over the search space of possible configurations of the network. The score measures how likely a particular structure is based on the data, and is divided into two categories: likelihood scores and Bayesian scores.

The likelihood scores rely mainly on the likelihood function, which is the probability of sampling the data given the structure, $L(\mathscr{G} \,|\, \mathscr{D}) = P(\mathscr{D} \,|\, \mathscr{G})$. The notation $\langle \mathscr{G}, \theta_{\mathscr{G}} \rangle$ denotes a BN, where $\mathscr{G}$ represents the structure and $\theta_{\mathscr{G}}$ the parameters of the network. The structure of the network is chosen so as to maximise the likelihood score, using the MLE parameters.

$$\max_{\mathscr{G}, \theta_{\mathscr{G}}} L(\langle \mathscr{G}, \theta_{\mathscr{G}} \rangle : \mathscr{D}) = \max_{\mathscr{G}} \left[\max_{\theta_{\mathscr{G}}} L(\langle \mathscr{G}, \theta_{\mathscr{G}} \rangle : \mathscr{D}) \right] = \max_{\mathscr{G}} L(\langle \mathscr{G}, \hat{\theta}_{\mathscr{G}} \rangle : \mathscr{D}).$$

The Bayesian scores have a similar approach as the Bayesian estimation for the parameters. First, we define a prior distribution over the structure $P(\mathscr{G})$ and a conditional prior over the parameters $P(\theta_{\mathscr{G}} \,|\, \mathscr{G})$. Then, we obtain the posterior distribution $P(\mathscr{G} \,|\, \mathscr{D})$ using the Bayes rule. Similar to the Bayesian estimation for the parameters, the denominator is a normalising factor and it remains the same for all the structures. Then, the score can be defined by taking the logarithm of the numerator:

$$\text{score}_B(\mathscr{G} : \mathscr{D}) = \log P(\mathscr{D} \,|\, \mathscr{G}) + \log P(\mathscr{G}),$$

where the second term, the prior, makes no significant difference in the score (see, e.g. [105, Section 18.3.2]). The first term, called *marginal likelihood*, is the average over all the possible choices of $\theta_{\mathcal{G}}$ based on the conditional probability provided before:

$$P(\mathcal{D} \mid \mathcal{G}) = \int_{\Theta_{\mathcal{G}}} P(\mathcal{D} \mid \theta_{\mathcal{G}}, \mathcal{G})\, P(\theta_{\mathcal{G}} \mid \mathcal{G})\, d\theta_{\mathcal{G}}. \tag{4.5}$$

The average over all the possible parameters makes the model more conservative, and hence it tries to avoid overfitting as we take into account the sensitivity to the values of the parameters.

Finally, we briefly describe the search space and the optimisation procedure for structure learning. The search space is a network itself where each of the nodes is a candidate structure $\mathcal{G}$. Given a node $\mathcal{G}$ corresponding to a structure in the search space network, the neighbours of $\mathcal{G}$ are structures obtained by either adding an edge, deleting an edge or reversing an edge. The Hill-Climbing algorithm follows the steps below:

1. Set initial BN structure to a network without edges $\mathcal{G}$.
2. Compute its score.
3. Consider all the neighbours of $\mathcal{G}$, obtained by either adding, deleting or reversing an edge in $\mathcal{G}$.
4. Choose the neighbour $\mathcal{G}_{\text{best}}$ which leads to the best improvement in the score.
5. Set $\mathcal{G} \leftarrow \mathcal{G}_{\text{best}}$ and repeat until no further improvement to the score is possible.

Some improvements can be made to this algorithm: ([105, Section 18.4.3], [106]).

4.3. Learning Bayesian networks from CDS data

As mentioned in Section 4.2, the BN literature has mostly focused on multinomial and multivariate normal data. In [97], the authors make the assumption that the residuals of the regressions on the log returns of the CDS spreads are normally distributed which is not supported by empirical data. In this work, we choose to work with discrete Bayesian networks. Therefore, we transform the continuous CDS time series data into a discrete distribution.

4.3.1. CDS dataset

The data used for the construction of the network are credit default swaps (CDS) spreads for different maturities obtained from Markit. These consist of daily CDS liquid spreads of Russian issuers from September 14$^{\text{th}}$ 2010 until August 15$^{\text{th}}$ 2015. This period is of particular interest because of the financial crisis in Russia in 2014-2015, which followed a sharp depreciation of the Russian ruble. Apart from the spreads, the dataset also includes information about the recovery rates, region, sector and average of the ratings from Standard & Poor's, Moody's, and Fitch Ratings for each issuer. We use the CDS spreads of issuers for the 5 year tenor for our analysis, since they are the most liquid quotes. Since recovery rates are not the same for all issuers, we have to normalise CDS spreads to do a

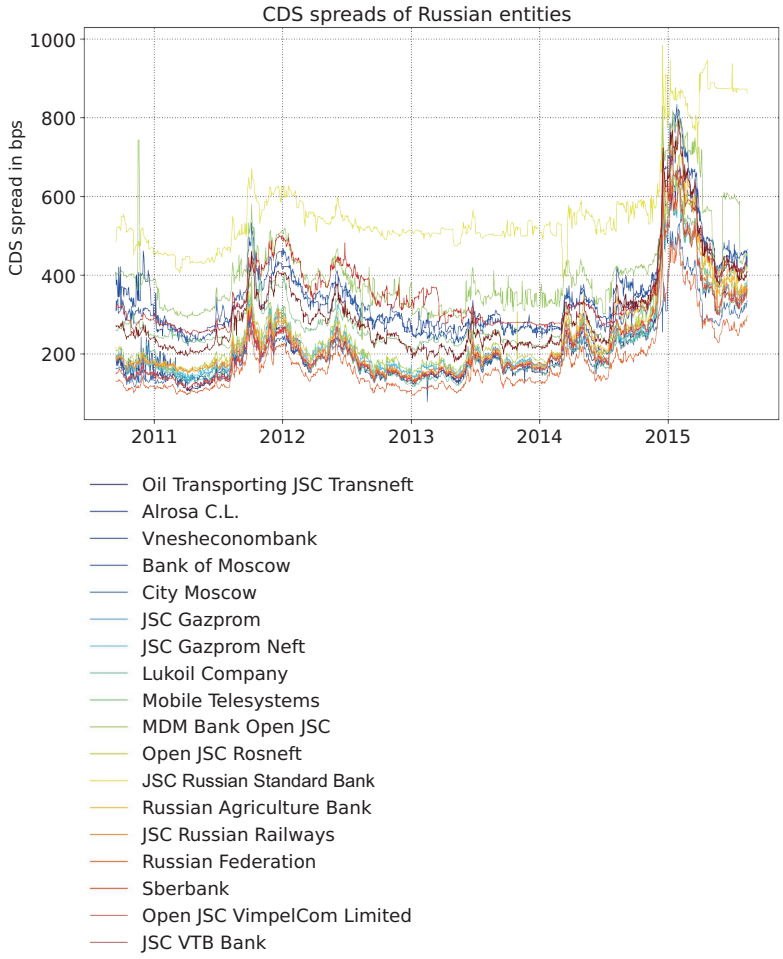

Figure 4.2: Normalised five year CDS spread of Russian issuers.

consistent analysis. The normalisation of CDS spreads for the recovery rate RR is done as follows:

$$\widehat{S} = S\frac{0.6}{(1-RR)}, \tag{4.6}$$

where $\widehat{S}$ denotes the normalised CDS spread, which corresponds to a recovery rate of 40%. The choice of normalising the CDS spreads using a recovery rate of 40% is based on the literature (see e.g., [107]) where the recovery rate is often assumed to be a constant. We use the normalised CDS spread of the five year tenor in our analysis. Figure 4.2 shows the normalised spreads for the Russian issuers in the portfolio.

4.3.2. Discretisation of CDS data

We use the notion of modified ϵ-drawups to transform the continuous CDS time series data into a discrete distribution. Modified ϵ-drawups build up on the notion of ϵ-drawups ([77, 108]) and can detect instances in the time series where significant upward jumps are present. For a more detailed definition of modified ϵ-drawups, the reader is refereed to Section 3.3.2. Note that, in the context of CDS spreads, upward jumps translate to rapid deteriorations in credit quality.

The CDS data can be transformed into a discrete distribution for learning the BN as follows. Firstly, we compute the modified ϵ-drawups for each of the time series. The ϵ parameter at time t is set to be the standard deviation in the time series between days $t-n$ and t, where n is chosen to be 10 days consistent with Chapter 3. Thus, each issuer i will either have either a modified ϵ-drawup at time t or nothing. We define a binary random variable X_i^t corresponding to the issuer i such that $X_i^t = 1$, if issuer i has a modified ϵ-drawup on day t, and 0, otherwise. Note that an issuer cannot have two modified ϵ-drawups on consecutive days by definition.

An additional step which is necessary to prepare the CDS data for learning the co-dependence of defaults is to introduce the concept of time-lag. This allows us to capture the fact that issuers can impact each other with a slight delay. For time-lag, we introduce a new categorical value, 0.5, in the following way. Let a company i have a modified ϵ-drawup on day t, so $X_i^t = 1$. If a different company j has a modified ϵ-drawup on at least one of the following three days, $t+1$, $t+2$ or $t+3$, and not on day t, then we set $X_j^t = 0.5$. Hence, the number of modified ϵ-drawups in the time series remains unchanged which ensures that the marginal probability of having a modified ϵ-drawup remains unchanged.

4.3.3. Bayesian network learning

To learn the structure of the network we use the Hill-Climbing algorithm based on two different scores: Bayesian Information Criterion (BIC) ([109]) which is a likelihood score, and Bayesian Dirichlet Sparse (BDs) ([110]), which is a Bayesian score. We refer to Section B.1 in the Appendix for details on the two scores.

To learn the network, we also applied a bootstrapping technique for ensuring the robustness of results ([111]). For the structure learning, we obtain the structure 1000 times and then we compute the average structure by including the edges which appear in at least 50% of the networks. The data set $\mathscr{D}_k$ used at iteration k is obtained by uniform sampling of $|\mathscr{D}|$ instances from the original training data $\mathscr{D}$.

Once the BN is learnt, we can evaluate the queries for conditional probabilities $P(Q|E)$, of events Q given evidence[2] E. To perform these queries, we use the logic sampling algorithm [112] which has the following steps. First, it orders the variables in the topological order implied by the structure $\mathscr{G}$. This means that the variables with no parents appear first followed by their children. Next, we set the counters $n_E = 0$ and $n_{E,Q} = 0$. Afterwards we generate a sufficiently large number of samples M where each sample consists of a vector of instances of all the random variables in the network. Note that generating the instance for X_i only requires the values of Pa_{X_i}. Then, for each sample if it includes E, set $n_E = n_E + 1$, and, if it includes both Q and E, set $n_{Q,E} = n_{Q,E} + 1$. Finally,

[2] An *event* in the BN terminology refers to a (some) random variable(s) taking a particular value(s). An *evidence* is mathematically the same as an event with the difference that it is known.

we can estimate $P(Q|E)$ by $n_{Q,E}/n_E$. This method is based on a Monte Carlo simulation, therefore a sufficiently large number of simulations is needed to assure a reliable result.

4.4. Numerical study

In this section we describe the setup of the problem and the results obtained in the calibrations and simulations.

4.4.1. Bayesian network learning and robustness

We use CDS data as described in Section 4.3 to learn the structure and the parameters of the BN. The `bnlearn` ([113]) library in R is used for the Hill-Climbing procedure. The numerical experiments were performed using two scores: BDs and BIC. Both scores resulted in similar structure of the network as shown in Figure 4.3, except for one edge: GAZPRU.Gneft → AKT which is present in the network learnt with BIC, whereas with BDs it is substituted by CITMOS → AKT, as we can see in Figure 4.3.

After learning the network, the next step is to estimate the conditional probability of default of an issuer, conditional on the default of the sovereign. In order to estimate these probabilities we run a Monte Carlo simulation of 100 iterations. For each of these iterations, we calculate the conditional probability using 4×10^5 samples. Finally, we take the mean of the Monte Carlo simulations as an estimate for conditional probabilities. We compare the probabilities for both BIC and BDs scores including mean, standard deviation and absolute difference in Table 4.1. Figure 4.4 shows the structure, with the nodes coloured according to their probability of default given sovereign default. The darker the colour of the node, the higher is the probability of default of the node conditional on sovereign default. We see that Gazprom and Gazprom Neft, the two nodes connected to the sovereign, are the ones more affected and the issuers which are further from the sovereign have relatively lower conditional default probabilities.

We observe that the standard deviation of the conditional probabilities estimates is quite small for all the issuers, ranging between 0.002 and 0.0035. This implies that the estimates are quite robust, and gives us a strong confidence on the reliability of the results. Moreover, we notice that the absolute difference of the probabilities from the two scores is smaller than the standard deviation except in two cases.

The main difference we note in the table has to do with Transneft, whose probability of default conditional on sovereign default decreases by more than 0.07 when changing the score from BIC to BDs. This is caused by the change in the structure, which directly affects this issuer. For the BIC score, Gazprom Neft is a parent of Transneft whereas City Moscow is not, and using BDs score it is the other way around. We see that with both scores Gazprom Neft is more affected by the sovereign default than City Moscow. This is also a confirmation of the fact that the stress spreads faster from one issuer to another if they are directly connected. The second difference in conditional probability has to do with MDM Bank. If we look at the structures, we see that MDM has only one parent, which is Transneft. As the parent (Transneft) is less affected in the structure learnt by BDs, its child also being less affected is in line with intuition. This causes a small but still noticeable difference in the conditional probabilities.

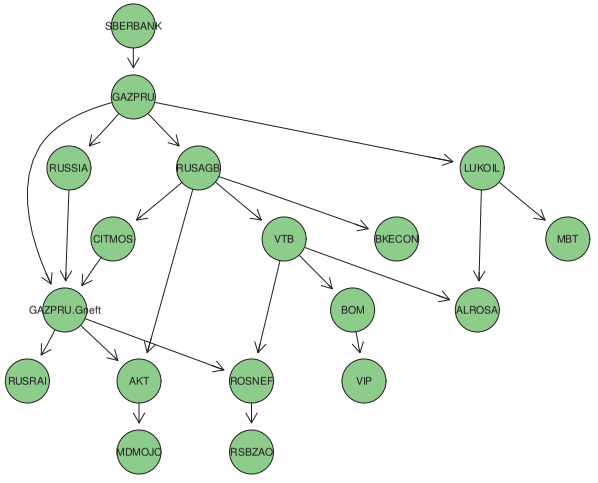

(a) Structure with BIC score.

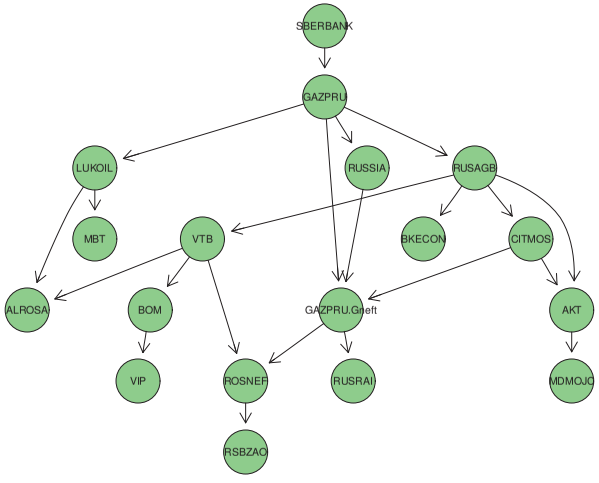

(b) Structure with BDs score.

Figure 4.3: Structure obtained with the different scores. Note that the visualisation system is mirroring the plot but close inspection reveals that the structure is not that different.

4.4.2. Comparative analysis

To investigate the impact of the contagion effects estimated using BNs on credit losses, we use the multi-factor Merton model described in Sections 3.2 and 3.3. We perform our numerical experiments for a Portfolio A from Chapter 3, consisting of 1 Russian government bond and 17 bonds issued by corporations registered and operating in the Russian Federation. The resulting risk measures for this portfolio are compared to those of the standard latent variable model with no contagion. Details on the credit quality of the issuers in the portfolio can be found in Table 3.2. The sectors represented are shown in table 3.3. The portfolio is assumed to be equally weighted with a total notional of €10 million.

In order to generate portfolio loss distributions and derive the associated risk measures we perform Monte Carlo simulations. This process entails generating joint realisations of the systematic and idiosyncratic risk factors, and comparing the resulting critical variables with the corresponding default thresholds. By this comparison we obtain the default indicator Y_i for each issuer and this enables us to calculate the overall portfolio loss for this trial. The only difference between the standard and the contagion model is that in the contagion model we first obtain the default indicators for the sovereigns, and their values determine which default thresholds are going to be used for the corporate issuers. A liquidity horizon of 1 year is assumed throughout and the figures are based on a simulation with 10^6 samples. Moreover, for the results shown we used the probabilities of default computed with the structure learnt via the BIC score. However, this choice does not make any notable difference in the quantiles of the loss distribution because the probabilities were almost the same and such tiny difference would not cause a large disturbance.

We compared the BN model with the CountryRank model of Chapter 3. In Table 4.2 we can observe the differences between the probabilities obtained with both methods, using the same data, and same parameters: 10 days to compute the standard deviation and 3 days as time lag. Following the sensitivity analysis in Chapter 3 we can expect that the 15% increase of the mean will not have a substantial impact on the quantiles of the loss distribution. This hypothesis can be confirmed by the results shown in Table 4.3 and the graph depicted in Figure 4.5.

4.5. Concluding remarks

In this chapter, we presented a novel method of estimating contagion effects from CDS data using BNs. Rather than assuming a certain distribution for CDS spreads, we introduced a method for learning BNs using ϵ-drawups. Different techniques to learn the structure and parameters of financial networks were studied and evaluated. We used CDS spreads of issuers in a stylised portfolio and incorporated the conditional probabilities in the credit portfolio model presented in Chapter 3. Simulations were carried out for a stylised portfolio and the impact on standard risk metrics was estimated. Contagion was shown to have a significant impact in the tails of the credit loss distribution, with the results being in line with results obtained by using the CountryRank metric.

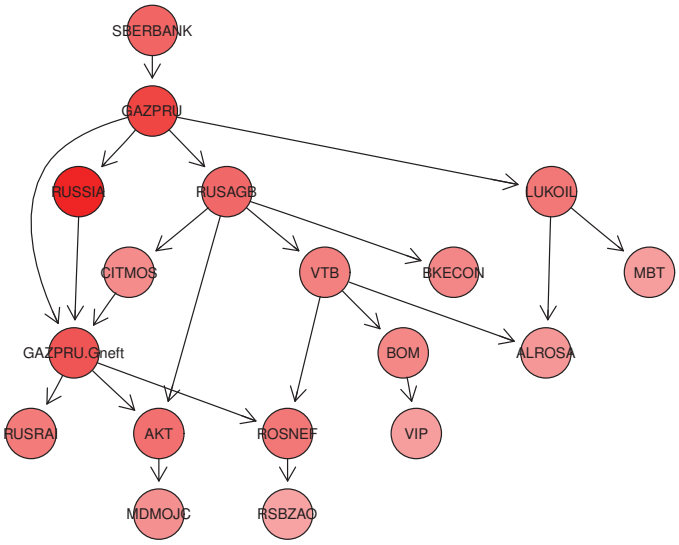

Figure 4.4: Bayesian network learnt with BIC with coloured nodes according to its probability of default given sovereign default. Note that having a darker colour means that the node has a higher conditional probability of default.

Order	Issuer	BIC		BDs		Abs diff
		γ_C	s.d.	γ_C	s.d.	
1	JSC Gazprom	0.7824	0.0030	0.7809	0.0028	0.0015
2	JSC Gazprom Neft	0.7024	0.0026	0.7018	0.0028	0.0006
3	Sberbank	0.6260	0.0034	0.6261	0.0032	0.0001
4	Russian Agriculture Bank	0.6165	0.0032	0.6167	0.0030	0.0002
5	Oil Transporting JSC Transneft	0.5754	0.0025	0.4983	0.0026	0.0771
6	Lukoil Company	0.5417	0.0024	0.5410	0.0023	0.0007
7	Open JSC Rosneft	0.5394	0.0030	0.5407	0.0025	0.0013
8	JSC Russian Railways	0.5186	0.0029	0.5189	0.0025	0.0003
9	JSC VTB Bank	0.4913	0.0027	0.4911	0.0030	0.0002
10	Vnesheconombank	0.4583	0.0028	0.4583	0.0024	$< 10^{-4}$
11	Bank of Moscow	0.4576	0.0027	0.4572	0.0025	0.0004
12	City Moscow	0.4377	0.0031	0.4375	0.0025	0.0002
13	MDM Bank Open JSC	0.4251	0.0026	0.4028	0.0032	0.0223
14	Alrosa C.L.	0.3890	0.0025	0.3885	0.0028	0.0005
15	Mobile Telesystems	0.3542	0.0025	0.3540	0.0023	0.0002
16	Open JSC VimpelCom Limited	0.3523	0.0022	0.3524	0.0023	0.0001
17	JSC Russian Standard Bank	0.3290	0.0024	0.3296	0.0021	0.0006

Table 4.1: Probabilities of default given sovereign default with BIC and BDs score.

Order	Issuer	BN	CountryRank	Diff
1	JSC Gazprom	0.7824	0.6220	0.1585
2	JSC Gazprom Neft	0.7024	0.5610	0.1415
3	Sberbank	0.6260	0.5854	0.0406
4	Russian Agric Bank	0.6165	0.5854	0.0312
5	Oil Transporting JSC Transneft	0.5754	0.5732	0.0022
6	Lukoil Company	0.5417	0.3381	0.2036
7	Open JSC Rosneft	0.5394	0.5244	0.0150
8	JSC Russian Railways	0.5186	0.5427	-0.0241
9	JSC VTB Bk	0.4913	0.6098	-0.1184
10	Vnesheconombank	0.4583	0.3339	0.1244
11	Bank of Moscow	0.4576	0.5305	-0.0729
12	City Moscow	0.4377	0.5122	-0.0745
13	MDM Bk Open JSC	0.4251	0.3131	0.1120
14	Alrosa C.L.	0.3890	0.2293	0.1596
15	Mobile Telesystems	0.3542	0.2446	0.1096
16	Open JSC VimpelCom Limited	0.3523	0.2964	0.0559
17	JSC Russian Standard Bank	0.3290	0.0869	0.2420
	Mean	0.5056	0.4405	0.0651

Table 4.2: Comparison of γ_C using BN and CountryRank model.

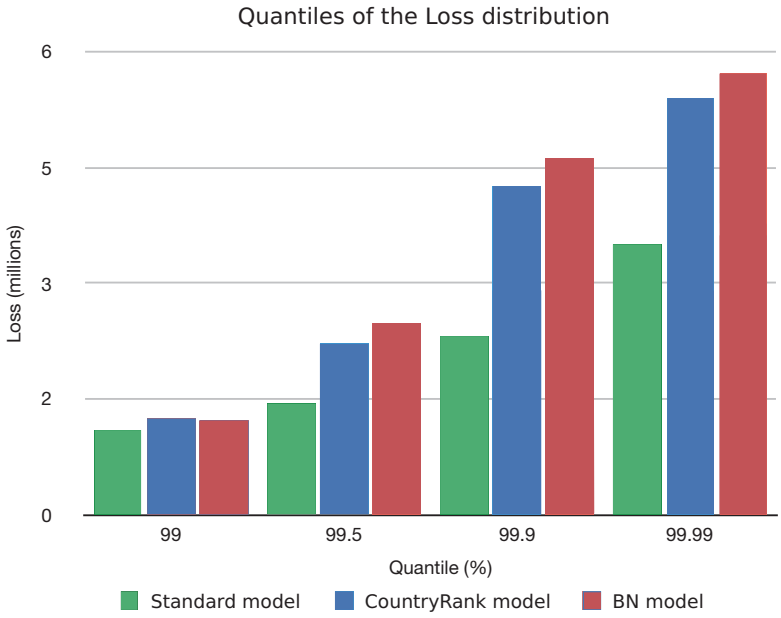

Figure 4.5: Quantiles of the Loss distribution without and with contagion with the BN and the CountryRank model.

Quantile	BN model Contagion impact		CountryRank model Contagion impact	
99%	117,341	11%	124,903	11%
99.5%	1,054,844	73%	769,694	53%
99.9%	2,302,667	99%	1,930,166	83%
99.99%	2,198,517	63%	1,883,240	54%

Table 4.3: Comparison of the contagion impact using Bayesian networks and CountryRank model.

The results presented are a first step in the application of BNs on portfolio credit risk models. However, the BN framework we developed is flexible enough to allow for wider applications. For instance, one can extend the contagion so that stress originates from any issuer and not only at the sovereign. Moreover, one can test scenarios where multiple issuers default. Two examples of such scenarios can be found in the Appendix B.2. These applications can be particularly useful for risk managers, who are often interested in building scenarios for catastrophic risks and testing the resilience of their portfolios to such scenarios.

In order to extend our analysis, we plan to further investigate applications of the developed probabilistic framework in problems beyond credit portfolio modelling. A promising direction looks to be using our framework in order to identify systemically important nodes in the financial system and measure systemic risk. This could be done by considering, in a recursive manner, the fact that a node is more systemically important if it impacts many systemically important nodes. Another interesting direction is the modelling of wrong-way risk (WWR) arising in the case of a sovereign default in the pricing of Credit Valuation Adjustment (CVA) and Funding Valuation Adjustment (FVA) for interest-rate and foreign exchange derivatives.

5

Community structure of the credit default swap market and portfolio default risk

One of the most challenging aspects in the analysis and modelling of financial markets, including Credit Default Swap (CDS) markets, is the presence of an emergent, intermediate level of structure standing in between the microscopic dynamics of individual financial entities and the macroscopic dynamics of the market as a whole. This elusive, mesoscopic level of organisation is often sought for via factor models that ultimately decompose the market according to geographic regions and economic industries. However, at a more general level the presence of mesoscopic structure might be revealed in an entirely data-driven approach, looking for a modular and possibly hierarchical organisation of the empirical correlation matrix between financial time series. The crucial ingredient in such an approach is the definition of an appropriate null model for the correlation matrix. Recent research showed that community detection techniques developed for networks become intrinsically biased when applied to correlation matrices. For this reason, a method based on Random Matrix Theory has been developed, which identifies the optimal hierarchical decomposition of the system into internally correlated and mutually anti-correlated communities. Building upon this technique, here we resolve the mesoscopic structure of the CDS market and identify groups of issuers that cannot be traced back to standard industry/region taxonomies, thereby being inaccessible to standard factor models. We use this decomposition to introduce a novel default risk model that is shown to outperform more traditional alternatives.

Parts of this chapter are based on [P4]

5.1. Introduction

The financial crisis of 2007-08 laid bare the downside of a highly interconnected financial system by evidencing that each link constitutes a channel through which shocks can propagate rapidly across markets and asset classes. This has been popularised by the *too-interconnected-to-fail* motto, stressing the impact that the failure of a highly central node would have on the rest of the network. Capturing financial complexity within models has been a major challenge since, for financial institutions and regulators alike.

Complexity-inspired models rest upon the evidence that economic and financial systems have many of the key properties characterising *natural* complex systems: they are composed by many heterogeneous units that interact with each other in a non-linear fashion, usually in the presence of feedback ([114, 115]). A tractable framework for the quantitative analysis of many complex systems is provided by *networks*. Techniques from network theory have been used to study a variety of financial assets, including equities ([115–117]), exchange rates ([118, 119]), commodities ([120]), bonds ([121]) and interest rates ([122]); however, despite the growing literature on networks in finance, the effort for incorporating these techniques in models used for the pricing and risk management of individual portfolios has remained at a very early stage, as seen in the previous chapters.

In addition to the complexity of the financial system, the global financial crisis uncovered the significant weaknesses of the regulatory framework for capitalising risks from trading activities. Since the onset of the crisis, a major source of losses and of the build up of leverage transpired in the trading book: an instrumental factor was that the existing capital framework for market risk, based on the 1996 Amendment to the Capital Accord to incorporate market risks ([123]), was not able to capture some key risks. In 2009, the Basel Committee on Banking Supervision introduced a set of revisions to the market risk framework to address the most crucial shortcomings, commonly referred to as the Basel 2.5 package of reforms ([124, 125]). These reforms included requirements for the banks to hold additional capital against default risk and rating migration risk, known as the Incremental Risk Charge (IRC). The IRC is calculated using a value-at-risk (VaR) model at the 99.9% confidence level over a one-year time horizon.

Although Basel 2.5 was an important improvement, some of the structural flaws of the market risk framework remained unaddressed. To this end, the Committee initiated a fundamental review of the trading book (FRTB) to enhance the design and coherence of the market risk capital standard, in line with the lessons learned from the global financial crisis ([64]). In FRTB the IRC is replaced with a Default Risk Charge (DRC) model. As an autonomous modelled approach, the IRC effectively dismisses diversification effects between credit-related risks and other risks. Moreover, the more complex IRC models were identified as source of undesired variability in the market risk weighted assets. Under the revised framework, the DRC models will measure the trading portfolio's default risk separate from all market risks. As an additional constraint, the DRC places limitations on the types of risk factors and correlations that can be used within the model. More specifically, banks must use a default simulation model with multiple systematic risk factors of two different types and default correlations must be based on credit spreads or on listed equity prices, covering a period of 10 years which includes a period of stress.

In order to meet the requirement of two different types of systematic factors for the default model, [126] proposed to use principal components analysis (PCA) to identify

the common systematic factors that drive issuer returns. While the factors obtained using this approach are explanatory in a statistical sense, they usually lack of an obvious economic meaning. Moreover, the stability of such factors over time might prove insufficient. A more common approach among practitioners is employing observable economic factors, representing the overall state of the economy or effects related to particular geographic regions or industry sectors. An example of this approach is described in [127].

Motivated by the absence of models encoding complexity-based 'inputs', in this chapter we take up the challenge by focusing on one of the key aspects of complex systems, i.e. the presence of a *community structure*. Detecting the presence of communities means individuating clusters of units sharing some kind of similarity: when considering financial systems, this usually boils down at identifying sets of stocks sharing similar *price dynamics*. We focus on credit default swap (CDS) spread time series with the aim of individuating clusters whose similarities cannot trace back to the standard, region- and sector-wise ones. To achieve this goal, we employ a recently-proposed community detection method that take as input the empirical correlation matrix induced by a given set of CDS time series ([128, 129]) and, then, we employ the output of such a method to identify communities of issuers and define a novel default risk model. The variant we propose is shown to outperform more traditional versions. Our contributions in this chapter are, therefore, threefold. First, to the best of our knowledge our study is the first one that detects mesoscopic communities of issuers by applying the approach based on Random Matrix Theory (RMT) on CDS time series. Second, on the basis of the detected communities we derive factors and develop a portfolio credit risk model that is in line with regulatory requirements for DRC calculations. Third, we set up four synthetic test portfolios and present the impact of considering different systematic factors on the quantiles of the generated loss distributions.

The remainder of the chapter is organised as follows. In Section 5.2 we provide a brief definition of CDS contracts and an overview of the dataset used for the present analysis. In Section 5.3 we describe the theoretical principles upon which the community detection method for correlation matrices employed here is based and analyse the results obtained using the data described in Section 5.2. Section 5.4 is, instead, dedicated to the description of our novel default risk model whose key ingredient is represented by a previously-ignored factor, i.e. the community-driven one, as well as a simulation study on synthetic test portfolios. Finally, in Section 5.5 we summarise our findings and draw conclusions.

5.2. Preliminary definitions

5.2.1. Credit default swaps

A credit default swap (CDS) is a financial contract in which a protection buyer, A, buys insurance from a protection seller, B, against the default of a reference entity, C. More specifically, regular coupon payments with respect to a contractual notional and a fixed rate, the CDS spread, are swapped with a payment of in the event of default of C, where RR, known as the recovery rate, is a contract parameter representing the fraction of investment which is assumed be recovered in the event of default of C.

CDS spreads reflect the market participants' view on probability of default. Thus, practitioners often rely on them to obtain market-implied parameters which are key inputs to their models. For instance, in the case of credit valuation adjustment (CVA)[1], the default probabilities are obtained from CDS spreads. Apart from derivatives valuation, CDS spreads are used extensively for estimating correlations in market risk and capital models ([64]).

5.2.2. Description of the data-set

The raw CDS data-set is provided by Markit and consists of daily CDS spreads for a range of maturities covering the period between 1 January 2007 and 31 December 2016. Markit maintains a network of market makers who contribute quotes from their official books and records for thousands of entities on a daily basis. Using the contributed quotes, the daily CDS spreads for each entity, as well as the daily recovery rates used to price the contracts, are calculated. In addition, the data-set contains information on the names of the underlying reference entities, recovery rates, seniority of the debt on which the contract is priced on, restructuring type, number of quote contributors, region, sector, average of the ratings from Standard & Poor's, Moody's, Fitch Group of each entity and currency of the quote.

Since Markit data are characterised by a number of attributes, it is possible to have multiple CDS data series for the same issuer. In order to obtain unique, representative time series, we apply a set of selection criteria. First, we select the CDS spreads of entities for the five-year tenor for our analysis; it is observed that Markit's raw data is more complete for this tenor, since five-year CDS contracts are the most liquid. For the same reason, we select senior unsecured debt for corporates and foreign debt for sovereigns. Finally, we set up a hierarchy for the document clause/restructuring type which defines what constitutes a credit event and select the series denominated in Euro for the European issuers and in U.S. dollar for issuers from the rest of the world. Besides the above steps, we apply a couple of additional filtering steps to the CDS data to retain the most liquid quotes. After applying these pre-processing steps, we are left with a total of 786 entities and 2608 trading days. The distribution of issuers across regions and sectors is shown in Table 5.1.

5.3. Community detection on CDS correlation matrices

5.3.1. Methods

Basic notation. In this subsection we introduce the basic notation and describe the community-detection method for time series introduced in [128]. Financial markets are represented as a set of time series $X_1 \dots X_N$, each one encoding the temporally ordered activity of the i-th unit of the system over, say, T time-steps, i.e.

$$X_i \equiv \{x_i(1) \dots x_i(T)\}, \forall\, i. \tag{5.1}$$

In our case i is a credit issuer. The mutual interactions between the series considered

[1] CVA is the difference between the risk-free portfolio value and the actual portfolio market value that takes into account the risk of a counterparty's default. Its magnitude depends on the probability of default of the counterparty, the future exposures of the underlying derivative or portfolio, and the loss given default.

Table 5.1: Distribution of 786 entities across regions and sectors.

Region	N	Sector	N
Africa	5	Basic materials	51
Asia	132	Consumer goods	104
Eastern Europe	14	Consumer services	94
Europe	239	Energy	51
India	7	Financials	164
Latin America	13	Government	63
Middle East	9	Health Care	33
North America	342	Industrials	85
Oceania	25	Technology	30
		Telecommunication services	42
		Utilities	69

above are summed up by an $X \times N$ *correlation matrix*, i.e. a matrix $\mathbf{C}$ whose generic entry C_{ij} reads

$$C_{ij} = \frac{\mathrm{Cov}[X_i, X_j]}{\sqrt{\mathrm{Var}[X_i] \cdot \mathrm{Var}[X_j]}}, \forall\, i, j \tag{5.2}$$

i.e. the Pearson coefficient between series i and j, with

$$\mathrm{Cov}[X_i, X_j] = \overline{X_i \cdot X_j} - \overline{X_i} \cdot \overline{X_j}, \forall\, i, j \tag{5.3}$$

and

$$\mathrm{Var}[X_i] = \overline{X_i^2} - \overline{X_i}^2, \forall\, i; \tag{5.4}$$

in the above equations, the bar is assumed to denote a temporal average, i.e.

$$\overline{X_i} = \frac{\sum_{t=1}^{T} x_i(t)}{T}, \forall\, i, \tag{5.5}$$

$$\overline{X_i^2} = \frac{\sum_{t=1}^{T} x_i^2(t)}{T}, \forall\, i, \tag{5.6}$$

$$\overline{X_i \cdot X_j} = \frac{\sum_{t=1}^{T} x_i(t) \cdot x_j(t)}{T}, \forall\, i, j. \tag{5.7}$$

As frequently done in order to filter out the inherent heterogeneity of time series, each series X_i has been *standardised* by subtracting the temporal average $\overline{X_i}$ and dividing the result by the standard deviation $\sigma_i = \sqrt{\mathrm{Var}[X_i]}$; in other words, X_i has been redefined as $(X_i - \overline{X_i})/\sigma_i$ in a such a way to ensure that $\overline{X_i} = 0$, $\mathrm{Var}[X_i] = 1$ and $C_{ij} = \mathrm{Cov}[X_i, X_j] = \overline{X_i \cdot X_j}$.

One of most challenging problems in the field of complex systems is that of extracting information from the matrix $\mathbf{C}$. As we are considering financial markets, we would be interested in individuating sets of issuers sharing a similar CDS spread dynamics. More

formally, this amounts at inspecting the community structure of the considered set of issuers, i.e. the presence of (internally cohesive) *modules of issuers*.

Over the past years, several techniques to retrieve information regarding the modularity of multiple time series have been proposed (see [128] and references therein). One of the most promising approach is that of applying community detection techniques to empirical correlation matrices: however, as existing methods are tailored on graphs, they suffer from statistical bias whenever applied 'as they are' to correlation matrices (see [128] and references therein).

Recently, a method based on Random Matrix Theory (RMT) ([130, 131]) has been proposed ([128]): when applied to financial time series, this algorithm has been proven to be able to capture the dynamical modularity of real markets, by identifying clusters of stocks which are positively correlated *internally* but anti-correlated with each other. In what follows, we will provide a brief explanation of the method. More details can be found in the original reference [128].

Spectral analysis of random correlation matrices. Let us start by inspecting the properties of random correlation matrices. The latter are constructed by considering N completely random time series of length T (more precisely, time series whose entries are independent, identically distributed random variables with zero mean and finite variance): the matrix encoding the correlations of this set of series is a $N \times N$ Wishart matrix, whose eigenvalues follow (in the limits $N \to +\infty$ and $T \to +\infty$ with $1 < T/N < +\infty$) the so-called Marcenko-Pastur distribution ([132]), reading

$$\rho(\lambda) = \frac{T}{N} \frac{\sqrt{(\lambda_+ - \lambda)(\lambda - \lambda_-)}}{2\pi\lambda} \quad \text{if} \quad \lambda_- \leq \lambda \leq \lambda_+ \tag{5.8}$$

and $\rho(\lambda) = 0$ otherwise, with λ_+ and λ_- being, respectively, the maximum and the minimum eigenvalue:

$$\lambda_\pm = \left[1 \pm \sqrt{\frac{N}{T}}\right]^2 . \tag{5.9}$$

The method we are going to describe implements the idea that, while the eigenvalues of an empirical correlation matrix falling within these boundaries can be attributed to random noise, any eigenvalue smaller than λ_- and larger than λ_+ is to be considered as representing some meaningful structure in the data. The result above leads to the possibility of expressing any empirical correlation matrix as the sum of two components, i.e.

$$\mathbf{C} = \mathbf{C}^{(r)} + \mathbf{C}^{(s)} \tag{5.10}$$

where $\mathbf{C}^{(r)}$ is the tensor *random component*, induced by the eigenvalues in the random bulk (i.e. $\forall\, i$ such that $\lambda_i \in [\lambda_-, \lambda_+]$) and reading

$$\mathbf{C}^{(r)} \equiv \sum_{\substack{i \\ (\lambda_- \leq \lambda_i \leq \lambda_+)}} \lambda_i |v_i\rangle\langle v_i| \tag{5.11}$$

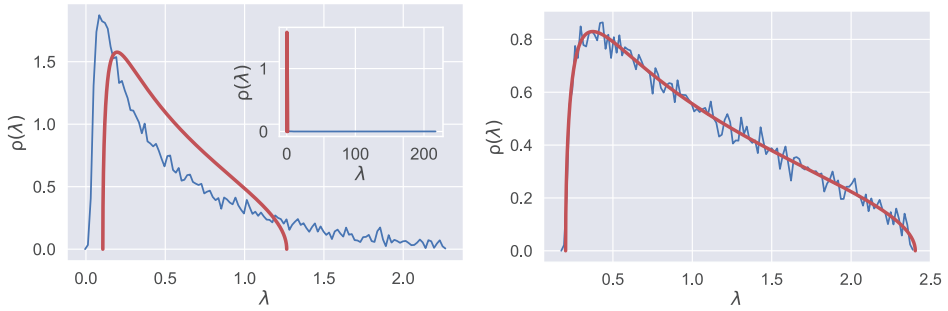

Figure 5.1: Left panel: smoothed eigenvalue density of the correlation matrix extracted from the CDS spreads of $N = 786$ issuers during the period 2007-2016 ($T = 2608$); for comparison we have plotted the Marcenko-Pastur density function (5.8) coming from N uncorrelated series of duration T. Inset: same plot, but including the highest eigenvalue corresponding to the 'market'. Right panel: eigenvalues density distribution of randomised CDS data. The figure shows the agreement between empirical (in blue) and random (in red) distributions once the original data are shuffled.

and $\mathbf{C}^{(s)}$ is the tensor *structural component*, aggregated from the remaining eigenvalues. The structural component $\mathbf{C}^{(s)}$ can be further subdivided, upon considering the existence of the so called *market mode*. As it has been shown in a number of previous studies ([128, 129, 132]), a representative characteristic of the spectrum of empirical correlation matrices is the existence of an eigenvalue λ_m which is orders of magnitude larger that the remaining ones; in case financial stocks are considered, such a leading eigenvalue embodies the common factor driving all the constituents of a given market. As the effect of λ_m is that of pushing all nodes into the same community, we need to properly discount it, by focusing on the 'reduced' portion of the structured spectrum defined by the condition $\lambda_i \in (\lambda_+, \lambda_m)$. This leads to a further decomposition of the correlation matrix, i.e.

$$\mathbf{C} = \mathbf{C}^{(r)} + \mathbf{C}^{(g)} + \mathbf{C}^{(m)} \tag{5.12}$$

where

$$\mathbf{C}^{(m)} \equiv \lambda_m |v_m\rangle\langle v_m| \tag{5.13}$$

represents the tensor portion induced by the market mode and

$$\mathbf{C}^{(g)} \equiv \sum_{i \atop (\lambda_+ < \lambda_i < \lambda_m)} \lambda_i |v_i\rangle\langle v_i| \tag{5.14}$$

represents the tensor portion filtered from both the random noise and the common factor. As a consequence, the correlations encoded in $\mathbf{C}^{(g)}$ are neither at the individual level nor at the level of the entire market but at the level of *groups of stocks* (i.e. at the *mesoscale* in the network jargon). Remarkably, the eigenvectors contributing to $\mathbf{C}^{(g)}$ have alternating signs, allowing for the detection of groups affected in a similar manner by some (other) common factors ([128, 130]).

In Figure 5.1 we plot the eigenvalue density distribution characterising the empirical correlation matrix of $N = 786$ CDS spreads (corresponding to $T = 2608$ daily log-returns

for the period 2007-2016) together with the Marcenko-Pastur distribution coming from N totally uncorrelated series of duration T (shown in red). The maximum expected eigenvalue amounts at approximately $\lambda_+ = 1.27$. The inset is the fully zoomed-out version of the plot, illustrating that the empirical correlation matrix has a maximum eigenvalue of about $\lambda_m = 216$ (i.e. the market mode), in addition to a few other eigenvalues lying between λ_+ and λ_m. The eigenvector $|v_m\rangle$ corresponding to λ_m has all positive signs. We also inspect whether the system follows the Marcenko-Pastur distribution once the original data re shuffled. To this aim, we, first, randomly permute the entries of each time series separately, thus destroying the daily correlations; then, we check if the eigenvalues of the correlation matrix of the shuffled set of series follow the Marcenko-Pastur distribution: as fig. 5.1 shows, this is indeed the case.

Community detection on filtered correlation matrices. Community detection is an active field of research within network theory. Among the many proposed approaches, the most popular one is based on the maximisation of the quantity known as *modularity*, a score function measuring the optimality of a given partition by comparing the empirical pattern of interconnections with the one predicted by a properly-defined benchmark model. It is defined as

$$Q(\boldsymbol{\sigma}) = \frac{1}{||A||} \sum_{i,j=1}^{N} \left[a_{ij} - \langle a_{ij} \rangle \right] \delta(\sigma_i, \sigma_j) \tag{5.15}$$

where a_{ij} is the generic entry of the network adjacency matrix $\mathbf{A}$, $\langle a_{ij} \rangle$ is the probability that nodes i and j establish a connection according to the chosen benchmark (i.e. the expectation of whether a link exists or not under some suitable null hypothesis), $\boldsymbol{\sigma}$ is the N-dimensional vector encoding the information carried by a given partition (the i-th component, σ_i, denotes the module to which node i is assigned) and the Kronecker delta $\delta(\sigma_i, \sigma_j)$ ensures that only the nodes within the same modules provide a positive contribution to the sum. The normalisation factor $||A|| = \sum_{i,j=1}^{N} a_{ij}$ guarantees that $-1 \leq Q(\boldsymbol{\sigma}) \leq 1$ (when undirected networks are considered, it equals twice the number of connections).

Much of the previous research in community detection for financial time series has explored the approach of considering the empirical correlation matrix $\mathbf{C}$ as a weighted network and searching for communities by using the weighted extension of the modularity, defined by posing $a_{ij} \equiv C_{ij}$ and

$$\langle a_{ij} \rangle = \langle C_{ij} \rangle = \frac{s_i s_j}{2W}, \forall\, i, j \tag{5.16}$$

with $s_i = \sum_{l=1}^{N} C_{il} = \mathrm{Cov}[X_i, X_{tot}]$ and $W = \sum_{i,j=1}^{N} C_{ij} = \mathrm{Var}[X_{tot}]$ (having defined $x_{tot}(t) = \sum_{t=1}^{T} x_i(t)$). According to [128], however, this approach may lead to biased results. As a consequence, a null model encoding the spectral properties of correlation matrices has been proposed, i.e.

$$\langle a_{ij} \rangle = \langle C_{ij} \rangle = C_{ij}^{(r)} + C_{ij}^{(m)}, \forall\, i, j \tag{5.17}$$

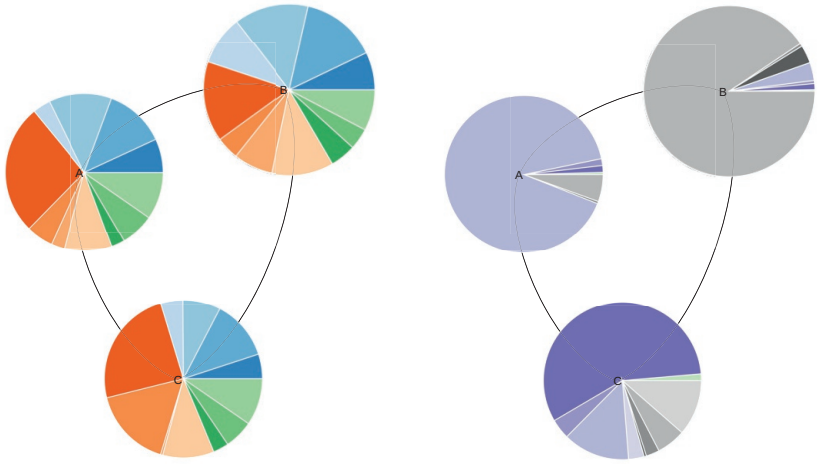

(a) (b)

Figure 5.2: CDS market community structure. The figure shows the communities detected on CDS spread data for 786 issuers during the period 1 January 2007-31 December 2016. The communities were generated by the modified Louvain algorithm ([128]) using daily log-returns. Individual communities are labelled A, B, C and the pie charts represent the relative breakdown of each community with respect to the sector (left panel) and region (right panel) of the component entities.

in turn leading to the following redefinition of modularity

$$Q(\boldsymbol{\sigma}) = \frac{1}{||C||} \sum_{i,j=1}^{N} \left[C_{ij} - \left(C_{ij}^{(r)} + C_{ij}^{(m)} \right) \right] \delta(\sigma_i, \sigma_j) \tag{5.18}$$

(with $||C|| = \sum_{i,j=1}^{N} C_{ij}$), a 'novel' quantity whose maximisation outputs a partition of a given set of time series upon filtering out the random noise and the market component.

5.3.2. Results

Community detection. We now proceed with the application of the methodology described in Section 5.3.1. Figure 5.2 shows the output of the Louvain algorithm when applied to the daily CDS spread data of 786 issuers, covering the period between 1 January 2007 and 31 December 2016. The algorithm is making use of the modularity defined in Equation (5.18), which is able to discount random as well as market-wide effects. With the CDS data, we obtain three mesoscopic communities, labelled A, B and C, characterised (as explained in the previous sections) by *positive correlations within them* and *negative correlations between them*. The pie charts represent the composition of each community according to the industry and region of the constituent issuers for Figure 5.2a and Figure 5.2b respectively. The colour legends can be found in Tables 5.2 and 5.3.

From the data in Figure 5.2a, it is apparent that every community contains a range of issuers from all industry sectors: no pattern of association between sector and community structure is immediately evident. For Community A, it can be seen that over a

Table 5.2: The 11 industry sectors with the colour representation used to highlight the sectors in the following figures.

Basic materials:		Health care:	
Consumer goods:		Industrials:	
Consumer services:		Technology:	
Energy:		Telecommunication services	
Financials:		Utilities:	
Government			

Table 5.3: The 9 regions with the colour representation used to highlight the sectors in the following figures.

Africa:		Latin America:	
Asia:		Middle East:	
Eastern Europe:		North America:	
Europe:		Oceania	
India:			

quarter of issuers are classified as Financials (■), while another quarter of the community comprises issuers from the Consumer Goods (■) and Consumer Services (■) sectors; the rest of the industry sectors are represented with lower percentages, ranging from slightly less than 10% for Utilities (■) to approximately 3% for Technology (■). Issuers from Financials (■) are slightly less frequent in Community B, accounting for approximately 15% of the total issuers, while consumer Goods (■), Consumer Services (■), and Industrials (■) sectors follow with similar percentages; the rest of the community consists of issuers from all sectors with lower percentages, such as Energy (■) and Utilities (■) with slightly less than 10% each. Almost 40% of Community C consists of Financials (■) and Government (■) issuers: interestingly, the proportion of Government (■) issuers in Community C is significantly higher than the corresponding proportion in Communities A and B and almost twice as high as the one in the full sample of 786 issuers; issuers from the Consumer Goods (■) and Industrials (■) sectors are also quite frequent, constituting approximately a quarter of Community C.

We now turn to the relative breakdown of the issuers of each community according to region. As Figure 5.2b demonstrates, the identified communities display a high degree of overlap with region classification. Communities A and B are dominated by the regions Europe (■) and North America (■) respectively. On the other hand, Community C contains the bulk of issuers from Asia (■), while issuers from Oceania (■) and India (■) are represented exclusively in this community. It is interesting, however, that a considerable amount of issuers from Europe (■) and North America (■) can be found in Community C, meaning that over the course of the ten-year period under analysis they were more correlated with issuers from Asia (■) or Oceania (■) than with most of the issuers located in their own region. A possible explanation is that some issuers such as international banks registered in Europe and North America have considerable exposure to Asia-Pacific.

Hierarchical community structure. The methodology described in Section 5.3.1 can be applied iteratively, to individuate smaller subcommunities which may be nested inside larger communities. As the leading eigenvalue of the correlation matrix represents something that all issuers in the market have in common, the leading eigenvalue of the correlation matrix restricted to a specific individual community can be interpreted as something that all issuers in *that* community have in common: by washing out the effects of this 'community mode', one can detect the 'residual' modular structure (internal to each community). Naturally, subcommunities within each parent community are anticorrelated with each other while being positively correlated internally.

The results of a single iteration over the communities A, B, and C (summarised in Figure 5.2) are illustrated in Figures 5.3 and 5.4. It can be seen from the graph that the degree of overlap with the sector-based classification is higher for subcommunities than for communities. Moreover, the overlap with the region-based classification is even more pronounced.

Community A is divided is four subcommunities labelled A1 through A4. A1 and A3 contain a range of issuers from all sectors, while A2 is dominated by Financials (■) and three quarters of A4 is constituted by Energy (■) and Utilities (■). In all four subcommunities, Europe (■) is the leading region and there is a small percentage of issuers from North America (■); moreover, Middle East (■), Eastern Europe (■) and Africa (■) are represented exclusively in A1 while issuers from Asia (■) can be found exclusively in A3.

Community B is split in five subcommunities. B1 is quite heterogeneous, including issuers from all different industry sectors. B2 includes issuers from the Energy (■) and Utilities (■) sectors. Approximately half of B3 and B4 include are constituted by Consumer Goods (■) and Consumer Services (■) issuers, with Industrials (■) and Health Care (■) accounting for another quarter of B4. Finally, B5 is dominated by Financials (■) and Government (■). From a geographic perspective, subcommunities of B are all dominated by North America (■), with some issuers from Europe (■) being present in B1 and to a lesser extent in B3 and B5. B2 contains issuers only from North America (■) and, with very few exceptions, the same holds for B3 and B4 as well. Most of the issuers from Latin America (■) can be found in B5 with almost a third of this subcommunity being from that region.

Moving to the four subcommunities of Community C, almost half of the issuers in subcommunity C1 are equally split among Consumer Goods (■) and Industrials (■). Issuers from the Government (■) and Financials (■) sectors constitute more than half of subcommunities C2 and C4. Financials (■) are frequent in subcommunity C3 as well, followed by Consumer Services (■), i.e. the second most frequent industry sector. In terms of regional classification, although Community C is more heterogeneous than A and B, its subcommunities reveal that issuers from Asia (■ are concentrated in subcommunities C1 and C4, with C4 containing almost all the issuers from India (■). C3 consists of issuers from Oceania (■), with a small number of issuers from Europe (■). The bulk of the European issuers in community C is concentrated in C2, making up almost 50% of the subcommunity. The rest of C2 consists of issuers from Eastern Europe (■) and North America (■) with about 15% each, and Middle East (■) with slightly over 10%.

In summary, these results provide important insights into the structure of the CDS market. It is suggested that the three communities initially detected are quite hetero-

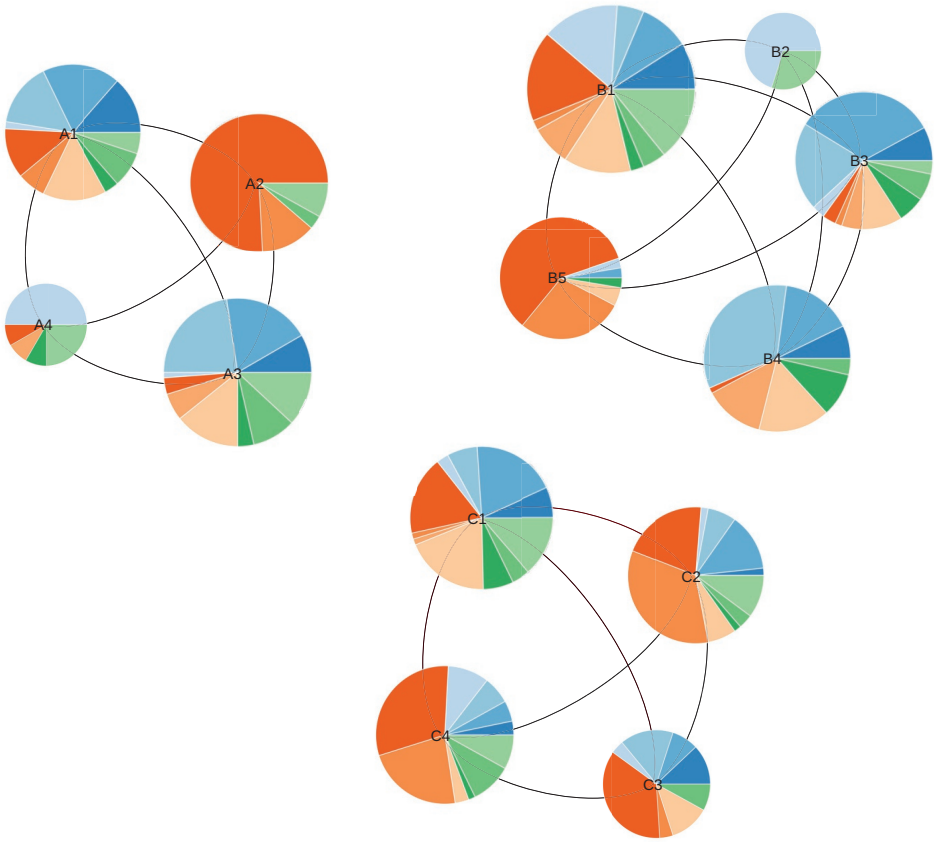

Figure 5.3: Subcommunity structure of the three communities of the CDS market by sector. Although at first glance the subcommunities seem quite heterogeneous with respect to sector, after close inspection it can be seen that some of them are dominated by certain sectors, for example A2 and B5 are dominated by Financials (■) and Government (■), while A4 and B2 are dominated by Energy (■) and Utilities (■).

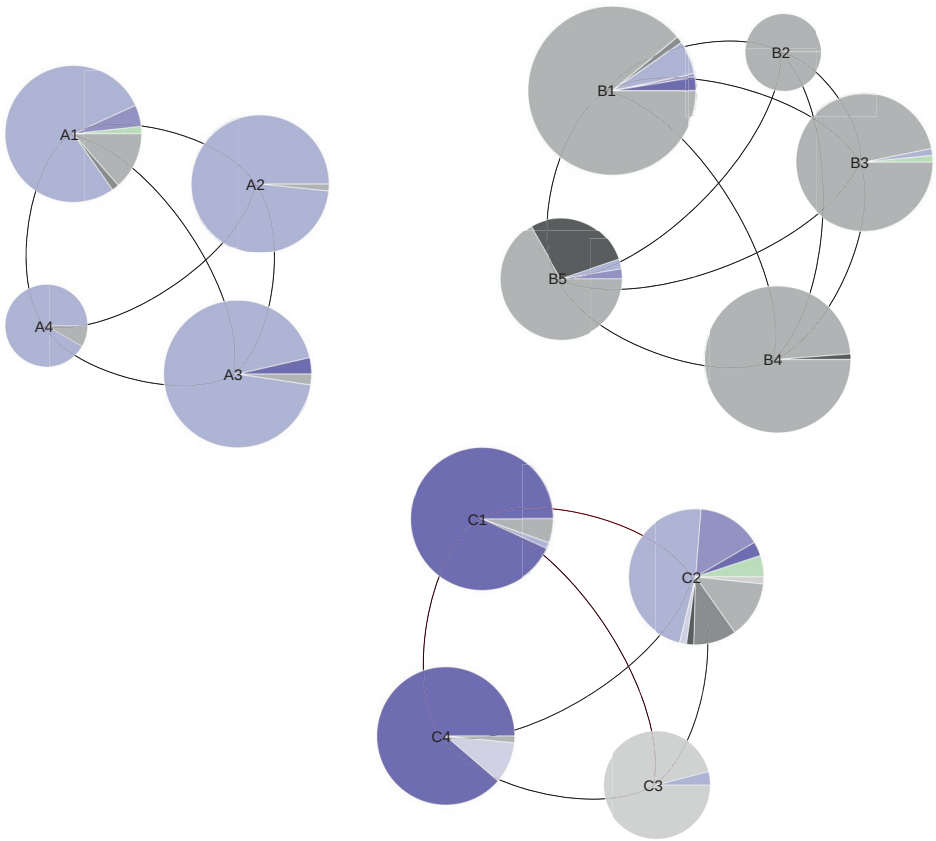

Figure 5.4: Subcommunity structure of the three communities of the CDS market by region. The overlap between region and subcommunities is better than the one between sectors and subcommunities.

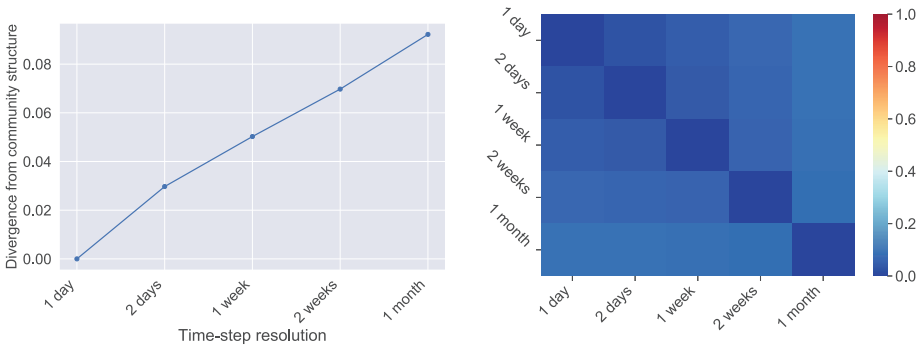

(a) (b)

Figure 5.5: Left panel (5.5a): Divergence from original community structure for the five data sets of different sampling frequencies. It can be seen that the VI is increasing steadily when moving from the finest to the coarsest resolution but does not exceed 10%, indicating a high level of similarity between partitions. Right panel (5.5b): Heat map illustrating the value of VI between each pair of the five data sets of different sampling frequencies. From the heat map, it is apparent that there is a considerable degree of consistency across sampling frequencies, but the similarity degrades steadily when moving from the finest to the coarsest resolution.

geneous as far as industry sectors are concerned, while they overlap to a greater extent when considering a regional-based classification of issuers. Interestingly, although Communities A and B are dominated by Europe (■) and North America (■), some European and North American issuers are clustered with issuers from Asia (■) and Oceania (■) in Community C. At the second iteration of the method, some of the obtained subcommunities are dominated by certain sectors: for instance, A2 and B5 are dominated by Financials (■) and Government (■), while A4 and B2 are dominated by Energy (■) and Utilities (■). The overlap between regions and subcommunities is even better than the one between sectors and subcommunities. These results have implications for the management of portfolios of credit risky instruments, demonstrating that after global effects have been filtered out, default risk dependence is related to regional effects to a larger extent than to sectoral effects. This seems to be in line with previous evidence from equity markets ([133]), indicating that industry-specific effects are less significant than region effects. In addition, as far as default risk is concerned, it appears that neither diversification over regions alone nor diversification over industries alone can achieve the optimal diversification benefits, a result that is aligned with [134].

Community detection: a temporal multiresolution analysis. Once the mesoscopic organisation of the CDS market has been detected, one may wonder how stable (i.e. 'robust over time') this organisation is. This amounts at investigating the presence of discrepancies from the original community structure once the log-returns constituting the time series are sampled at different frequencies, e.g. weekly or monthly. For consistency with the results presented so far, the same period of ten years is considered but our analysis is now focused on the set of time series induced by the following array of time resolutions

$$\Delta_t \in \{1\text{ day}, 2\text{ days}, 1\text{ week}, 2\text{ weeks}, 1\text{ month}\}. \tag{5.19}$$

To measure the effects of the temporal resolution, we employ the index known as *variation of information* (VI), an information-theoretic measure quantifying the difference between any two partitions. Two different partitions can be represented by two N-dimensional vectors $\vec{\sigma}_1$ and $\vec{\sigma}_2$ whose i-th component σ_i denotes the module to which node i belongs. The (normalised) variation of information is defined as

$$VI(\vec{\sigma}_1 : \vec{\sigma}_2) = 1 - \frac{I(\vec{\sigma}_1 : \vec{\sigma}_2)}{H(\vec{\sigma}_1 : \vec{\sigma}_2)} \tag{5.20}$$

where $I(\vec{\sigma}_1 : \vec{\sigma}_2)$ is the *mutual information*, which is defined as follows

$$I(\vec{\sigma}_1 : \vec{\sigma}_2) = \sum_{i=1}^{N}\sum_{j=1}^{N} p(\sigma_i^1, \sigma_j^2) \log\left[\frac{p(\sigma_i^1, \sigma_j^2)}{p(\sigma_i^1)p(\sigma_j^2)}\right] \tag{5.21}$$

(with $p(\sigma_i^1)$ being the probability for a node to belong to σ_i in partition 1, $p(\sigma_j^2)$ being the probability for a node to belong to σ_j in partition 2 and $p(\sigma_i^1, \sigma_j^2)$ being the joint probability distribution for a node to belong to σ_i in partition 1 *and* to σ_j in partition 2) and $H(\vec{\sigma}_1 : \vec{\sigma}_2)$ is the *joint entropy*, which is defined as follows

$$H(\vec{\sigma}_1 : \vec{\sigma}_2) = \sum_{i=1}^{N}\sum_{j=1}^{N} p(\sigma_i^1, \sigma_j^2) \log\left[p(\sigma_i^1, \sigma_j^2)\right]. \tag{5.22}$$

Notice that, unlike mutual information, the variation of information is a true metrics since it satisfies the triangle inequality. The divergence from the community structure presented in Section 5.3.2, for each additional set of time series is depicted by Figure 5.5a. From the chart, it is apparent that VI is increasing steadily when moving from the finest to the coarsest resolution but does not exceed 10% in any case, indicating a high level of similarity between partitions. The value of the VI between each pair of data-sets is, instead, shown in Figure 5.5b. This result provides some support for the conceptual premise that community structure does not (strongly) depend on the level of temporal resolution at which our data-set is considered.

The VI-based analysis contributes to our understanding of the robustness of the community structure with respect to different temporal resolutions; however, we would like to extend this kind of analysis at the issuer level, by assessing how robust is the assignment of issuers to communities by measuring the frequency with which any two issuers are assigned to the same community over different temporal partitions. The results of this analysis are presented in Figure 5.6. The heat map shows how frequently issuers co-occur within the same communities across the time resolutions considered here. In case two issuers are found within the same community for *each* time resolution, the entry corresponding to the considered pair of issuers in the heat map is drawn in white, while if they are *never* found within the same community the entry is drawn in black. As the heat map shows, three 'hard cores' of issuers appear, indicating that the issuers belonging to them are assigned to the same community for the vast majority of the temporal resolutions; in addition, there are also few 'soft issuers' who move across

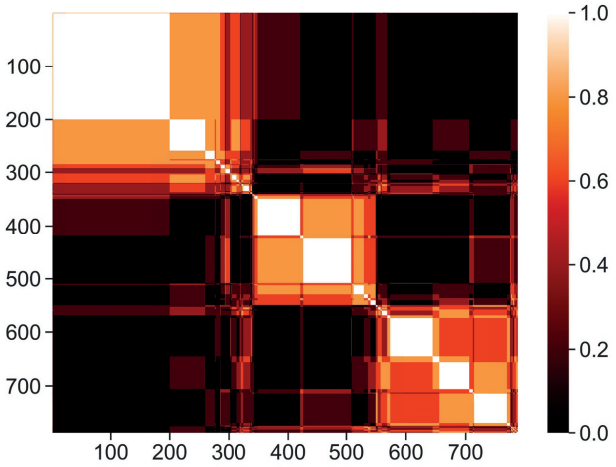

Figure 5.6: Multifrequency heat map showing the normalised co-occurrence of different pairs of issuers within the same community, for the same time period but over various temporal resolutions of the original time series. The issuers have been ordered using hierarchical clustering with average linkage to position issuers with a high degree of co-occurrence next to each other.

communities for different time resolutions, offering an explanation for the small variation observed in Figure 5.5.

Community detection: temporal stability. One of the major challenges that managers measuring portfolio risk face is that of determining the appropriate period of history to use when estimating correlations to be used in their models. According to [135], using a relatively short period of data might be dangerous: in case the employed period is uncharacteristically stable, in fact, the estimated correlations may be lower than average, leading to excessive risk taking; on the other hand, if the used interval is relatively volatile, the resulting correlations can be unrealistically high, leading to excessive risk aversion. However, choosing a longer time series is not guaranteed to produce more reliable estimates: the ever-evolving nature of financial markets deems undesirable to rely on data from the distant past. In order to be confident that the results presented in Section 5.3.2 can provide useful insights for risk managers, it is required to study the time dynamics of the detected communities.

To analyse the stability of communities over the course of time, we employ a non-overlapping sliding window of six months. Figure 5.7a illustrates the divergence from the community structure detected using the first six-month window throughout the years. It can be seen that there are no significant fluctuations, with VI not exceeding 10% for any of the six-month periods. To further improve our understanding on the community coherence, in Figure 5.7b we provide a heat map showing the mutual VI between every two pairs of six-month windows. Each square in the matrix represents the value of VI between the i-th and j-th six-month period, while the last row and column represent the value of VI between each six-month period and the partition obtained using the full

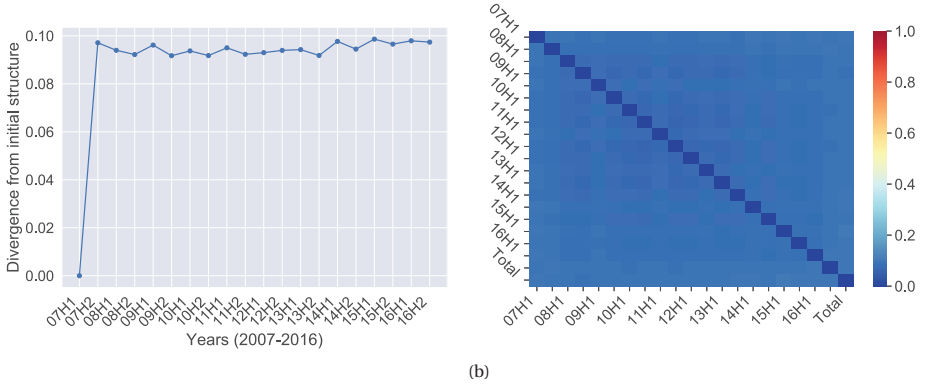

(a) (b)

Figure 5.7: Left panel (5.7a): Divergence from initial community structure for the ensuing six-month windows. The values of VI do not exceed 10% for any of the six-month windows, while no particular trend can be observed. Right panel (5.7b): The heat map illustrates the value of VI between every pair of six-month time windows, as well as the VI between each window and the total ten-year period (rightmost column and bottom row). It can be seen that there is a high degree of community coherence over time.

ten-year sample. The results indicate that there was little movement of issuers between communities during the ten-year period. In addition, it can be seen that there is little difference between these periods and the community structure obtained when we using the entire ten-year period.

Finally, having determined that the communities do not exhibit significant fluctuations over time, we use the same sliding window to examine the stability of communities over time at the issuer level. In a similar fashion to the temporal multiresolution analysis, we plot a heat map containing the frequency with which each pair of issuers can be found within the same community over the course of the ten-year time frame. As Figure 5.8 shows, pairs of issuers appearing to be in the same community for all the six-month windows have white entries in the heat-map, while the entries corresponding to pairs of issuers never appearing within the same community are drawn in black. After a closer inspection, it can be seen that the three communities detected by using the full ten-year history appear to be tight-knit and unwavering, thus maintaining a high degree of coherence over the course of time. A small number of issuers moving fluidly from one community to another can still be appreciated.

5.4. Default risk charge model

5.4.1. Model specification

Consider a portfolio of m issuers, indexed by $i = 1,2...m$ and a fixed time horizon of $T = 1$ year. The overall portfolio loss is modelled by a random variable L, defined as the sum of the individual losses on issuers' default, i.e. $L = \sum_{i=1}^{m} L_i$, with

$$L_i = q_i e_i Y_i \tag{5.23}$$

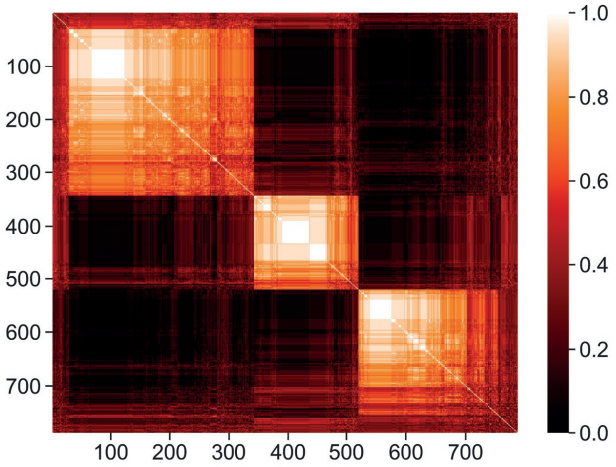

Figure 5.8: Coherence of communities over time. The heat map shows the frequency of co-occurrence of different pairs of issuers within the same community over time. The communities appear to be tight-knit and unwavering, maintaining coherence over the course of the ten-year time frame. The issuers have been ordered using hierarchical clustering with average linkage to position issuers with a high degree of co-occurrence next to each other.

where $L_i = q_i e_i Y_i$ denotes the loss on issuer i, with e_i and q_i being, respectively, the *exposure at default* and the *loss given default* of issuer i and Y_i being the random default indicator taking the value 1 if issuer i defaults before time T and 0 otherwise. In order to define the probability distributions of L_i's, as well as their dependence structure, we rely on a factor model approach, descending from the structural model of Merton ([23]), which is widely used for portfolio default risk modelling by regulators and financial institutions alike. Notable examples of this approach include the Asymptotic Single Risk Factor (ASRF) model ([24]), which is at the heart of Basel II credit risk capital charge, as well as industrial adaptations of Merton model such as the CreditMetrics ([63]) and KMV models ([61, 62]).

Let us introduce a random variable X_i representing issuer i's creditworthiness. In the same spirit of Merton's structural model, we specify that default occurs before time T if the value of X_i lies below a threshold d_i, or equivalently:

$$Y_i := \mathbf{1}_{[-\infty, d_i]}(X_i), \tag{5.24}$$

where $\mathbf{1}_A(\cdot)$ is the indicator function of set A. Hence, modelling Y_i's boils down to model the creditworthiness indices X_i with $i = 1...m$, which are linearly dependent on a vector $\mathbf{F}$ of $p < m$ systematic factors satisfying $\mathbf{F} \sim N_p(0, \Omega)$. Issuer i's creditworthiness index is assumed to be driven by an issuer-specific combination $\tilde{F}_i = \boldsymbol{\alpha}_i' \mathbf{F}$ of the systematic factors:

$$X_i = \sqrt{\beta_i}\tilde{F}_i + \sqrt{1-\beta_i}\epsilon_i, \tag{5.25}$$

where $\tilde{F}_i$ and $\epsilon_1 ... \epsilon_m$ are independent, standard normal variables (i.e. $\tilde{F}_i \sim N(0,1)$, $\forall\, i$ and $\epsilon_i \sim N(0,1)$, $\forall\, i$) and the latter ones model the idiosyncratic risk. The coefficient β_i can be seen as a measure of sensitivity of X_i to systematic risk, as it represents the proportion of the X_i variation that is explained by the systematic factors. The assumption that $\text{Var}[\tilde{F}_i] = 1$ implies that $\boldsymbol{\alpha}_i' \Omega \boldsymbol{\alpha}_i = 1$ for all i. The correlations between asset returns are given by

$$\begin{aligned} \rho(X_i, X_j) &= \text{Cov}[X_i, X_j] \\ &= \left(1 - \beta_i\right) \mathbf{1}_{\{i=j\}} + \sqrt{\beta_i \beta_j}\, \text{Cov}[\tilde{F}_i, \tilde{F}_j] \\ &= \left(1 - \beta_i\right) \mathbf{1}_{\{i=j\}} + \sqrt{\beta_i \beta_j}\, \boldsymbol{\alpha}_i' \Omega \boldsymbol{\alpha}_j \end{aligned} \tag{5.26}$$

(since $\tilde{F}_i$ and $\epsilon_1 ... \epsilon_m$ are independent, standard normal variables and $\text{Var}[X_i] = 1$). In order to set up the model we need to determine $\boldsymbol{\alpha}_i$ and β_i for each issuer and Ω (while ensuring that $\boldsymbol{\alpha}_i' \Omega \boldsymbol{\alpha}_i = 1$).

We choose d_i such that $\mathbb{P}(Y_i = 1) = p_i$, where p_i is the marginal *probability of default* of issuer i. As a result, $d_i = F_{X_i}^{-1}(p_i)$, with $F_{X_i}(\cdot)$ being the cumulative distribution function of X_i. Given the normality of X_i, it follows that $d_i = \Phi^{-1}(p_i)$, with $\Phi^{-1}(\cdot)$ denoting the standard normal cumulative distribution function. The portfolio loss can, then, be written as follows:

$$L = \sum_{i=1}^{m} q_i e_i \mathbf{1}_{[-\infty, \Phi^{-1}(p_i)]} \left(\sqrt{\beta_i}\, \tilde{F}_i + \sqrt{1 - \beta_i}\, \epsilon_i \right). \tag{5.27}$$

For $p = 1$, the specification above is equivalent to the ASRF model. In this model, the single systematic factor affecting all issuers is usually interpreted as the state of the economy and the correlation coefficients are regulatory prescribed. In multi-factor models ($p \geq 2$), latent or observable factors encompassing regional or industry characteristics are typically used by modellers to capture the portfolios correlation structure.

5.4.2. Model calibration

Models used by banks for DRC calculations are required to account for systematic risk via multiple systematic factors of two different types [64, Paragraph 186(b)]. For the first systematic factor, we consider a global factor that is common to all issuers, reflecting the overall state of the economy. We adopt this approach due to relevant literature suggesting strong dependence of changes in default risk on global effects ([134]). For the second systematic factor we consider factors representing industry and region effects, as well as community and subcommunity effects. Even though a model with three types of systematic factors would not be in line with the regulatory requirements for the calculation of DRC, for comparison purposes we also consider a model with global, industry, and region systematic factors, an approach commonly adopted in the industry for the calculation of IRC.

In addition to the types of systematic factors, the regulatory rule-set specifies that correlations must be calibrated using credit spreads or listed equity prices over a period of at least ten years that includes a period of stress. We calibrate the model presented

in Section 5.4.1 using CDS spreads covering the period between 1 January 2007-31 December 2016 which includes the 'stressed' period between 2007 and 2009. In our model setting, the liquidity horizon is set as one year and, as a result, the correlations should be measured over the same horizon. However, non-overlapping annual log-returns from ten years history contain only nine points, which is not sufficient to yield a reliable correlation estimate. If overlapping log-returns are considered alternatively, the sample size can be sufficiently big, but the linear relation between the data series can be distorted. Moreover, certain bias can be introduced into the correlation estimate via auto-correlation, which usually leads to over-estimations. Instead of using overlapping annual returns, we chose to use to monthly non-overlapping returns over the ten-year period. This approach leads to a sufficient number of data points for correlation estimation and can be seen as a reasonable compromise. The implied hypothesis is that correlations measured over monthly and annual horizons are interchangeable and can be used as a predictor for future one-year correlations. According to [127], this assumption can be questioned, but, it is hard to reject from a statistical point of view, if one takes into account the uncertainty of the correlation measurement itself.

We start by scaling each individual time series to have zero mean and unit variance. At each time point, global ($X_{G,t}$), industry ($X_{I(j),t}$), region ($X_{R(k),t}$), community ($X_{C(l),t}$) and subcommunity ($X_{S(n),t}$) returns are derived from the corresponding cross-section of the issuer returns. All the resulting factor time series have zero mean. The dependence of the region, industry, community and subcommunity factors on global returns is explored by running the following linear regression models

$$\begin{aligned} X_{I(j),t} &= \gamma_{I(j)} X_{G,t} + \varepsilon_{I(j),t}, \\ X_{R(k),t} &= \gamma_{R(k)} X_{G,t} + \varepsilon_{R(k),t}, \\ X_{C(l),t} &= \gamma_{C(l)} X_{G,t} + \varepsilon_{C(l),t}, \\ X_{S(n),t} &= \gamma_{S(n)} X_{G,t} + \varepsilon_{S(n),t} \end{aligned} \tag{5.28}$$

where $\gamma_{I(j)}$, $\gamma_{R(k)}$, $\gamma_{C(l)}$ and $\gamma_{S(n)}$ are coefficients weighing the global factor and $\varepsilon_{I(j),t}$, $\varepsilon_{R(k),t}$, $\varepsilon_{C(l),t}$ and $\varepsilon_{S(n),t}$ are the industry-, region-, community- and subcommunity-specific residuals, respectively. The full regression results on the basis of Equation (5.28) for the period between January 2007 to December 2016 can be found in Table C.1 in Appendix C.1. The majority of the factor returns move in line with the global returns, with coefficients not significantly different from one. In addition, the proportion of variance explained by the global returns is high (as indicated by the values of R^2, between 63% and 96%), highlighting the leading role of the global factor.

Turning now to the case of a single issuer, it is important to note that by regressing the industry ($X_{I(j)}$), region ($X_{R(k)}$), community ($X_{C(l)}$) and subcommunity ($X_{S(n)}$) returns against the global returns (X_G), we have essentially orthogonalised the rest of the factors relative to the global factor. Hence, in addition to the global returns (X_G), we use the residuals $\varepsilon_{I(j)}, \varepsilon_{R(k)}, \varepsilon_{C(l)}$, and $\varepsilon_{S(n)}$ from eq. (5.28) as explanatory factors for the returns of a single issuer, representing industry, region, community, and subcommunity effects respectively. In the following we discuss the calibration of a model with a global and a subcommunity factor; calibration of other model variants should then be straightforward. Recall that issuer i's creditworthiness index X_i follows the dynamics presented in

Table 5.4: The table provides the statistics for the R^2 between the individual issuers and systematic factor(s). The model estimation is based on the following settings: global factor only (Model 1); global and industry factors (Model 2); global and region factors (Model 3); global, region, and industry factors (Model 4); global and community factors (Model 5); and global and subcommunity factors (Model 6). Industry, region, community, and subcommunity factors are defined as cross-sectional averages at each time point and taken as already decomposed into a global factor and residuals. The estimation is based on non-overlapping monthly log-returns and conducted from January 2007 to December 2016, which was identified as a recent 10-year period which included the 'stressed' period between 2007 and 2009.

Individual R^2 versus systematic factors	Model 1: Global factor only	Model 2: Global and industry factors	Model 3: Global and region factors	Model 4: Global, region, and industry factors	Model 5: Global and community factors	Model 6: Global and subcommunity factors
Average	48.1%	54.5%	54.2%	58.1%	55.4%	58.2%
SD	15.8%	16.4%	17.6%	17.5%	16.7%	18.0%
Minimum	0.0%	0.6%	0.0%	1.4%	1.4%	0.8%
Maximum	0.82%	84.1%	96.3%	96.5%	88.4%	92.6%

Section 5.4.1. In our case, $\tilde{F}_i := \alpha_{G(i)} X_G + \alpha_{S(i)} \epsilon_{S(i)}$, where the coefficients $\alpha_{G(i)}$ and $\alpha_{S(i)}$ have been rescaled so that $\tilde{F}_i \sim N(0,1)$, i.e.

$$\alpha_{G(i)} := \frac{\hat{\alpha}_{G(i)}}{\Psi_i}, \qquad \alpha_{S(i)} := \frac{\hat{\alpha}_{S(i)}}{\Psi_i} \tag{5.29}$$

with $\hat{\alpha}_{G,i}$ and $\hat{\alpha}_{S,i}$ being the factor loadings of the regression model

$$X_{i,t} = \hat{\alpha}_{G(i)} X_{G,t} + \hat{\alpha}_{S(i)} \epsilon_{S(i),t} + \varepsilon_{i,t} \tag{5.30}$$

and $\Psi_i = \sigma\left[\hat{\alpha}_{G(i)} X_G + \hat{\alpha}_{S(i)} \epsilon_{S(i)}\right]$. Thus, we calibrate the factor loadings $\hat{\alpha}_{G(i)}$ and $\hat{\alpha}_{S(i)}$ by running the above regression. If we collect X_G and $\epsilon_{S(i)}$ into a matrix F_i, then the least squares estimator $\hat{\boldsymbol{\alpha}}_i$ equalises the two sides of the following equation:

$$X_i = F_i \hat{\boldsymbol{\alpha}}_i \tag{5.31}$$

or, in other words, $\hat{\boldsymbol{\alpha}}_i$, $\forall\, i$ represent estimates of the coefficients appearing in Equation (5.30):

$$\hat{\boldsymbol{\alpha}}_i = (F_i' F_i)^{-1} (F_i' X_i). \tag{5.32}$$

Finally, the coefficient β_i from Section 5.4.1 is the R^2 of this regression, representing the proportion of variance for X_i explained by the systematic factors.

We estimate the parameters of six model variants on the basis of the calibration process described previously: global factor only (Model 1); global and industry factors (Model 2); global and region factors (Model 3); global, region, and industry factors (Model 4); global and community factors (Model 5) and global and subcommunity factors (Model 6). The statistics for the individual R^2 versus systematic factors are compared in Table 5.4. As it can be seen from the table, not surprisingly, the model based only on the global factor provides the worst fit to the data with an average R^2 of 48.2%. After the introduction of the industry factor the average R^2 increases to 54.5%. A comparable value (54.2%) is obtained if instead of the industry factor we introduce a region factor. The model based on

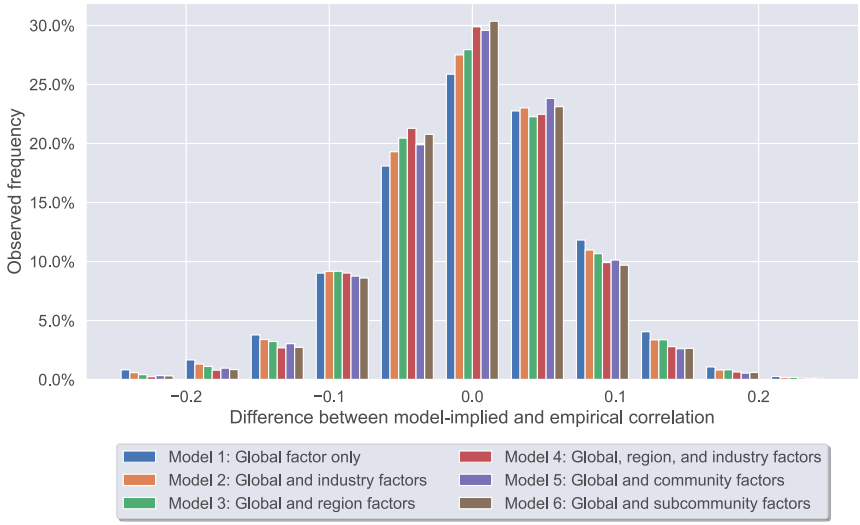

Figure 5.9: The figure shows the distribution of the differences between the model-implied and empirical (pairwise) correlations. As for the model, the six variants (global factor only, global/industry, global/region, global/industry/region, global/community, global/subcommunity factors) are explored.

global and community factors (Model 5) provides a slightly better fit than the other two-factor models with an average R^2 of 55.4%. The best fit is achieved by the model based on global and subcommunity factors (Model 6) with an average R^2 of 58.2%, outperforming even the three-factor model based on global, region, and industry factors. This result is particularly interesting since the difference in the average R^2 between Model 6 and the other two-factor models is comparable to the difference between the other two-factor models and the model based only on the global factor.

Having estimated the factor loadings and covariance matrices for the six model variants, we are able to obtain the distribution of the differences between the model-implied and empirical (pairwise) correlations (shown in Figure 5.9): after close inspection, it becomes evident that the distributions of the correlation errors based on Model 4 and Model 6 are heavier around zero and have thinner tails. The distribution of the actual empirical correlations is shown in Figure C.1 in Appendix C.2.

5.4.3. Numerical experiments

In order to study the properties of the framework presented in Section 5.4 we set up four synthetic test portfolios:

- **Portfolio A**: Long-only portfolio consisting of 36 sovereign issuers from the iTraxx SovX index family.

- **Portfolio B**: Long-only portfolio consisting of 89 corporate issuers (Financials and Non-Financials) from the iTraxx Europe index.

Table 5.5: The table provides the historical default rates per rating. Source [136, 137]

Rating	Corporates (1981-2018)	Sovereigns (1975-2018)
AAA	0.00	0.00
AA	0.02	0.00
A	0.06	0.00
BBB	0.17	0.00
BB	0.65	0.49
B	3.44	2.82
CCC/C	26.63	41.56

- **Portfolio C**: Long-only consisting of 125 issuers from Portfolio and Portfolio B combined.
- **Portfolio D**: Long-short portfolio consisting of 22 long positions on issuers from Financials and 22 short positions on issuers from Non-Financials from the iTraxx Europe index selected such that the average default probability between the two groups is the same.

For the purposes of our numerical experiments, we use historical default rates per rating from [136] and [137] as *probabilities of default*. The historical defaults rates per rating are shown in Table 5.5. In accordance with regulatory requirements [64, Paragraph 186(b)], probabilities of default are subject to a floor of 3 bps. The detailed composition of the synthetic portfolios in terms of rating, as well as the mean and standard deviation of the corresponding probabilities of default are shown in Table 5.6.

As far as the *exposure at default* is concerned, for the long-only portfolios we consider a constant and equally weighted exposure for each issuer such that $e_i = 1/m$ for all $i = 1...m$ and $\sum_{i=1}^{m} = 1$. For the long-short portfolio we consider $e_{i \in Financials} = 1/22$ and $e_{i \notin Financials} = -1/22$, and as a result $\sum_{i=1}^{m} e_i = 0$. Finally, for the sake of simplicity, the *loss given default* parameter is set to 1 for all issuers, i.e. $q_i = 1$, $i = 1...m$.

We, then, generate portfolio loss distributions and derive the associated risk measures by means of Monte Carlo simulations. This process entails generating joint realizations of the systematic and idiosyncratic risk factors and comparing the resulting critical variables with the corresponding default thresholds. By this comparison, we obtain the default

Table 5.6: The table provides the composition of the synthetic test portfolios in terms of rating, as well as the mean and standard deviation for the corresponding probabilities of default.

	AAA	AA	A	BBB	BB	Average PD	SD PD
Portfolio A	4	7	6	14	5	0.09%	0.16%
Portfolio B	-	6	32	51	-	0.12%	0.05%
Portfolio C	4	13	38	65	5	0.11%	0.10%
Portfolio D	-	6	30	8	-	0.08%	0.05%

Table 5.7: The table provides the quantiles of the loss distribution for the corresponding portfolios and for each of the six model configurations.

	α	Model 1: Global factor only	Model 2: Global and industry factors	Model 3: Global and region factors	Model 4: Global, region, and industry factors	Model 5: Global and community factors	Model 6: Global and subcommunity factors
Portfolio A:	0.99	2.8%	2.8%	2.8%	2.8%	2.8%	2.8%
Sovereign bonds,	0.995	2.8%	5.6%	5.6%	5.6%	2.8%	2.8%
long position	0.999	8.3%	11.1%	11.1%	11.1%	8.3%	11.1%
Portfolio B:	0.99	3.4%	3.4%	2.2%	2.2%	3.4%	3.4%
Corporate bonds,	0.995	5.6%	5.6%	5.6%	5.6%	5.6%	5.6%
long position	0.999	14.6%	14.6%	16.9%	16.9%	15.7%	16.9%
Portfolio C:	0.99	2.4%	2.4%	2.4%	2.4%	2.4%	2.4%
Combination of	0.995	4.8%	4.8%	4.8%	4.8%	4.8%	4.8%
portfolios A and B	0.999	12.8%	12.8%	13.6%	13.6%	12.8%	13.6%
Portfolio D:	0.99	0.0%	0.0%	0.0%	0.0%	0.0%	0.0%
Corporate bonds,	0.995	4.5%	4.5%	4.5%	0.0%	4.5%	4.5%
long/short position	0.999	9.1%	13.6%	9.1%	9.1%	13.6%	13.6%

indicator Y_i for each issuer and this enables us to calculate the overall portfolio loss for this trial. A liquidity horizon of 1 year is assumed throughout and the results are based on calibrations according to Section 5.4.2 and simulations with ten million sample paths each. For a given confidence level $\alpha \in [0,1]$, the VaR_α is defined as the α-quantile of the loss distribution:

$$\text{VaR}_\alpha(L) = \inf\{l \in \mathbb{R} : \mathbb{P}(L \leq l) \geq \alpha)\}. \tag{5.33}$$

Since both IRC in Basel 2.5 and DRC in FRTB are calculated based on a 99.9% VaR over a capital horizon of one year, we rely on this risk measure in order to compare the impact of different correlation model configurations on portfolio risk. We calculate $\text{VaR}_\alpha(L)$ for selected confidence levels $\alpha \in \{0.99, 0.995, 0.999\}$, including the 0.999 which corresponds to DRC, for each of the six model configurations and the synthetic test portfolios. The results are illustrated in Table 5.7 and Figure 5.10.

For Portfolio A, consisting of long positions on sovereign issuers, Model 1 and Model 5 yield a DRC figure of 8.3%, while the other model variants yield a slightly more conservative figure at 11.1%. For Porfolio B, consisting of long positions on corporates, the values are higher and more variable, with Model 1 and Model 2 producing a DRC at 14.6%, Model 5 at 15.7%, and the rest of the models at 16.9%. For the more diversified Portfolio C, models 1,2, and 5 produce a DRC of 12.8%, while models 3,4,6 produce slightly higher figures at 13.6%. Finally, for the long/short Portfolio D, models 1,3, and 4 yield a DRC of 9.1%, while models 2,5, and 6 yield a more conservative 13.6%.

In general, different model variants produce less variable losses for lower quantiles. Furthermore, although it is not straightforward to draw solid conclusions on one model being consistently more conservative, it seems that model based on global and subcommunity factors (Model 6) is among the most conservative models for all four portfolios, while the one-factor model (Model 1) is consistently among the least conservative. In addition, the DRC values produced by models 3 and 4 are in agreement for all the portfolios.

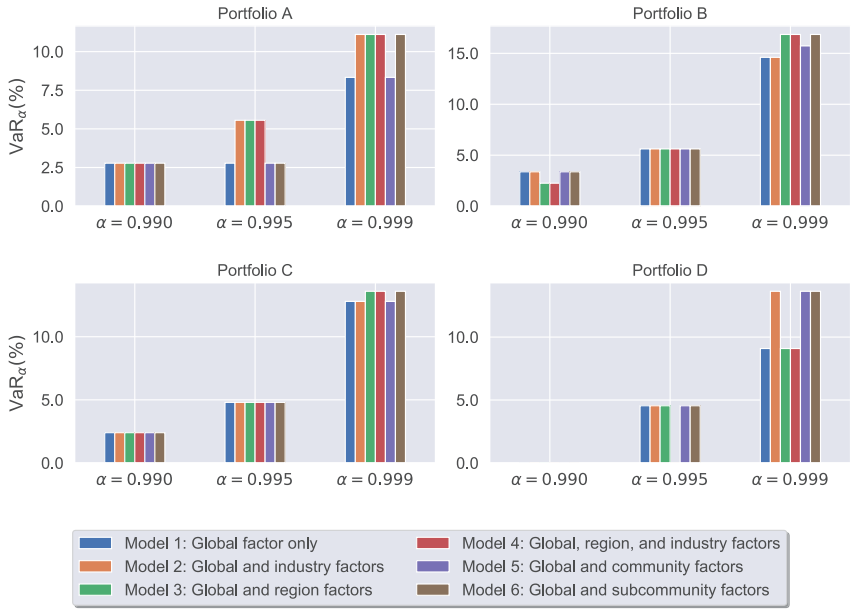

Figure 5.10: Quantiles of the loss distributions obtained from the six model variants (global factor only, global/industry, global/region, global/industry/region, global/community, global/subcommunity factors) for the four synthetic test portfolios.

Another noteworthy observation has to do with the tails of the generated loss distributions. By analysing the relationship between the quantiles presented in Table 5.7, it can be seen that all model variants seem to produce distributions with heavier tails than the standard normal distribution. For instance, the ratio between the 0.999 and the 0.99 quantile for Portfolio A is 2.96 for Model 1 and Model 5, and 3.96 for all the other model variants, compared to 1.33 for the standard normal distribution. Similar tail behaviour can be observed for all the portfolios.

5.5. Concluding remarks

One of the most challenging problems in the study of complex systems is that of identifying the mesoscopic organisation of the constituting units. This amounts to detecting groups of units which are more densely connected internally than with the rest of the system. In case the units are represented by time series, a common approach is to regard correlation matrices as weighted networks and employ standard network community detection methods. Since such an approach can introduce biases, in this chapter we adopt a principled approach based on Random Matrix Theory, leading to an algorithm that is able to identify internally correlated and mutually anti-correlated communities, in a multiresolution fashion.

Our methods are applied to the analysis of CDS time series with the aim of identifying mesoscopic groups of issuers whose similarities cannot be traced back to industry

sectors or geographical regions. We use ten years of data including the stressed period between 2007 and 2009. The analysis reveals several interesting results with regards to the community structure. In addition, our results show that different time resolutions yield similar community structures and that these structures are stable over time; this renders the obtained communities useful for risk models.

Based on the detected communities, we derive factors and build a model for portfolio credit risk that is in line with regulatory requirements for the calculation of DRC. This model is then compared with industry-standard models based on global, country, and region factors. The models based on global, communities, and subcommunities factors provide a better fit to the data and lower error between the model-implied and the empirical pairwise correlations compared to the other two-factor models.

To further explore the properties of the obtained factor models we set up four synthetic portfolios and generate loss distributions via Monte Carlo simulations. The results show that the model based on global and subcommunity factors is consistently among the most conservative. As a more general observation, all models produce distributions with heavy tails and the variability is higher in the higher quantiles, including the 0.999 which is of particular interest for DRC.

The present work represents a first step towards incorporating community detection in risk models that can be used in a realistic set up. Further research could usefully explore applications in portfolio optimisation and hedging of credit sensitive instruments. An interesting avenue for further study that would establish the value of our findings for portfolio construction could be a rigorous analysis of the diversification potential for portfolios of risky instruments across communities and subcommunities, similar to the one conducted by [134] for country and industry factors.

6

Conclusion

The aim of this thesis was to develop novel risk management models which would be able to capture financial markets as complex systems prone to sudden and major changes and consisting of many interacting nodes. The techniques and tools developed here should provide an innovative approach to risk modelling and the calculation of capital buffers. The encompassing body of work includes new methods for empirical analysis, as well as computational and mathematical tools, which were used in combination with a range of real-world datasets to develop an integrated complex systems framework for risk models. By merging new conceptual paradigms such as network theory and data-driven methods into practical simulation and risk measurement tools, we penned the outline of the upcoming paradigm shift within risk management.

The thesis was faced with three key challenges, namely the importance of extremes, the interdependence of risks, and the problem of scale. Firstly, in financial markets, as in other complex systems, extreme values occur much more frequently than what normal models would suggest. In this thesis, we considered models that depart from the Gaussian framework and account for extreme phenomena in a data-driven manner and without the use of jump processes or stochastic volatility. Secondly, the ability to accommodate for situations where many extreme outcomes occur simultaneously presents a particular challenge in the multivariate modelling set-up of portfolio credit risk. State-of-the-art models often underestimate the probability of joint large movements of risk factors. In the work presented here, we argued about the importance of considering an alternative channel of default dependence and incorporating network effects in standard credit models. Thirdly, the scale of most realistic portfolios poses a problem due to the fact that, often, portfolios in question may contain the entire position of a bank in credit-risky instruments. Dimension reduction is the only plausible option and it is often achieved by the calibration of factor models that ultimately decompose the market according to geographic regions and economic industries. In this thesis we chose a different path by adopting an entirely data-driven approach, looking for a modular and possibly hierarchical organisation of the empirical correlation matrix between financial time series.

In Chapter 2, a hidden Markov model (HMM) for the evolution of exchange rates was presented. In contrast to the widely used geometric Brownian motion (GBM), the proposed model can account for extreme behaviour that may persist for several periods, and thus prevent underestimation of counterparty exposure and the corresponding capital buffers. In our numerical experiments, scenarios were generated for a range of exchange rates and a rigorous backtesting exercise was performed. The performances of GBM and HMM were found to be very similar, with HMM being slightly more conservative. However, when the generated scenarios were used to calculate exposure profiles for foreign exchange options, we found significant differences between the results of the two models, especially for deep out-of-the-money options. In addition, our study highlighted the necessity for careful interpretation as far as backtesting results are concerned.

Chapters 3 and 4 were concerned with the interdependence of risks. An extended factor model for portfolio credit risk which offers a breadth of possible applications to capital calculations, as well as to the analysis of structured credit products, was presented in Chapter 3. In the proposed framework, systematic risk factors were augmented with an infectious default mechanism which affects the entire portfolio. Unlike models based on copulas with more extreme tail behaviour, where the dependence structure of defaults is specified a priori, our approach is more intuitive. First the way sovereign defaults may affect the default probabilities of corporate issuers is specified and then the joint default distribution is derived. The impact of sovereign defaults was quantified using a credit stress propagation network constructed from real data. Under this framework, loss distributions for synthetic test portfolios were generated and the contagion effect was shown to have a profound impact on the upper tails. In an attempt to obtain an improved approximation of the joint default distribution of issuers in credit stress propagation networks, in Chapter 4 we presented a novel method of estimating contagion effects from CDS data using Bayesian networks (BNs). Rather than assuming a certain distribution for CDS spreads, we introduced a method for learning BNs using ϵ-drawups. A range of techniques to learn the structure and parameters of financial networks was studied and evaluated. We used CDS spreads of issuers in a stylised portfolio and incorporated the conditional probabilities in the credit portfolio model presented in Chapter 3. Simulations were carried out and the impact on standard risk metrics was estimated. Contagion was shown to have a significant impact in the tails of the credit loss distribution, with the results being in line with those obtained by using the CountryRank metric in Chapter 3.

Finally, in Chapter 5 the focus was on identifying the mesocoscopic structure of the CDS market in an entirely data-driven manner, looking for a modular and possibly hierarchical organisation of the empirical correlation matrix between CDS time series. A recently developed method based on Random Matrix Theory was used to identify the optimal hierarchical decomposition of the system into internally correlated and mutually anti-correlated communities. Building upon this technique, we identified groups of issuers that cannot be traced back to standard industry/region taxonomies, thereby being inaccessible to standard factor models. We used this decomposition to introduce a novel credit risk model that was shown to outperform more traditional alternatives. Synthetic portfolios were set up and loss distributions were generated to further explore the properties of the obtained factor models. The results showed that the proposed model was consistently among the most conservative in terms of capital requirements.

The main conclusion of this thesis is that in order for quantitative risk management to be able to cope with the complex, interconnected nature of modern financial systems, a paradigm shift is inevitable. Complexity-inspired models, in combination with more traditional modelling and simulation frameworks, can open up new avenues for risk management and fill some of the gaps and inadequacies of regulatory frameworks revealed by the global financial crisis. The proposed methods were built on this assumption and showed that, by using models that account for characteristics of complex systems such as regime shifts and contagion, the impact on capital requirements may be significant.

This study lays the groundwork for further research into complex systems approaches for quantitative risk management and the calculation of capital buffers. A number of questions still remains to be answered. Future research could usefully explore whether the quantitative results of the models presented in this thesis are sensitive to specific parametrisation assumptions. In Chapter 3 we touched upon the sensitivity of the contagion impact by stressing a set of chosen parameters to assess their influence on the results. Even though such an approach is widely used in the financial industry to evaluate the sensitivity of model results, it suffers from the fact that it is only local, and thus highly dependent on the chosen parameter values. In addition, local sensitivity analyses do not take into consideration possible interactions between parameters and non-linear relationships that are frequently encountered in risk models. In recent decades, global sensitivity analysis methods have been developed in the applied mathematics and engineering fields as part of the more broad area of uncertainty quantification. While in local methods of sensitivity analysis only small parameter uncertainties around a few selected reference points are considered, global methods provide a quantitative characterisation of the uncertainty across a wide range of parameter space and propagate it through the model to evaluate the importance of each parameter along with interactions between parameters. A greater focus on global sensitivity analysis could produce interesting findings that could contribute to the credibility of the models presented in this thesis but also to the general advancement of quantitative risk management as a field.

A natural progression of the work presented in this thesis is to further investigate the relation between the credit stress propagation networks constructed from market data and causality. The questions asked here were, from a formal perspective, of a probabilistic nature and without the necessity to interpret networks as causal models whose edges carry some causal significance. For instance, in Chapter 4 the BN structures may be directed, but it is not required for the directions of the edges to have some causal meaning. All things considered, if a network structure can provide a correct representation of the underlying joint distribution, the answers that we obtain to probabilistic queries are the same, regardless of whether the network structure corresponds to some notion of causal influence. On the other hand, in situations where intervention is necessary, for example when a government needs to decide whether it is willing to bail out a financial institution or not, it is essential to understand the causal relationships in our models. The issue of causality is thus an intriguing one and could be a fruitful area to explore.

Finally, a challenge that remains to be tackled involves further research to assess the impact of using the models described in this thesis on financial stability and systemic risk. From the point of view of an individual bank, it is clear that the methods developed here may result in increased capital requirements. A rigorous study is required to de-

termine the impact of using such models to the risk and profitability of the industry as a whole. This could be achieved by setting up agent-based simulations, wherein each bank represents an agent using one of the models presented here to calculate their capital requirements. In this fashion, one could examine whether using a particular model improves the stability of the financial system. A simulation of this nature would enable regulators and financial institutions to test policies and strategies for better capital management.

A

Chapter 3 CDS spread data and stability of the ϵ parameter

A.1. CDS spread data

The data used to calibrate the credit stress propagation network for European issuers is the CDS spread data of Dutch, German, Italian and Spanish issuers as shown in Figures A.1 and A.2.

A.2. Stability of the ϵ parameter

The plot in Figure A.3 shows the time series of the epsilon parameter for different number days used for ϵ-drawup calibration.

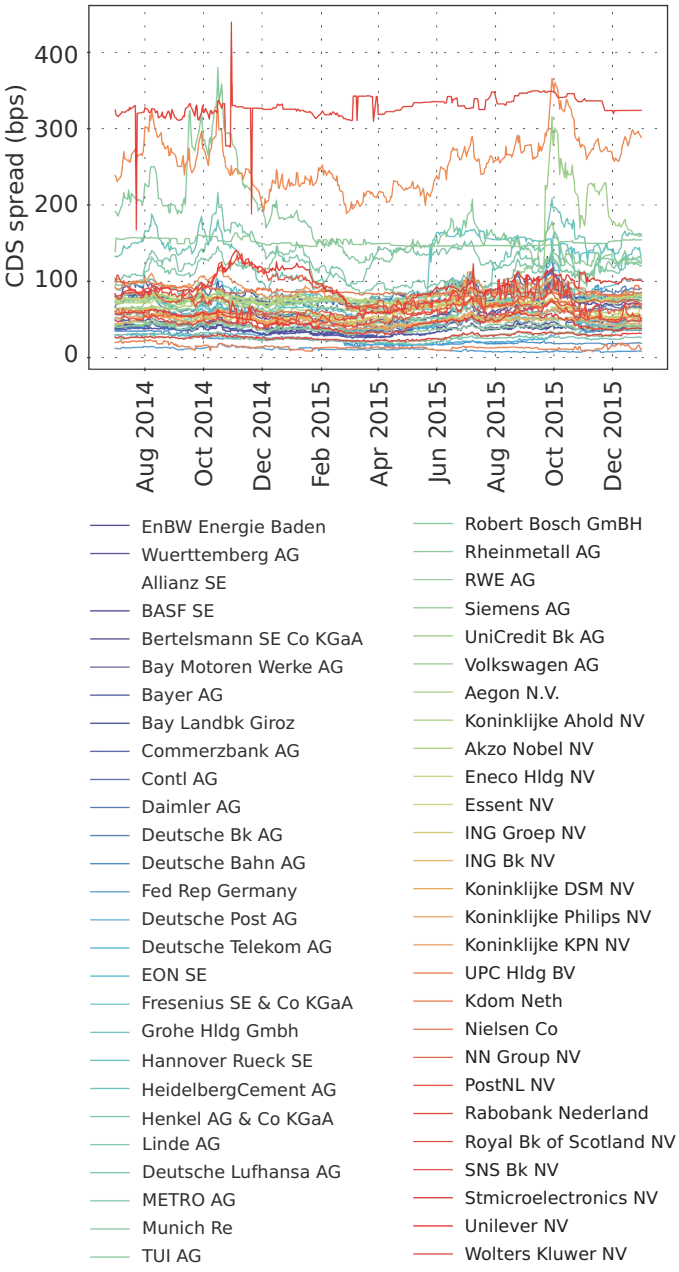

Figure A.1: Time series of CDS spreads of Dutch and German entities.

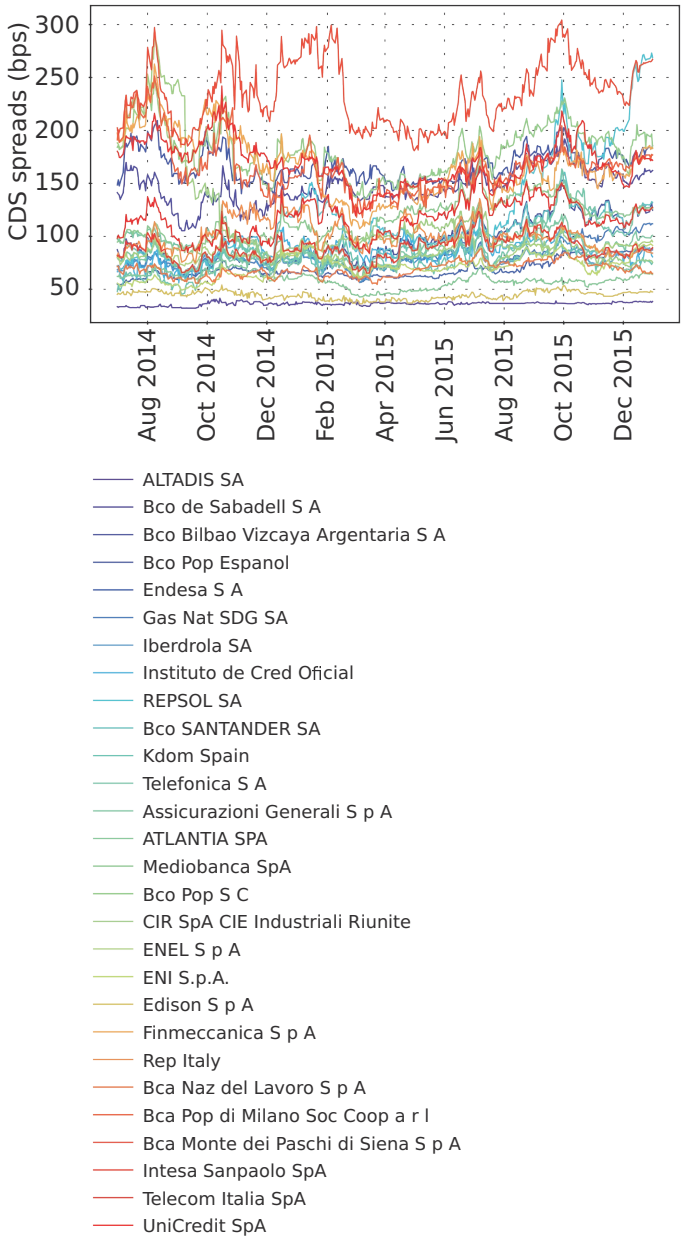

Figure A.2: Time series of CDS spreads of Spanish and Italian entities.

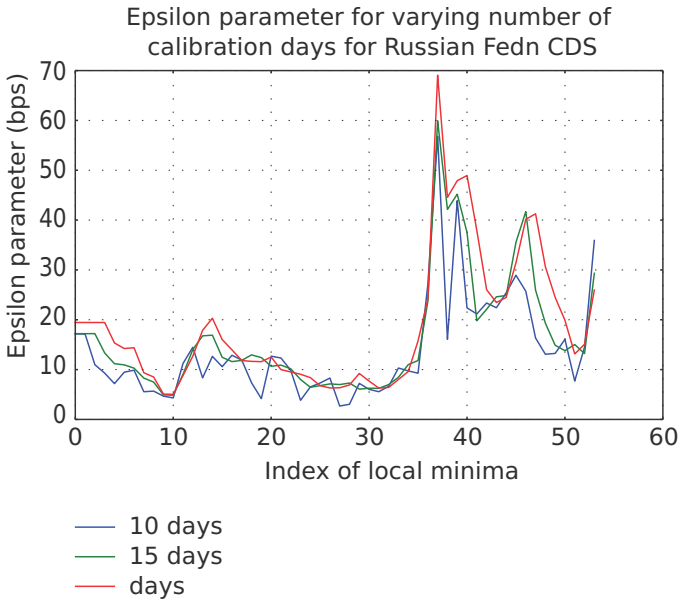

Figure A.3: Stability of ϵ parameter for Russian Federation CDS.

B

Bayesian network scores and stress scenarios

B.1. Scores

We briefly describe the two scores namely the BIC and BDs used for BN learning. For details, we refer to [105, Section 18.3]. BIC is a likelihood score defined as:

$$\text{score}_{BIC}(\mathscr{G}:\mathscr{D}) = \log L(\mathscr{G}:\mathscr{D}) - \frac{1}{2}|\mathscr{G}|\log N,$$

where $|\mathscr{G}|$ is the complexity of the network, the number of independent parameters in the network. This score penalises explicitly the score with the number of independent parameters, hence assigning higher scores to sparser structures.

The following expression is the closed-form derived for the marginal-likelihood of the structure score:

$$P(\mathscr{D}\,|\,\mathscr{G}) = \prod_i \prod_{k=1}^{q_i} \frac{\Gamma(\alpha_{X_i|k})}{\Gamma(\alpha_{X_i|k} + M[k])} \prod_{j=1}^{r_i} \left[\frac{\Gamma(\alpha_{j|k} + M[j,k])}{\Gamma(\alpha_{j|k})} \right], \tag{B.1}$$

where $\alpha_{X_i|k} = \sum_{j=1}^{r_i} \alpha_{j|k}$.

BDs is derived from a different score, BDeu, which is obtained from B.1 by assuming a uniform prior distribution over the parameters (Dirichlet distribution with all the hyperparameters taking the same value α). Let $\alpha_{j|k} = \alpha_i/(r_i q_i)$ and $\alpha_i = \alpha$, where r_i is the number of states of X_i and q_i is the number of configurations of parents of X_i, the number of parents configuration of X_i. Then score BDeu is defined as follows

$$\text{BDeu}(\mathscr{G},\mathscr{D};\alpha) = \prod_i \prod_{k=1}^{q_i} \frac{\Gamma(r_i\alpha_i)}{\Gamma(r_i\alpha_i + M[k])} \prod_{j=1}^{r_i} \frac{\Gamma(\alpha_i + M[j,k])}{\Gamma(\alpha_i)}. \tag{B.2}$$

[110] argues that choosing uniform prior distributions over $\theta_{\mathscr{G}X_i|\mathrm{Pa}_{X_i}}$ and $\mathscr{G}$ can have a negative effect over the quality of the results obtained with the score BDeu. To avoid this he introduces the score BDs.

In the first place we see that if $P(k) = 0$ for some $k \in \{1,\dots,q_i\}$ and $i \in [n]$, or if the sample size of $\mathscr{D}$ is very small, it may happen that $M[k] = 0$ for some configurations of Pa_{X_i} which do not appear in $\mathscr{D}$, then we can split

$$\mathrm{BDeu}(\mathscr{G},\mathscr{D};\alpha) = \prod_i \left(\left(\prod_{\substack{k=1) \\ M[k]=0}}^{q_i} \frac{\Gamma(r_i\alpha_i)}{\Gamma(r_i\alpha_i)} \prod_{j=1}^{r_i} \frac{\Gamma(\alpha_i)}{\Gamma(\alpha_i)} \right) \left(\prod_{\substack{k=1 \\ M[k]>0}}^{q_i} \frac{\Gamma(r_i\alpha_i)}{\Gamma(r_i\alpha_i + M[k])} \prod_{j=1}^{r_i} \frac{\Gamma(\alpha_i + M[j,k])}{\Gamma(\alpha_i)} \right) \right).$$

We note that as the number of parent configurations which appear in the data $\mathscr{D}$ decreases, the effective imaginary sample size decreases, as

$$\sum_{k:M[k]>0} \sum_j \alpha_i \leq \sum_{k,j} \alpha_i = \alpha. \tag{B.3}$$

This induces the posterior to converge to the corresponding likelihood estimation and hence leaning towards overfitting and including spurious edges in $\mathscr{G}$. To avoid this problem we define:

$$\tilde{q}_i = \left|\{k \in \{1,\dots,q_i\} : M[k] > 0\}\right| \quad \text{and} \quad \tilde{\alpha}_i = \begin{cases} \alpha/(r_i\tilde{q}_i) & \text{if } \tilde{q}_i > 0, \\ 0 & \text{otherwise.} \end{cases}$$

With this new definition the expression B.3 becomes an equality, $\sum_{k:M[k]>0}\sum_j \alpha_i = \alpha$. Moreover, we see that the uniform prior that we just defined is on the conditional distribution which can be estimated from $\mathscr{D}$, so this is a empirical Bayesian score. Finally, we substitute α_i in B.2 by $\tilde{\alpha}_i$ and obtain:

$$\mathrm{BDs}(\mathscr{G},\mathscr{D};\alpha) = \prod_i \prod_{\substack{k=1 \\ M[k]>0}}^{q_i} \frac{\Gamma(r_i\tilde{\alpha}_i)}{\Gamma(r_i\tilde{\alpha}_i + M[k])} \prod_{j=1}^{r_i} \frac{\Gamma(\tilde{\alpha}_i + M[j,k])}{\Gamma(\tilde{\alpha}_i)}. \tag{B.4}$$

B.2. Stress scenarios

The first scenario is stressing three banks in the network, BKECON, BOM and SBERBANK. Figure B.1 depicts the network with the nodes coloured according to the probabilities obtained in that scenario, shown next to it. We observe that the values obtained are similar to the ones of the scenario where the sovereign is stressed. This may be due to the strong connections of the sovereign with big companies such as GAZPRU and GAZPRU.Gneft and because the stressed banks are in the periphery of the network.

As the Russian crisis of 2014 was strongly related to oil industry, in the second scenario we stress four of the largest oil companies: AKT, GAZPRU, LUKOIL, and ROSNEF. Figure B.2 shows the network and the probabilities for this case. It is noticeable that the oil

Issuer	Prob.
BKECON	1
BOM	1
SBERBANK	1
RUSAGB	0.7757
VTB	0.7287
GAZPRU	0.69
AKT	0.5797
GAZPRU.Gneft	0.5593
ROSNEF	0.5514
RUSSIA	0.5351
CITMOS	0.5107
LUKOIL	0.4948
VIP	0.4742
RUSRAI	0.4528
ALROSA	0.4244
MDMOJC	0.4242
MBT	0.3379
RSBZAO	0.3319

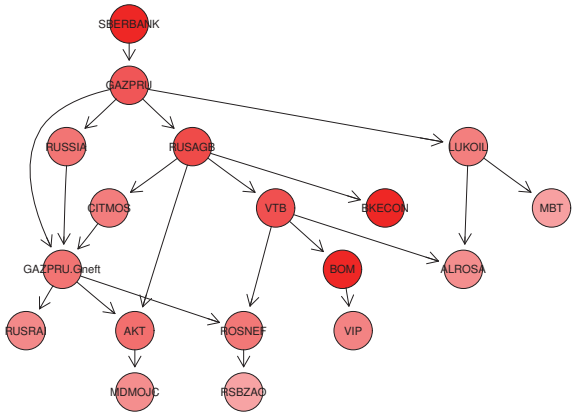

Figure B.1: Probabilities and network in the scenario of three banks stressed.

companies have a larger impact on the network. Note also that in this case four nodes are stressed. However, one can see that these nodes are more centred and the rest of the nodes are more stressed.

Issuer	Prob.
AKT	1
GAZPRU	1
LUKOIL	1
ROSNEF	1
GAZPRU.Gneft	0.8382
RUSAGB	0.7867
SBERBANK	0.7563
RUSSIA	0.6469
VTB	0.6028
RUSRAI	0.5814
MDMOJC	0.5321
BKECON	0.5273
CITMOS	0.5133
MBT	0.5078
BOM	0.4972
ALROSA	0.4708
RSBZAO	0.4053
VIP	0.366

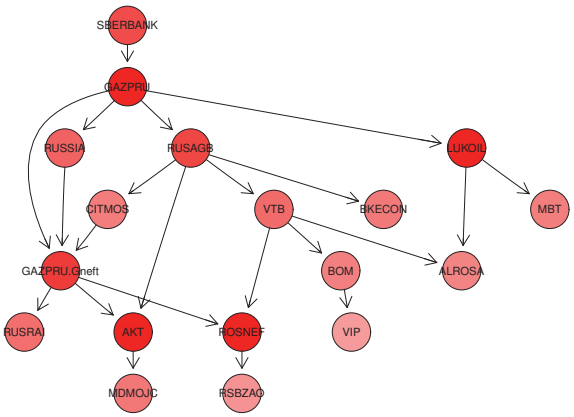

Figure B.2: Probabilities and network in the scenario of four oil companies stressed.

C

Chapter 5 regression results and empirical correlations

C.1. Full regression results on the basis of Equation (5.28)

This appendix presents the full regression results for the time-series regression models that are presented in Equation (5.28) for Chapter 5.

Table C.1: This table provides the results of the industry, region, and community factor analysis derived from CDS spread returns. The analysis is based on non-overlapping monthly log-returns and conducted over the period January 2007 through December 2016. After standardization the CDS returns are used to derive global, industry, region and community factors as cross-sectional averages at each time point. The industry, region, and community factors are regressed onto the global factor; coefficients (γ_I, γ_R, γ_C, and γ_{SC} respectively) as well as R^2 are provided in the table, complemented by the standard deviation of the residual returns. t-tests are conducted to evaluate whether the coefficients differ from one.

Industry	γ_I	t-statistic	p-value	R^2	σ_I	σ_G
Basic Materials	1.027	0.993	32.3%	92.3%	20.1%	
Consumer goods	0.988	-0.586	55.9%	95.2%	15.1%	
Consumer services	0.962	-1.676	9.6%	93.7%	16.9%	
Energy	1.021	0.491	62.5%	82.7%	31.7%	
Financials	1.019	0.603	54.8%	90.1%	23.0%	
Government	1.042	1.035	30.3%	84.6%	30.2%	67.9%
Health care	0.880	-3.306	0.1%	83.2%	26.9%	
Industrials	1.028	1.493	13.8%	96.3%	13.6%	
Technology	0.890	-4.178	0.0%	90.7%	19.4%	
Telecommunication services	1.023	0.982	32.8%	94.0%	17.5%	
Utilities	1.009	0.350	72.7%	93.2%	18.5%	
Region	γ_R	t-statistic	p-value	R^2	σ_R	σ_G
Africa	1.056	0.936	35.1%	72.8%	43.8%	
Asia	1.115	2.883	0.5%	86.9%	29.3%	
Eastern Europe	1.065	1.056	29.3%	71.8%	45.3%	
						67.9%

Europe	1.021	0.928	35.5%	94.5%	16.7%	
India	1.131	1.792	7.6%	67.1%	53.8%	
Latin America	1.072	1.221	22.4%	73.6%	43.6%	
Middle East	0.928	-1.282	20.2%	69.7%	41.6%	
North America	0.926	-3.702	0.0%	94.9%	14.6%	
Oceania	1.104	2.688	0.8%	87.3%	28.7%	
Community	γ_C	t-statistic	p-value	R^2	σ_C	σ_G
A	0.967	-1.196	23.4%	91.5%	20.1%	
B	0.987	-0.526	60.0%	92.6%	18.9%	67.9%
C	1.061	1.852	6.6%	89.9%	24.2%	
D	0.989	-0.220	82.6%	76.8%	36.9%	
Subcommunity	γ_S	t-statistic	p-value	R^2	σ_S	σ_G
A1	0.943	-1.665	0.098	86.5%	25.3%	
A2	0.934	-2.052	0.042	87.6%	23.9%	
A3	1.093	2.260	0.026	85.6%	30.4%	
A4	0.999	-0.015	0.988	76.5%	37.5%	
B1	0.952	-1.516	0.132	88.5%	23.2%	
B2	1.067	2.267	0.025	91.8%	21.7%	
C1	1.022	0.474	0.636	80.4%	34.3%	
C2	0.995	-0.141	0.888	88.4%	24.5%	67.9%
C3	1.154	3.665	0.000	86.5%	31.0%	
D1	1.026	0.379	0.705	65.5%	50.5%	
D2	0.895	-3.202	0.002	86.4%	24.1%	
D3	0.980	-0.295	0.768	62.8%	51.2%	
D4	1.123	1.664	0.099	66.2%	54.6%	
D5	1.081	1.122	0.264	65.7%	53.0%	
D6	1.011	0.168	0.867	65.0%	50.4%	

C.2. Empirical pairwise correlations

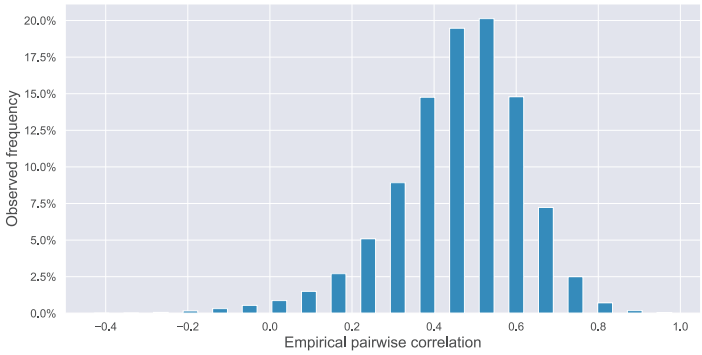

Figure C.1: Empirical pairwise correlation. The figure shows the distribution of the CDS spread correlation during the period January 2007 through December 2016, based on Markit data for 786 issuers. The return correlation is calculated from non-overlapping monthly log-returns.

Bibliography

[1] S. Battiston, J. D. Farmer, A. Flache, D. Garlaschelli, A. G. Haldane, H. Heesterbeek, C. Hommes, C. Jaeger, R. May, and M. Scheffer, *Complexity theory and financial regulation,* Science **351**, 818 (2016).

[2] A. Turner, *The Turner review: a regulatory response to the global banking crisis.* Financial Services Authority (2009).

[3] W. Weaver, *Science and complexity,* American Scientist **36**, 536 (1948).

[4] J. D. Farmer, *Economics needs to treat the economy as a complex system,* in *Papers for the INET Conference "Rethinking Economics and Politics"*, Vol. 14 (2012).

[5] H. A. Simon, *The architecture of complexity,* Proceedings of the American Philosophical Society **106**, 467 (1962).

[6] F. A. Hayek, *The theory of complex phenomena,* in *The Critical Approach to Science and Philosophy*, edited by M. Bunge (The Free Press, Glencoe, 1964) Chap. 22, pp. 332–349.

[7] P. W. Anderson, K. Arrow, and D. Pines, eds., *The economy as an evolving complex system* (Westview Press, Boulder, 1988).

[8] W. B. Arthur, S. N. Durlauf, and D. A. Lane, eds., *The Economy as an Evolving Complex System II.* (Westview Press, Boulder, 1997).

[9] F. Allen and D. Gale, *Financial contagion,* Journal of Political Economy **108**, 1 (2000).

[10] P. Gai and S. Kapadia, *Contagion in financial networks,* Proceedings of the Royal Society of London A: Mathematical, Physical and Engineering Sciences **466**, 2401 (2010).

[11] P. Glasserman and H. P. Young, *How likely is contagion in financial networks?* Journal of Banking & Finance **50**, 383 (2015).

[12] M. Elliott, B. Golub, and M. O. Jackson, *Financial networks and contagion,* American Economic Review **104**, 3115 (2014).

[13] D. Acemoglu, A. Ozdaglar, and A. Tahbaz-Salehi, *Systemic risk and stability in financial networks,* American Economic Review **105**, 564 (2015).

[14] R. Cont, A. Moussa, and E. B. Santos, *Network structure and systemic risk in banking systems,* in *Handbook on Systemic Risk:*, edited by J.-P. Fouque and J. A. Langsam (Cambridge University Press, Cambridge, 2013) pp. 327–368.

[15] S. Battiston, M. Puliga, R. Kaushik, P. Tasca, and G. Caldarelli, *DebtRank: Too central to fail? financial networks, the FED and systemic risk,* Scientific Reports **2** (2012), 10.1038/srep00541.

[16] M. Bardoscia, S. Battiston, F. Caccioli, and G. Caldarelli, *DebtRank: A microscopic foundation for shock propagation,* PLoS ONE **10**, e0130406 (2015).

[17] S. Battiston, G. Caldarelli, M. D'Errico, and S. Gurciullo, *Leveraging the network: a stress-test framework based on DebtRank,* Statistics & Risk Modeling **33**, 117 (2016).

[18] M. Bardoscia, F. Caccioli, J. I. Perotti, G. Vivaldo, and G. Caldarelli, *Distress propagation in complex networks: The case of non-linear DebtRank,* PLoS ONE **11**, 1 (2016).

[19] S. Fortunato, *Community detection in graphs,* Physics reports **486**, 75 (2010).

[20] A. J. McNeil, R. Frey, and P. Embrechts, *Quantitative risk management: Concepts, techniques and tools*, 2nd ed. (Princeton university press, 2015).

[21] H. F. Kloman, *Risk management agonistes 1,* Risk Analysis **10**, 201 (1990).

[22] J. C. Hull, *Options, Futures, and Other Derivatives*, 7th ed. (Pearson Prentice Hall, New York, 2009).

[23] R. C. Merton, *On the pricing of corporate debt: The risk structure of interest rates,* The Journal of Finance **29**, 449 (1974).

[24] M. Gordy, *A risk-factor model foundation for ratings-based bank capital rules,* Journal of Financial Intermediation **12**, 199 (2003).

[25] Moody's Global Credit Policy, *Emerging market corporate and sub-sovereign defaults and sovereign crises: Perspectives on country risk,* Moody's Investor Services (2009).

[26] I. T. Jolliffe, *Principal component analysis*, 2nd ed., Springer series in statistics (Springer-Verlag, New York, 2002).

[27] Basel Committee on Banking Supervision, *Basel III: A global regulatory framework for more resilient banks and banking systems,* Bank for International Settlements (2010).

[28] Basel Committee on Banking Supervision, *Sound practices for backtesting counterparty credit risk models,* Bank for International Settlements (2010).

[29] F. Anfuso, D. Karyampas, and A. Nawroth, *Credit exposure models backtesting for Basel III,* Risk **9**, 82 (2014).

[30] I. Ruiz, *Backtesting counterparty risk: how good is your model?* The Journal of Credit Risk **10**, 87 (2014).

[31] Basel Committee on Banking Supervision, *Supervisory framework for the use of "backtesting" in conjunction with the internal models approach to market risk capital requirements,* Bank for International Settlements (1996).

[32] P. Boothe and D. Glassman, *The statistical distribution of exchange rates: empirical evidence and economic implications,* Journal of International Economics **22**, 297 (1987).

[33] B. H. Juang and L. R. Rabiner, *Hidden Markov models for speech recognition,* Technometrics **33**, 251 (1991).

[34] A. Krogh, M. Brown, I. S. Mian, K. Sjölander, and D. Haussler, *Hidden Markov models in computational biology: Applications to protein modeling,* Journal of Molecular Biology **235**, 1501 (1994).

[35] A. D. Wilson and A. F. Bobick, *Parametric hidden Markov models for gesture recognition,* IEEE Transactions on Pattern Analysis and Machine Intelligence **21**, 884 (1999).

[36] Z. Ghahramani, *An introduction to hidden Markov models and bayesian networks,* in *Hidden Markov models: applications in computer vision* (World Scientific, 2001) pp. 9–41.

[37] J. D. Hamilton, *Rational-expectations econometric analysis of changes in regime: An investigation of the term structure of interest rates,* Journal of Economic Dynamics and Control **12**, 385 (1988).

[38] J. D. Hamilton, *A new approach to the economic analysis of nonstationary time series and the business cycle,* Econometrica: Journal of the Econometric Society , 357 (1989).

[39] T. Rydén, T. Teräsvirta, and S. Åsbrink, *Stylized facts of daily return series and the hidden Markov model,* Journal of Applied Econometrics **13**, 217 (1998).

[40] J. Bulla, S. Mergner, I. Bulla, A. Sesboüé, and C. Chesneau, *Markov-switching asset allocation: do profitable strategies exist?* Journal of Asset Management **12**, 310 (2011).

[41] P. Nystrup, H. Madsen, and E. Lindström, *Stylised facts of financial time series and hidden Markov models in continuous time,* Quantitative Finance **15**, 1531 (2015).

[42] A. Ang and G. Bekaert, *How regimes affect asset allocation,* Financial Analysts Journal **60**, 86 (2004).

[43] M. Guidolin and A. Timmermann, *Asset allocation under multivariate regime switching,* Journal of Economic Dynamics and Control **31**, 3503 (2007).

[44] P. Nystrup, B. W. Hansen, H. Madsen, and E. Lindström, *Regime-based versus static asset allocation: Letting the data speak,* The Journal of Portfolio Management **42**, 103 (2015).

[45] V. Naik, *Option valuation and hedging strategies with jumps in the volatility of asset returns,* The Journal of Finance **48**, 1969 (1993).

[46] X. Guo, *An explicit solution to an optimal stopping problem with regime switching,* Journal of Applied Probability **38**, 464 (2001).

[47] N. P. Bollen, *Valuing options in regime-switching models,* The Journal of Derivatives **6**, 38 (1998).

[48] L. E. Baum and T. Petrie, *Statistical inference for probabilistic functions of finite state Markov chains,* The Annals of Mathematical Statistics **37**, 1554 (1966).

[49] L. E. Baum and J. A. Eagon, *An inequality with applications to statistical estimation for probabilistic functions of Markov processes and to a model for ecology,* Bulletin of the American Mathematical Society **73**, 360 (1967).

[50] L. R. Rabiner, *A tutorial on hidden Markov models and selected applications in speech recognition,* in *Readings in Speech Recognition* (Elsevier, Amsterdam, 1990) pp. 267–296.

[51] A. P. Dempster, N. M. Laird, and D. B. Rubin, *Maximum likelihood from incomplete data via the em algorithm,* Journal of the Royal Statistical Society. Series B (methodological) **39**, 1 (1977).

[52] F. X. Diebold, T. A. Gunther, and A. Tay, *Evaluating density forecasts,* International Economic Review **39**, 863 (1997).

[53] W. Zucchini, I. L. MacDonald, and R. Langrock, *Hidden Markov models for time series: an introduction using R* (Chapman and Hall/CRC, London, 2016).

[54] S. H. Zhu and M. Pykhtin, *A guide to modeling counterparty credit risk,* GARP Risk Review **37** (2007).

[55] J. Gregory, *Counterparty credit risk and credit value adjustment: A continuing challenge for global financial markets* (John Wiley & Sons, Hoboken, 2012).

[56] E. Picoult, *Quantifying the risks of trading* (Cambridge University Press, Cambridge, 2002).

[57] M. B. Garman and S. W. Kohlhagen, *Foreign currency option values,* Journal of international Money and Finance **2**, 231 (1983).

[58] Basel Committee on Banking Supervision, *The standardised approach for measuring counterparty credit risk exposures,* Bank for International Settlements (2014).

[59] J. Berkowitz, *Testing density forecasts, with applications to risk management,* Journal of Business & Economic Statistics **19**, 465 (2001).

[60] G. Amisano and R. Giacomini, *Comparing density forecasts via weighted likelihood ratio tests,* Journal of Business & Economic Statistics **25**, 177 (2007).

[61] J. R. Bohn and S. Kealhofer, *Portfolio management of default risk,* KMV working paper (2001).

[62] P. J. Crosbie and J. R. Bohn, *Modeling default risk,* KMV working paper (2002).

[63] JP Morgan, *Creditmetrics™–technical document,* JP Morgan, New York (1997).

[64] Basel Committee on Banking Supervision, *International convergence of capital measurement and capital standards,* Bank of International Settlements (2004).

[65] D. Duffie, L. H. Pedersen, and K. J. Singleton, *Modeling sovereign yield spreads: A case study of Russian debt,* The Journal of Finance **58**, 119 (2003).

[66] P. J. Schönbucher and D. Schubert, *Copula-dependent default risk in intensity models,* Available at SSRN 301968 (2001).

[67] S. R. Das, D. Duffie, N. Kapadia, and L. Saita, *Common failings: How corporate defaults are correlated,* The Journal of Finance **62**, 93 (2007).

[68] R. Frey, A. J. McNeil, and M. Nyfeler, *Copulas and credit models,* Risk **10** (2001).

[69] E. Lütkebohmert, *Concentration risk in credit portfolios* (Springer Science & Business Media, New York, 2008).

[70] M. Davis and V. Lo, *Infectious defaults,* Quantitative Finance **1**, 382 (2001), http://dx.doi.org/10.1080/713665832 .

[71] K. Giesecke and S. Weber, *Credit contagion and aggregate losses,* Journal of Economic Dynamics and Control **30**, 741 (2006).

[72] D. Lando and M. S. Nielsen, *Correlation in corporate defaults: Contagion or conditional independence?* Journal of Financial Intermediation **19**, 355 (2010).

[73] R. A. Jarrow and F. Yu, *Counterparty risk and the pricing of defaultable securities,* the Journal of Finance **56**, 1765 (2001).

[74] D. Egloff, M. Leippold, and P. Vanini, *A simple model of credit contagion,* Journal of Banking & Finance **31**, 2475 (2007).

[75] S. Sourabh, M. Hofer, and D. Kandhai, *Credit valuation adjustments by a network-based methodology,* BigDataFinance Winter School on Complex Financial Networks (2017).

[76] S. Battiston, D. D. Gatti, M. Gallegati, B. Greenwald, and J. E. Stiglitz, *Liaisons dangereuses: Increasing connectivity, risk sharing, and systemic risk,* Journal of Economic Dynamics and Control **36**, 1121 (2012).

[77] R. Kaushik and S. Battiston, *Credit default swaps drawup networks: Too interconnected to be stable,* PLoS ONE **8**, e61815 (2013).

[78] J. Gregory, *The xVA Challenge: Counterparty Credit Risk, Funding, Collateral, and Capital* (John Wiley & Sons, Chichester, 2015).

[79] A. Green, C. Kenyon, and C. Dennis, *KVA: capital valuation adjustment by replication,* Risk **27** (2014).

[80] S. Sourabh, M. Hofer, and D. Kandhai, *Liquidity risk in derivatives valuation: an improved credit proxy method,* Quantitative Finance **18**, 467 (2018).

[81] C. S. de Graaf, Q. Feng, D. Kandhai, and C. W. Oosterlee, *Efficient computation of exposure profiles for counterparty credit risk,* International Journal of Theoretical and Applied Finance **17**, 1450024 (2014).

[82] C. S. L. de Graaf, D. Kandhai, and C. Reisinger, *Efficient exposure computation by risk factor decomposition,* Quantitative Finance **18**, 1657 (2018).

[83] S. Simaitis, C. S. L. de Graaf, N. Hari, and D. Kandhai, *Smile and default: the role of stochastic volatility and interest rates in counterparty credit risk,* Quantitative Finance **16**, 1725 (2016).

[84] T. Squartini, I. Van Lelyveld, and D. Garlaschelli, *Early-warning signals of topological collapse in interbank networks,* Scientific reports **3**, 3357 (2013).

[85] S. Poledna, S. Thurner, J. D. Farmer, and J. Geanakoplos, *Leverage-induced systemic risk under Basel II and other credit risk policies,* Journal of Banking & Finance **42**, 199 (2014).

[86] N. Musmeci, V. Nicosia, T. Aste, T. Di Matteo, and V. Latora, *The multiplex dependency structure of financial markets,* Complexity **2017** (2017).

[87] B. Hambly, S. Ledger, and A. Sojmark, *A McKean–Vlasov equation with positive feedback and blow-ups,* arXiv preprint arXiv:1801.07703 (2018).

[88] B. Hambly and A. Sojmark, *An spde model for systemic risk with endogenous contagion,* arXiv preprint arXiv:1801.10088 (2018).

[89] V. Kaushansky and C. Reisinger, *Simulation of particle systems interacting through hitting times,* arXiv preprint arXiv:1805.11678 (2018).

[90] V. Kaushansky, A. Lipton, and C. Reisinger, *Semi-analytical solution of a McKean-Vlasov equation with feedback through hitting a boundary,* arXiv preprint arXiv:1808.05311 (2018).

[91] S. Nadtochiy, M. Shkolnikov, *et al.*, *Particle systems with singular interaction through hitting times: application in systemic risk modeling,* The Annals of Applied Probability **29**, 89 (2019).

[92] M. Galley, K. McKeown, J. Hirschberg, and E. Shriberg, *Identifying agreement and disagreement in conversational speech: Use of Bayesian networks to model pragmatic dependencies,* in *the 42nd Annual Meeting on Association for Computational Linguistics* (Association for Computational Linguistics, 2004) p. 669.

[93] I. A. Beinlich, H. J. Suermondt, R. M. Chavez, and G. F. Cooper, *The alarm monitoring system: A case study with two probabilistic inference techniques for belief networks,* in *AIME 89* (Springer, 1989) pp. 247–256.

[94] M. Fishelson and D. Geiger, *Optimizing exact genetic linkage computations,* Journal of Computational Biology **11**, 263 (2004).

[95] A. Denev, *Credit portfolio models in the presence of forward-looking stress events,* The Journal of Risk Model Validation **7**, 83 (2013).

[96] C. Chong and C. Klüppelberg, *Contagion in financial systems: A Bayesian network approach,* SIAM Journal on Financial Mathematics **9**, 28 (2018).

[97] C. Kitwiwattanachai, *Learning Network Structure of Financial Institutions from CDS Data,* Available at SSRN 2533606 (2015).

[98] K. B. Korb and A. E. Nicholson, *Bayesian artificial intelligence* (CRC press, London, 2003).

[99] F. V. Jensen and T. D. Nielsen, *Bayesian networks and decision graphs* (Springer, New York, 2007).

[100] R. Nagarajan, M. Scutari, and S. Lèbre, *Bayesian networks in R* (Springer, New York, 2013).

[101] R. M. May and N. Arinaminpathy, *Systemic risk: the dynamics of model banking systems,* Journal of the Royal Society Interface **7**, 823 (2009).

[102] P. Gai and S. Kapadia, *Contagion in financial networks,* Proceedings of the Royal Society A: Mathematical, Physical and Engineering Sciences **466**, 2401 (2010).

[103] J. P. Gleeson, T. Hurd, S. Melnik, and A. Hackett, *Systemic risk in banking networks without monte carlo simulation,* in *Advances in Network Analysis and its Applications*, edited by E. Kranakis (Springer-Verlag, Berlin Heidelberg, 2012) pp. 27–56.

[104] T. R. Hurd and J. P. Gleeson, *On watts' cascade model with random link weights,* Journal of Complex Networks **1**, 25 (2013).

[105] D. Koller and N. Friedman, *Probabilistic graphical models: principles and techniques* (MIT press, 2009).

[106] F. Glover, *Tabu search fundamentals and uses,* Boulder: Graduate School of Business, University of Colorado. (1995).

[107] S. R. Das and P. Hanouna, *Implied recovery,* Journal of Economic Dynamics and Control **33**, 1837 (2009).

[108] D. Sornette and W.-X. Zhou, *Predictability of large future changes in major financial indices,* International Journal of Forecasting **22**, 153 (2006).

[109] G. Schwarz, *Estimating the dimension of a model,* Annals of Statistics **6**, 461 (1978).

[110] M. Scutari, *An empirical-bayes score for discrete Bayesian networks,* in *Conference on Probabilistic Graphical Models* (2016) pp. 438–448.

[111] N. Friedman, M. Goldszmidt, and A. Wyner, *Data analysis with Bayesian networks: a bootstrap approach,* in *Fifteenth conference on Uncertainty in artificial intelligence*, UAI'99 (Morgan Kaufmann Publishers Inc., San Francisco, 1999) pp. 196–205.

[112] M. Henrion, *Propagating uncertainty in Bayesian networks by probabilistic logic sampling,* in *Machine Intelligence and Pattern Recognition*, Vol. 5 (Elsevier, 1988) pp. 149–163.

[113] M. Scutari, *Learning Bayesian networks with the bnlearn R package,* Journal of Statistical Software **35**, 1 (2010).

[114] L. A. Amaral and J. M. Ottino, *Complex networks,* The European Physical Journal B **38**, 147 (2004).

[115] R. N. Mantegna, H. E. Stanley, *et al.*, *An introduction to econophysics: correlations and complexity in finance*, Vol. 9 (Cambridge university press, Cambridge, 2000).

[116] R. N. Mantegna, *Hierarchical structure in financial markets,* The European Physical Journal B-Condensed Matter and Complex Systems **11**, 193 (1999).

[117] J.-P. Onnela, A. Chakraborti, K. Kaski, J. Kertesz, and A. Kanto, *Dynamics of market correlations: Taxonomy and portfolio analysis,* Physical Review E **68**, 056110 (2003).

[118] M. McDonald, O. Suleman, S. Williams, S. Howison, and N. F. Johnson, *Detecting a currency's dominance or dependence using foreign exchange network trees,* Physical Review E **72**, 046106 (2005).

[119] M. McDonald, O. Suleman, S. Williams, S. Howison, and N. F. Johnson, *Impact of unexpected events, shocking news, and rumors on foreign exchange market dynamics,* Physical Review E **77**, 046110 (2008).

[120] P. Sieczka and J. A. Hołyst, *Correlations in commodity markets,* Physica A: Statistical Mechanics and its Applications **388**, 1621 (2009).

[121] M. Bernaschi, L. Grilli, and D. Vergni, *Statistical analysis of fixed income market,* Physica A: Statistical Mechanics and its Applications **308**, 381 (2002).

[122] T. Di Matteo, T. Aste, and R. N. Mantegna, *An interest rates cluster analysis,* Physica A: Statistical Mechanics and its Applications **339**, 181 (2004).

[123] Basel Committee on Banking Supervision, *Amendment to the capital accord to incorporate market risks,* Bank for International Settlements (1996).

[124] Basel Committee on Banking Supervision, *Guidelines for computing capital for incremental risk in the trading book,* Bank for International Settlements (2009).

[125] Basel Committee on Banking Supervision, *Revisions to the basel ii market risk framework,* Bank for International Settlements (2011).

[126] J.-P. Laurent, M. Sestier, and S. Thomas, *Trading book and credit risk: How fundamental is the basel review?* Journal of Banking & Finance **73**, 211 (2016).

[127] S. Wilkens and M. Predescu, *Default risk charge: Modeling framework for the'basel'risk measure,* Journal of Risk **19** (2017).

[128] M. MacMahon and D. Garlaschelli, *Community detection for correlation matrices,* Physical Review X **5**, 021006 (2015).

[129] A. Almog, F. Besamusca, M. MacMahon, and D. Garlaschelli, *Mesoscopic community structure of financial markets revealed by price and sign fluctuations,* PLoS ONE **10**, e0133679 (2015).

[130] M. Potters, J.-P. Bouchaud, and L. Laloux, *Financial applications of random matrix theory: Old laces and new pieces,* arXiv preprint arXiv:physics/0507111 (2005).

[131] M. L. Mehta, *Random matrices*, Vol. 142 (Elsevier, Amsterdam, 2004).

[132] L. Laloux, P. Cizeau, J.-P. Bouchaud, and M. Potters, *Noise dressing of financial correlation matrices,* Physical Review Letters **83**, 1467 (1999).

[133] S. L. Heston and K. G. Rouwenhorst, *Does industrial structure explain the benefits of international diversification?* Journal of Financial Economics **36**, 3 (1994).

[134] K. Aretz and P. F. Pope, *Common factors in default risk across countries and industries,* European Financial Management **19**, 108 (2013).

[135] M. Loretan and W. B. English, *III. Special feature: Evaluating changes in correlations during periods of high market volatility,* BIS Quarterly Review , 29 (2000).

[136] S&P Global Ratings, *Default, transition, and recovery: 2018 annual sovereign default and rating transition study,* S&P (2019).

[137] S&P Global Ratings, *Default, transition, and recovery: 2018 annual global corporate default and rating transition study,* S&P (2019).

List of Publications

[P1] **I. Anagnostou** and D. Kandhai, *Risk factor evolution for counterparty credit risk under a hidden Markov model*, Risks **7**, 66 (2019).

Contributions: Both authors conceived and planned the research. **I. Anagnostou** performed the numerical experiments. Both authors discussed the results and contributed to the final version of the manuscript.

[P2] **I. Anagnostou**, S. Sourabh, and D. Kandhai, *Incorporating contagion in portfolio credit risk models using network theory*, Complexity **2018** (2018).

Contributions: **I. Anagnostou** and S. Sourabh conceived the research, carried out the numerical experiments and wrote the manuscript. D. Kandhai supervised the research and revised the manuscript. All authors approved the final version of the manuscript.

[P3] **I. Anagnostou**, J. Sánchez Rivero, S. Sourabh, and D. Kandhai, *Contagious defaults in a credit portfolio: A Bayesian network approach*, Journal of Credit Risk **16**, 1 (2020)

Contributions: **I. Anagnostou** and S. Sourabh conceived the research. **I. Anagnostou** and J. Sánchez Rivero performed the data analysis and numerical experiments and wrote the manuscript. S. Sourabh revised the manuscript. D. Kandhai supervised the research and revised the manuscript. All authors approved the final version of the manuscript.

[P4] **I. Anagnostou**, T. Squartini, D. Garlaschelli, and D. Kandhai, *Uncovering the mesoscale structure of the credit default swap market to improve portfolio risk modelling*, in preparation for Quantitative Finance (2020)

Contributions: **I. Anagnostou** collected and analysed the data, performed the numerical experiments, and wrote the first version of the manuscript. T. Squartini contributed the community detection methods part and revised the rest of the manuscript. D. Garlaschelli and D. Kandhai supervised the research and revised the manuscript. All authors approved the final version of the manuscript.

I have undertaken additional research during my PhD that I do not include in this thesis due to its disparate nature. For completeness, I include the publication resulting from this work below

[P5] G. Moysiadis, **I. Anagnostou**, and D. Kandhai, *Calibrating the mean-reversion parameter in the Hull-White model using neural networks.*, ECML PKDD 2018 Workshops, 23 (2018)

Contributions: All authors conceived the research. G Moysiadis performed the research, carried out the numerical experiments, and wrote the manuscript. **I. Anagnostou** and D. Kandhai supervised the research and revised the manuscript. All authors approved the final version of the manuscript.

Preliminary results of [P1] and [P3] were presented at the below international conferences:

- *Financial time series regime detection* (invited talk), The 13th Fixed Income Conference, Florence, Italy, October 19, 2017.
- *Contagious defaults in a credit portfolio: a Bayesian network approach*, SIAM Conference on Financial Mathematics and Engineering (FM19) Toronto, Canada, June 4, 2019.

Acknowledgements

I would like to express my sincere gratitude to my supervisor, Prof. Drona Kandhai for offering me the opportunity to pursue a PhD in his group and for providing me with encouragement and support whilst giving me the room to explore and develop my own approach. Drona, thank you for creating opportunities and opening doors for collaborations, for helping me connect the dots in order to build a story, and for always having in mind the big picture. I would also like to thank Prof. Alfons Hoekstra for his role in this PhD and the members of the doctoral committee for their efforts in assessing this thesis and acting as opponents during its defence.

I am grateful to Grigorios and Erik, with whom I started working on the idea of modelling default contagion during my MSc in Edinburgh and who were the ones recommending me to Drona.

Throughout my PhD, the person I have worked the closest with was Sumit. Sumit, thank you for the collaboration, for the insights into doing a PhD and writing scientific papers, and for being such a good conference buddy. Many thanks to Marcel and Jori for our countless interesting discussions, for reviewing my work and giving me feedback, as well as for translating the summary of this thesis to Dutch.

In the past four years I have had the pleasure of working with many talented students and I am grateful to all of them, with special thanks to Javier and George. Javier, thank you for the hard work fuelled by Thai food and fresh coconuts at IAS during the heatwave. George, thank you for presenting in Dublin despite the obstacles and for helping me retrieve my stolen bike.

Many thanks to Tiziano and Diego for making me feel welcome at IMT Lucca; the time spent there is among the fondest memories from my PhD journey. I would also like to thank Emiliano, Matteo, Beyza, Dimitris, Afrodite, Elisa, Mirko, and the other researchers for the coffee breaks at Mara Meo, conversations about our research, and for exploring the Tuscan country side with me.

Thanks to Anna, Ben, Britt, and Vishnu for always being there to discuss the common challenges of working towards a PhD and reminding me every path has its curves with its ups and downs. Thanks to my office mates Lourens, Donwei, David, and Mark for providing nice working environment. Thanks to Peter, Jaap, Mike, Rick, Valeria, and Gabor for making CSL such a great place to work. The CSL outings - be it the kayaking through the canals of Amsterdam, mountain biking in the Ardennes, watching seals in the Wadden sea or simply having some beer at Oerknal - contributed to my sanity while pursuing my research. I would also like to thank the CSL members present at the beginning: Kees, Omri, Louis, Amir, Eva, Yukki, Saad, Debraj, and Philip.

A big thank you to Markus, Shashi, Patrik, Lech, Vlad, Arne, Alexios, Thorsten, Ibrahim, Eduard and the rest of my colleagues at ING who made me feel welcome from the very first days and were always eager to discuss research ideas. The weekly squash sessions

organised by Thorsten helped me release some pressure and contributed to my body's ability to function beyond the premises of my computer screen.

I consider myself very lucky that my PhD was part of the BigDataFinance Marie Curie Innovative Training Network. I would like to express my gratitude to all the ESRs and supervisors. Attending the training events and conferences with all of you was truly memorable and I look forward to our future collaborations.

Thank you to those of my friends scattered around the world who figured as a constant in my life, providing me with laughs, advice, and support no matter the weather.

I would like to thank my parents, Georgios and Kyriaki. I would not be here if it was not for you and your sacrifices. Your love and support has been a constant source of encouragement and comfort for me. Many thanks to my brother, Antonios. Despite living far apart, you are all close to my heart.

Last and foremost, I would like to thank my beautiful wife, Thess. Thank you for always believing in me, for encouraging me when most needed and for giving me that extra push to go for it when I was hesitating. Thank you for the countless flights and video calls, for leaving behind your job and your favourite place in the world in order to be with me in Amsterdam. Thank you for reading my papers and thesis and for always providing me with smart comments. Thank you for inspiring me every day to do my best. I am thankful to have you in my life.